UNIVERSITY OF OKLAHOMA

GRADUATE COLLEGE

NOVEL, LOW-COST ALUMINUM (HYDR)OXIDE BASED MATERIALS FOR FLUORIDE-IMPACTED DRINKING-WATER: BATCH AND COLUMN STUDIES

A DISSERTATION

SUBMITTED TO THE GRADUATE FACULTY

in partial fulfillment of the requirements for the

Degree of

DOCTOR OF PHILOSOPHY

By

JUNYI DU
Norman, Oklahoma
2016

NOVEL, LOW-COST ALUMINUM (HYDR)OXIDE BASED MATERIALS FOR FLUORIDE-IMPACTED DRINKING-WATER: BATCH AND COLUMN STUDIES

A DISSERTATION APPROVED FOR THE
SCHOOL OF CIVIL ENGINEERING AND ENVIRONMENTAL SCIENCE

BY

_____
Dr. Elizabeth Butler, Chair

_____
Dr. David Sabatini, Co-Chair

_____
Dr. Robert Nairn

_____
Dr. Tohren Kibbey

_____
Dr. Andrew Elwood Madden

DEDICATION

This dissertation is gratefully dedicated to my mother

Hongxia Zhang

And in memory of my late father

Xihua Du

My late grandmother *Huailan Li* and my late grandfather *Xikong Zhang*

Acknowledgements

It is impossible to write this dissertation without the tutoring of Dr. Elizabeth Butler and Dr. David Sabatini. I owe my deepest gratitude to them who have devoted plenty of time to mentoring me with their insightful comments and consistent encouragement.

I have been especially lucky to have Dr. Butler as my advisor who encouraged me to develop my own ideas and provided guidance whenever my research was struggled. Her meticulous attitude, thought-provoking comments as well as constructive criticisms brought me to a high research level and facilitated me to build solid skills of critical thinking and manuscript writing.

My advisor, Dr. David Sabatini, has been always patient to listen and give advice. I am thankful to him for the detailed reading and editing on numerous revisions of manuscripts. It is my fortune to work with Dr. Sabatini who introduced me to the field of water, health and sanitation for developing world and inspired me to think over water and environmental issues from a multidisciplinary perspective. With his guidance, I first time realized the necessity of considering sociocultural, economic, and political factors in dealing with practical environmental problems, and became aware of the effectiveness and importance of non-technological solutions such as social entrepreneurship to water treatment and supply. I am also deeply grateful to Dr. Sabatini and Mrs. Sabatini for all their encouragement, comfort, and home receptions during my Ph.D. study.

I am indebted to all my committee members, Dr. Tohren Kibbey, Dr. Robert Nairn, and Dr. Andrew Madden with whom I have interacted through classes and personal discussion. I warmly appreciate all the valuable concepts and ideas learned

from their lectures and seminar talks that help broaden my research scope and enrich my background in environmental modeling, ecological engineering, and mineralogy. I would like to acknowledge their time and effort spent on improving the quality of final dissertation. I am also thankful to my committee members for allowing me to use their laboratory equipment (peristaltic pump and light scattering detector from Dr. Kibbey's lab, muffle furnace in Dr. Nairn's lab) and giving me the access to characterization facilities (BET pore analyzer and XRD in Dr. Madden's lab).

I would like to give a special mention for Dr. Jim Chamberlain who taught me practical skills of water supply, disinfection, and well drilling and provided valuable suggestions for my research and studies. I have been always impressed and cheered by Jim's optimistic spirit and unwavering passion towards his work.

I am grateful to my fellow graduate students (Dr. Chodchanok Attaphong, Dr. Laura Brunson, Chris Cope, Dr. Linh Do, Dr. Lili Hou, Ying Lan, Anisha Nijhawan, Hayley Ryckman, and Teshome L. Yami) who give me various forms of assistance, support and encouragement. Whenever I need help, they are ready to reach out. I feel so lucky to have the opportunity to work with and learn from them during my Ph.D.

I would like to acknowledge many other people who give me a lot of help on my research and studies (CEES Staff: Audre Carter, Brenda Clouse, Ronald Conlon, Cindy Murphy, Mike Schmitz, Molly Smith, and Susan Williams; Dr. Mark Nanny—Nanopure water system, Dr. Zaman—muffle furnace, Dr. Preston Larson—SEM and EDS, Pritchet Brittany—XRD, Ibrahim Al-Habbo and Jessica Johnston—laboratory experiments, Angela Rodriguez—crucible making, and Leonard Flotz—kindly providing *Pinus patula*).

Many friends have given me unselfish help especially when I first came to the US and spoke very poor English. It is their support and care that helped me get through the adaptation period and adjust to a new country.

I am appreciative of Dr. Daishe Wu at Nanchang University and my relatives for their aid and encouragement throughout this endeavor. They have been a constant source of support, concern, comfort, and strength.

My cordial love and thanks are to my dear wife, Kangmei Zhao. I am blessed to have Kangmei as my companion, the best gift I have ever had in my life. Her support and concern helped me carry through my toughest time after my father's decease and recover from disappointment and agony. I greatly value her love and trust through these difficult times.

Most importantly, my deepest gratitude is to my parents to whom this dissertation is dedicated to. None of this work would have been possible without their sincere support, love and understanding. They sacrificed too much in support of my decision to study abroad. I often feel anxious and guilty whenever I compare my parents' sacrifice with my selfishness. Although I know whatever I have been doing cannot reciprocate their kindness, I hope to use this work to at least show that I am doing something good and will continue my work to benefit more people and to relay their love.

Finally, I would like to thank the financial support for my research from the National Science Foundation (NSF) (CBET-1066425), Oklahoma University Graduate Senate Research Grant, Oklahoma University Graduate College Research Grant, and WaTER Center.

Table of Contents

List of Tables

List of Figures

Abstract

Simple aluminum (hydr)oxides and layered double hydroxides were synthesized using common chemicals and equipment by varying synthesis temperature, concentrations of extra sulfate and citrate, and metal oxide amendments. Aluminum (hydr)oxide samples were aged at either 25 or 200 ^{o}C during synthesis and, in some cases, calcined at 600 ^{o}C. Despite yielding increased crystallinity and mineral phase changes, higher temperatures had a generally negative effect on fluoride adsorption. Addition of extra sulfate during synthesis of aluminum (hydr)oxides led to significantly higher fluoride adsorption capacity compared to aluminum (hydr)oxides prepared with extra citrate or no extra ligands. X-ray diffraction results suggest that extra sulfate led to the formation of both pseudoboehmite (γ-AlOOH) and basaluminite ($Al_4SO_4(OH)_{10}\cdot 4H_2O$) at 200 ^{o}C; energy dispersive X-ray spectroscopy confirmed the presence of sulfur in this solid. Treatment of aluminum (hydr)oxides with magnesium, manganese, and iron oxides did not significantly impact fluoride adsorption. While layered double hydroxides exhibited high maximum fluoride adsorption capacities compared to aluminum (hydr)oxides, their adsorption capacities at dissolved fluoride concentrations close to the World Health Organization drinking water guideline of 1.5 mg/L were much lower than those for the aluminum (hydr)oxides.

Molecular sieves and zeolites showed increased fluoride adsorption capacities when amended with aluminum (hydr)oxide (AlOOH). When normalized by the AlOOH content, the adsorption capacities of most amended molecular sieves were higher than the maximum theoretical value expected for monolayer surface coverage, suggesting fluoride removal from processes beyond adsorption, such as precipitation.

Although the mass-normalized adsorption capacities of most amended materials were less than that of an equivalent mass of pure AlOOH, several molecular sieves with pores of one to several nanometers showed mass-normalized adsorption capacities similar to pure AlOOH, possibly due to their larger pores, which may have facilitated fluoride adsorption after aluminum (hydr)oxide precipitation. Energy dispersive X-ray spectroscopy detected elevated fluorine in a representative AlOOH-amended molecular sieve after repeated fluoride adsorption, also consistent with fluoride uptake by processes beyond only monolayer coverage. Regeneration of the adsorbents with low-concentration sodium hydroxide solution led to partial recovery of the fluoride adsorption capacity, which decreased over the course of sequential adsorption batch experiments, possibly due to loss of aluminum.

Pure aluminum (hydr)oxide (AlOOH) and AlOOH-amended sodalite (prepared with 0.6 M aluminum chloride, 0.18-0.425 mm sodalite, and at pH 5.3) exhibited good performance in column fluoride removal in terms of service time (time until breakthrough), energy consumption, and cost. The long service time (1370 and 2000 bed volumes for AlOOH-amended sodalite and pure AlOOH, respectively) was primarily due to a large mass loading of AlOOH in amended materials when using small-size substrate zeolite and high aluminum concentration, and secondarily to the amorphous state of AlOOH formed at a slightly acidic pH (5.3). Column effluent water showed signs of aluminum leaching for the first 70 bed volumes due to the outflow of AlOOH particles. Once AlOOH particles smaller than 0.2 μm stopped exiting the column, the effluent aluminum concentration stayed below 0.2 mg/L, from 70 bed volumes to breakthrough. However, aluminum concentrations increased after

breakthrough; this was attributed to fluoride-induced AlOOH dissolution and formation of aqueous aluminum-fluoride complex. There was no significant reduction of fluoride removal capacity from competing solutes (bicarbonate, silicate, sulfate, and pyromellitic acid) present at five times higher concentration than the fluoride content. The estimated energy requirement of 2.13×10^{-4} and 0.011 kWh/m^3 treated water for household and community-scale filters is much lower than the energy consumption of electrocoagulation (10.8 kWh/m^3) and reverse osmosis (5 kWh/m^3), and is favorable for the practical use of these materials. In the absence of continuous power supply, hydrostatic energy can be used to run the community-scale filter using an elevated water tank about four meters above the ground. The cost advantage ($0.97 and $1.05 per cubic meters of treated water for producing pure AlOOH and amended sodalite) makes these materials appealing to developing regions compared to the production cost of activated alumina ($2.94/$m^3$ treated water). The cost can be further decreased by using aluminum sulfate during amendment or reusing adsorbents after one cycle of regeneration with 0.01 M sodium hydroxide.

Chapter 1 : Introduction

Motivation of the Research

Fluoride, a naturally occurring element in the environment, is beneficial to the growth of human teeth when present at a low concentration but is harmful to human health at an elevated level (Edmunds and Smedley 2013). When consuming drinking-water with fluoride concentration between 1.5 and 4.0 mg/L, dental fluorosis occurs with symptoms of teeth mottling and embrittlement (Mohapatra et al. 2009). With prolonged exposure at fluoride concentration of 4.0 to 10.0 mg/L, skeletal fluorosis occurs as manifested by densification and embrittlement of bones (Mohapatra et al. 2009). Excessive intake of drinking water with fluoride concentration above 10 mg/L, skeletal fluorosis progresses to crippling fluorosis with spine and joints deformities and physical disability (Ozsvath 2009). Aside from health impacts, effects of fluorosis include impairment of self-dignity and reduction in economic income due to the change in appearance and loss in physical ability (Hobdell et al. 2003), particularly for the people living in emerging regions with limited coverage of medical care and a low income levels. Therefore, fluoride removal from drinking water is imperative to mitigate the fluorosis problem.

This study focused on drinking-water fluoride mitigation for endemic fluorosis areas. Impacted by igneous bedrocks originating from volcanic activities, many endemic fluorosis areas, such as the Rift Valley in Ethiopia (Haimanot et al. 1987) and Northern Rajasthan State in India (Suthar et al. 2008), have drinking water fluoride concentrations ranging from 2 mg/L in groundwater wells to 200 mg/L in lakes (Tekle-Haimanot et al. 2006, Suthar et al. 2008, Rango et al. 2010), far above the fluoride level

(1.5 mg/L) recommended by the World Health Organization for drinking water. These areas are also densely populated regions; Amalraj and Pius (2013) estimated that more than 200 million residents are threatened by fluorosis. Even worse, most of the residents in these areas facing the risk of fluoride-contaminated drinking water live on an income lower than the extreme poverty line set by the World Bank, i.e. $1.90 per day (Wondwossen et al. 2006, Saravanan et al. 2008, Chen et al. 2013, Firempong et al. 2013). The high rate of illiteracy in many developing countries, e.g., estimated to be 61% in Ethiopia and 31% in India (UNICEF 2015), exacerbates the difficulty for fluorosis prevention. It would be arduous for fluoride treatment professionals to teach less-educated communities the complex knowledge about fluoride chemistry and train them to use sophisticated techniques such as reverse osmosis. As a result, to be compatible with local economic and educational levels, it is necessary to design fluoride-removal techniques that can be affordable to and simply operated by such communities.

Currently, a number of fluoride-removal technologies have been implemented in fluorosis areas, such as adsorption, precipitation, electrocoagulation, and membrane filtration (Meenakshi and Maheshwari 2006). Nevertheless, many of these techniques fail to provide a long-term service as they are constrained by inefficient fluoride removal capacity, generation of a large amount of waste, or prohibitive cost in energy consumption and materials procurement (Mohapatra et al. 2009). Among all candidate techniques, adsorption is efficient, economical and free of sophisticated operational skills (Feenstra et al. 2007). It is usually conducted in columns packed with adsorbents through which fluoride-contaminated water is infiltrated (Feenstra et al. 2007). When

using this technique, adsorbent is the most critical component with its performance dictating the efficiency of fluoride removal; consequently a wide variety of adsorbents originating from industrial products or natural materials have been developed and applied in practice such as bone char, hydroxyapatite, and clay minerals (Bhatnagar et al. 2011). Within all available materials aluminum (hydr)oxides (AlOOH) are among the most effective materials (Bhatnagar et al. 2011). AlOOH consists of a group of materials precipitated from aluminum (hydr)oxide colloids and post-treated by dewatering or calcination (Wefers and Misra 1987). AlOOH has promising fluoride removal capacity which could be ascribed to the high affinity between aluminum and fluoride (Wu et al. 2007).

Designed to reduce the cost, AlOOH with high fluoride binding affinities can also be loaded on low-cost substrate materials. To date, numerous efforts have been made to treat different types of substrate materials with AlOOH (Jagtap et al. 2011, Tomar and Kumar 2013) such as wood char (Brunson and Sabatini 2015), resins (Luo and Inoue 2004), and clay (Agarwal et al. 2003). However, these efforts are typically constrained by low aluminum loading in the amended materials (Agarwal et al. 2003, Brunson and Sabatini 2015) and limited availability of commercial substrate materials, e.g., ion-exchange resins (Luo and Inoue 2004), in endemic fluorosis areas, particularly of developing countries.

There is still a knowledge gap in the mineral phases and surface chemistry of AlOOH related to fluoride adsorption. As a result, this dissertation endeavors to bridge this gap by studying the relationship between AlOOH speciation and fluoride adsorption, as well as to develop cost-effective fluoride removal materials based on

inexpensive substrate material and simple chemicals available to most endemic fluorosis areas.

In general, the overall objective of this dissertation was to develop economical fluoride removal materials and adsorption techniques for endemic fluorosis areas, especially those in developing countries. To accomplish this objective, detailed tasks, methods and results are elaborated in the following three chapters, i.e., the low-cost synthesis of AlOOH by changing the temperature and composition of colloidal systems (Chapter Two), preparation of AlOOH-modified materials with various cheap and locally available substrate materials (Chapter Three), and evaluation of AlOOH and AlOOH-amended zeolites in fluoride treatment with column filtration with respect to fluoride adsorption capacity, energy consumption and cost (Chapter Four). The dissertation is closed with a final chapter (except the Supporting Information), general conclusions and recommendations for future research and practice (Chapter Five). Below is the brief introduction to following chapters.

Chapter Two: Aluminum (Hydr)oxides Based Minerals

Aluminum (hydr)oxide based minerals are among the best performing fluoride removal materials with their high fluoride removal capacity (Bhatnagar et al. 2011) and specificity to fluoride (Chauhan et al. 2007). The good performance of AlOOH can be attributed to the high affinity of aluminum to fluoride (Wu et al. 2007), which was evidenced by a positive correlation between aluminum content and fluoride removal amount in AlOOH based materials (Bower and Hatcher 1967, Ganvir and Das 2011, Xie et al. 2001). This can be further evidenced by higher complexation coefficients

between fluoride and aluminum (e.g., $Al^{3+} + 2\ F^- = AlF_2^+$ log K = 12.6) compared to iron (e.g., $Fe^{3+} + 2\ F^- = FeF_3^+$ log K = 10.7) or lanthanum (e.g., $La^{3+} + 2\ F^- = LaF_2^+$ log K = 3.6) (Smith and Martell 2004).

Conventionally, activated alumina is the most widely used AlOOH based mineral for drinking-water fluoride treatment around the world (Fawell et al. 2006, Onyango and Matsuda 2006); nonetheless it may be an inappropriate choice for many developing regions due to its limited capacity (Ghorai and Pant 2005) and high cost (Kasprzyk-Hordern 2004). Therefore, researchers began exploring the potential of other AlOOH materials in fluoride removal to replace activated alumina. Varying synthesis conditions (e.g., temperature, pressure, and aging time) is a common approach employed by researchers to produce innovative AlOOH with an improved fluoride removal capacity (Pietrelli 2005, Shimelis et al. 2006, Wang et al. 2009, Kumar et al. 2011). As formed under diverse conditions including various synthesis temperature and pressure, aging time and calcination temperature, a wide range of properties including crystallinity, particle size, surface area, and surface charge have been reported for AlOOH (Wefers and Misra 1987, Kosmulski 2009). In an attempt to link these properties to fluoride removal, it is found that fluoride removal capacity was dependent on the surface charge (surface potential) and surface area (particle size) of AlOOH (James et al. 2005, Liu et al. 2011). High surface charge and a larger surface area (smaller particle size) often corresponded to an increased fluoride removal capacity (James et al. 2005, Liu et al. 2011). In practice, there are many ways to control the surface area (particle size) and surface charge for AlOOH by tuning synthesis pH, temperature and pressure to appropriate levels by use of autoclaves (Watanabe et al.

2002, Liu et al. 2008, Liu et al. 2011). However, considering the scarcity of pressurized equipment and limited access to energy service in developing regions, it is not easy in these settings to control temperature and pressure for a large surface area and reduced particle size.

Alternatively, the same result (a large surface area and reduced particle size) could be attained by addition of extra ligands (e.g., sulfate and citric acid) under room temperature and ambient pressure. The added ligands can bind with aluminum and impede the crystallization of AlOOH (Violante and Huang 1984, Violante and Huang 1993). Concomitantly, a mineral phase, pseudoboehmite, could form in this process with amorphous crystal structure and a small particle size (Violante and Huang 1984). The produced pseudoboehmite phase upon the addition of ligands remained amorphous and did not transform to other AlOOH minerals with extending aging time (Violante and Huang 1984). Nevertheless, the selection of the type and concentration of ligands must be made carefully for two reasons. First, the aluminum complexation constant and concentration of ligands were shown to affect the speed of AlOOH crystallization (Violante and Huang 1984, Violante and Huang 1993). And second, the ligands with high aluminum complexation constant and of elevated concentration might form tight bond with AlOOH during synthesis and compete with fluoride for binding sites during adsorption.

In addition to the adjustment of crystallinity and particle size, metal doping is another possible way to increase fluoride adsorption. Exchange between fluoride and surface hydroxyl groups could be promoted through crystal lattice distortion and bond weakening between aluminum and hydroxyl groups (Martínez and McBride 2000,

Gaudry et al. 2003). There are two kinds of doping methods which differ in the time when extra metal is added, i.e. during synthesis and after synthesis. The preparation of layered double hydroxides (LDH) can be considered as an example of in-synthesis metal doping. By mixing aluminum with magnesium in a solution, an LDH mineral of a special layered structure with anions intercalated in interlayer space can be produced (Maliyekkal et al. 2006, Lv 2007). These interspace anions are exchangeable with fluoride and served as a complement to surface aluminum sites for fluoride removal (Maliyekkal et al. 2006, Lv 2007). The second type of metal-doping mainly refers to the coating of metal oxides on synthesized AlOOH. Examples using this type of metal-doping such as preparations of magnesia-coated activated alumina (Maliyekkal et al. 2008) and lanthanum-modified activated alumina (Cheng et al. 2014) can be found in literature. It was shown that the coated metal oxides could increase the pH_{PZC} (or zeta potential at a given pH) (Maliyekkal et al. 2008, Cheng et al. 2014) compared to the original activated alumina which might help enhance the fluoride removal capacity.

In short, the task of Chapter Two was to develop efficient AlOOH-based minerals including pure AlOOH, Mg-Al layered double hydroxides, and metal oxides impregnated AlOOH for fluoride treatment with inexpensive chemicals (such as aluminum salts and caustic soda) and normal temperature and pressure.

Chapter Three: Aluminum (Hydr)oxides Amended Materials and Their Regeneration

Despite its good fluoride removal efficiency, pure AlOOH also has some limitations. First, because of small particle size, pure AlOOH is prone to cause a high head loss

during column operation (Wasay et al. 1996). In order to improve the hydraulic performance and adapt the use of AlOOH to developing countries, indigenous or low-cost materials were employed as supporting substrates for AlOOH. With favorable mechanical strength and a large particle size these substrate materials are expected to provide a firm anchorage for AlOOH and at the same time reduce the head loss. Substrate materials such as char and silica sand have been used in the amendment with aluminum and showed an improved fluoride removal capacity relative to their parent materials (Ramos et al. 1999, Brunson and Sabatini 2009, Tchomgui-Kamga et al. 2010).

For an ideal substrate for fluoride removal, it is desirable to have a large surface area and ample accessible pore volume. Biochar and molecular sieves fall into this category owing to their particular porous structure and vast internal volume. In endemic fluorosis areas, there are abundant resources that can be exploited to obtain biochar and zeolites. To name a few, eucalyptus is a common plant and a popular material in the Rift Valley to make wood char (Jagger and Pender 2003). The pine species *Pinus patula*, which is an invasive species for Ethiopia, is also widely-spread in the Rift Valley so that can be used as the raw material for wood char production (Yirdaw 2001). Zeolites are widely-distributed, naturally occurring minerals available in many endemic fluorosis areas, e.g., sodalite contained in bedrock outcrops has been identified in the Chacopampean plain in Argentina **(**Gomez et al. 2008**)**, thus opening the door for the use of zeolites as substrate materials.

Therefore, task one of Chapter Three was to precipitate AlOOH on wood char, zeolites, and other substrate materials that are frequently applied in water treatment

including fibrous materials (cellulose, steel wool, and glass wool), wood char, and various resins at different aluminum concentrations and pH values. The substrate materials which showed the highest fluoride removal capacity after AlOOH amendment were selected for following studies. In addition, fluoride removal capacity appeared to be a function of pH used to prepare AlOOH precipitate (Gong et al. 2012). Amorphous AlOOH with high fluoride removal capacity formed at slightly acidic pH values (e.g., pH 5) compared to more crystalline AlOOH (boehmite and bayerite) precipitated at basic pH values (e.g., pH 9) with relatively lower defluoridation capacity (Gong et al. 2012). Thus, effects of the pH values as well as aluminum concentrations used in AlOOH precipitation on fluoride removal capacity of AlOOH-amended materials were also examined.

Upon the selection of well-performing AlOOH-amended materials, reusability was investigated. Reusability of an adsorbent is generally described as the ability of the adsorbent to maintain significant adsorption capacity during repeated uses (Yokoi et al. 2004, Chularueangaksorn et al. 2013). A reusable adsorbent is always desirable as it can minimize the required amount of material and save the cost of operation. Experimentally, how much adsorption capacity is recovered each time after regeneration is a good measurement of the reusability of adsorbents (Chularueangaksorn et al. 2013, Yokoi et al. 2004).

A number of regeneration methods for AlOOH-based adsorbents have been discussed (Ghorai and Pant 2004, Ghorai and Pant 2005, Tripathy et al. 2006, Mohapatra et al. 2009), of which sodium hydroxide is viewed as the most efficient regenerant. With size approximate to the diameter of fluoride ion, hydroxide could

exchange with the fluoride previously adsorbed to surface (Maliyekkal et al. 2008). It was also observed that a higher sodium hydroxide concentration was conducive to fluoride desorption (Maliyekkal et al. 2008). However, concentrated sodium hydroxide (e.g., > 0.1 M) may dissolve AlOOH with concurrent release of aluminum (Panias et al. 2001, Abelló et al. 2009). This was illustrated by Panias et al. (2001) that the dissolution rate of aluminum was correlated to the concentration of sodium hydroxide. Other than sodium hydroxide, assorted regenerants such as aluminum sulfate and sodium chloride have also been applied in the regeneration of AlOOH-based adsorbents, yet their reported regeneration ability differed significantly and was generally inferior to sodium hydroxide (Boruff 1934, Wu et al. 2007).

Task two of Chapter Three was the regeneration of best-performing AlOOH-amended materials selected in the first task. The optimum regenerant and its concentration were determined by comparing the fluoride removal capacity after the regeneration batch when using different solutes. Fluoride adsorption isotherms of materials after each regeneration batch were plotted to illustrate the reusability of materials over a broad initial concentration range.

Chapter Four: Evaluation of AlOOH and AlOOH-amended zeolites performance in Fluoride Treatment using Column Filtration

Chapter Four focused on practical aspects such as a column setup similar to the packed filters. The column performance of AlOOH and AlOOH-amended zeolites for fluoride treatment was evaluated. Column experiments are an indispensable step to fill the gap between batch experiments and field implementations. Fluoride removal

capacity of materials determined in column experiments is similar to the capacity in large-scale filters due to the resemblance in rates of surface diffusion, advective and dispersive transport and intra-particle mass transfer of fluoride between small and large columns (Crittenden et al. 1986). The first objective of this chapter was to evaluate the performance of AlOOH and AlOOH-amended zeolites in column fluoride adsorption. Criteria encompassing service time (fluoride removal capacity), energy consumption, and material production cost were employed in the appraisal of materials for drinking-water fluoride treatment.

For filtration techniques, energy is mainly consumed to compensate for the head loss across the packed adsorbents during water flow through (Stephens et al. 2010). Hence, as an indicator for energy consumption, head loss across the column over the course of operation was tracked by monitoring the backpressure at the column inlet.

To identify limiting factors for column performance, effects of pH of AlOOH precipitation, aluminum concentrations, and substrate size on fluoride removal capacity and backpressure were examined. Parameters such as fluoride concentration, pH, and flow rate of inlet water were maintained constant such that the column performance of different materials could be compared on the basis of common operational conditions. In column studies, fluoride concentration and pH values were used that are representative of those found in the natural groundwater.

For column defluoridation with AlOOH, there are often concerns about competitive adsorption and aluminum leaching. In natural groundwater, there exist many solutes that may compete with fluoride adsorption (Tang et al. 2009). Because of their high concentrations and valence, these solutes such as phosphate and silicate may

compete with fluoride for the accessible adsorption sites on the surface of adsorbents (Cai et al. 2012, Sujana et al. 1998). Aluminum leaching is another potential risk to cause damage to human neural system and bones (Boegman and Bates 1984). Considering the potential health risk associated with aluminum leaching and the high cost to reduce the effluent aluminum concentration to a very low value when using AlOOH-based minerals in water treatment, a level for aluminum in drinking water at 0.2 mg/L is recommended by the World Health Organization (2004). Moreover, AlOOH is more susceptible to dissolution in fluoride-containing solution as the attachment of fluoride to material surface weakened aluminum-oxygen bond and made it liable to break (Phillips et al. 1997). Despite this fact, the pattern of aluminum release in column fluoride removal is rarely studied. As a result, it is necessary to check effluent aluminum concentrations periodically to delineate the aluminum release pattern over column adsorption. Thus, the final objective of Chapter Four was to look into the competing effect exerted by common groundwater solutes (sulfate, bicarbonate, silicate, pyromellitic acid used as a surrogate for natural organic matter) and the potential aluminum leaching when using pure AlOOH and AlOOH-amended zeolite.

Chapter Five: Conclusions and Recommendations

In the final chapter, overall conclusions summarizing the key findings in previous chapters are given to reiterate the critical factors that affect AlOOH precipitation and fluoride removal and to offer guidance to the practical use of AlOOH-amended zeolites in the field. Recommendations for future research and practice are also provided which relate to the process of fluoride removal by AlOOH and practical issues that need to pay

attention to other than material preparation in drinking-water fluoride treatment especially in developing countries.

References

Abelló, S., Bonilla, A. and Pérez-Ramírez, J. (2009). "Mesoporous ZSM-5 zeolite catalysts prepared by desilication with organic hydroxides and comparison with NaOH leaching." Appl. Catal. A-Gen. 364(1-2): 191-198.

Agarwal, M., Rai, K., Shrivastav, R. and Dass, S. (2003). "Deflouridation of water using amended clay." J. Clean. Prod. 11(4): 439-444.

Amalraj, A. and Pius, A. (2013). "Health risk from fluoride exposure of a population in selected areas of Tamil Nadu South India." Food Science and Human Wellness 2(2): 75-86.

Bhatnagar, A., Kumar, E. and Sillanpää, M. (2011). "Fluoride removal from water by adsorption—A review." Chem. Eng. J. 171(3): 811-840.

Boegman, R. J. and Bates, L. A. (1984). "Neurotoxicity of aluminum." Can. J. Physiol. Pharm. 62(8): 1010-1014.

Boruff, C. S. (1934). "Removal of fluorides from drinking waters." Ind. Eng. Chem. 26(1): 69-71.

Bower, C. A. and Hatcher, J. T. (1967). "Adsorption of fluoride by soils and minerals." Soil Sci. 103(3): 151-154.

Brunson, L. R. and Sabatini, D. A. (2009). "An evaluation of fish bone char as an appropriate arsenic and fluoride removal technology for emerging regions." Environ. Eng. Sci. 26(12): 1777-1784.

Brunson, L. R. and Sabatini, D. A. (2015). "Role of surface area and surface chemistry during an investigation of eucalyptus wood char for fluoride adsorption from drinking water." J. Environ. Engi. 141(2): 04014060.

Cai, P., Zheng, H., Wang, C., Ma, H., Hu, J., Pu, Y. and Liang, P. (2012). "Competitive adsorption characteristics of fluoride and phosphate on calcined Mg-Al-CO_3 layered double hydroxides." J. Hazard. Mater. 213-214: 100-108.

Chen, S., Li, B., Lin, S., Huang, Y., Zhao, X., Zhang, M., Xia, Y., Fang, X., Wang, J., Hwang, S. A. and Yu, S. (2013). “Change of urinary fluoride and bone metabolism indicators in the endemic fluorosis areas of southern China after supplying low fluoride public water." BMC Public Health 13(1): 1-10.

Cheng, J., Meng, X., Jing, C. and Hao, J. (2014). “La^{3+}-modified activated alumina for fluoride removal from water." J. Hazard. Mater. 278: 343-349.

Chularueangaksorn, P., Tanaka, S., Fujii, S. and Kunacheva, C. (2013). “Regeneration and reusability of anion exchange resin used in perfluorooctane sulfonate removal by batch experiments." J. App. Polym. Sci. 130(2): 884-890.

Crittenden, J. C., Berrigan, J. K. and Hand, D. W. (1986). “Design of rapid small-scale adsorption tests for a constant diffusivity." J.Water Pollut. Con. F. 58(4): 312-319.

Edmunds, W. M. and Smedley, P. (2013). Fluoride in natural waters. In: O. Selinus (ed.) *Essentials of Medical Geology*. Springer Netherlands: 311-336.

Fawell, J., Bailey, K., Chilton, J., Dahi, E., Fewtrell, L. and Magara, Y. (2013). “Fluoride in drinking-water." Water Intelligence Online 12: 9781780405803.

Feenstra, L., Vasak, L. and Griffioen, J. (2007). “Fluoride in groundwater: Overview and evaluation of removal methods." International Groundwater Reservation Assessment Center, Report no. SP 1.

Firempong, C. K., Nsiah, K., Awunyo-Vitor, D. and Dongsogo, J. (2013). "Soluble fluoride levels in drinking water-a major risk factor of dental fluorosis among children in Bongo community of Ghana." Ghana Medical Journal 47(1): 16-23.

Ganvir, V. and Das, K. (2011). “Removal of fluoride from drinking water using aluminum hydroxide coated rice husk ash." J. Hazard. Mater. 185(2-3): 1287-1294.

Gaudry, E., Kiratisin, A., Sainctavit, P., Brouder, C., Mauri, F., Ramos, A., Rogalev, A. and Goulon, J. (2003). “Structural and electronic relaxations around substitutional Cr^{3+} and Fe^{3+} ions in corundum." Phys. Rev. B 67(9): 094108.

Ghorai, S. and Pant, K. (2004). “Investigations on the column performance of fluoride adsorption by activated alumina in a fixed-bed." Chem. Eng. J. 98: 165-173.

Ghorai, S. and Pant, K. (2005). “Equilibrium, kinetics and breakthrough studies for adsorption of fluoride on activated alumina." Sep. Purif. Technol. 42: 265 - 271.

Gomez, M. L., Blarasin, M. T. and Martínez D. E. (2009). “Arsenic and fluoride in a loess aquifer in the central area of Argentina." Environ. Geol. 57(1), 143-155.

Gong, W.-X., Qu, J.-H., Liu, R.-P. and Lan, H.-C. (2012). “Adsorption of fluoride onto different types of aluminas." Chem. Eng. J. 189-190(0): 126-133.

Haimanot, R. T., Fekadu, A. and Bushra, B. (1987). “Endemic fluorosis in the Ethiopian Rift Valley." Trop. Geogr. Med. 39(3): 209-217.

Ho, T.-L. (1975). “Hard soft acids bases (HSAB) principle and organic chemistry." Chem. Rev. 75(1): 1-20.

Hobdell, M., Petersen, P. E., Clarkson, J. and Johnson, N. (2003). “Global goals for oral health 2020." Int. Dent. J. 53(5): 285-288.

Jagger, P. and Pender, J. (2003). “The role of trees for sustainable management of less-favored lands: the case of eucalyptus in Ethiopia." Forest Policy Econ. 5(1): 83-95.

Jagtap, S., Yenkie, M., Das, S. and Rayalu, S. (2011). “Synthesis and characterization of lanthanum impregnated chitosan flakes fopr fluoride removal in water." Desalination 273: 267-275.

James, G., Sabatini, D. A., Chiou, C. T., Rutherford, D., Scott, A. C. and Karapanagioti, H. K. (2005). “Evaluating phenanthrene sorption on various wood chars." Water Res. 39(4): 549-558.

Kasprzyk-Hordern, B., Raczyk-Stanisławiak, U., Świetlik, J. and Nawrocki, J. (2006). “Catalytic ozonation of natural organic matter on alumina." Appl. Catal. B-Environ. 62(3): 345-358.

Kosmulski, M. (2009). “Compilation of PZC and IEP of sparingly soluble metal oxides and hydroxides from literature." Adv. Colloid Interfac. 152(1-2): 14-25.

Kumar, E., Bhatnagar, A., Kumar, U. and Sillanpää, M. (2011). “Defluoridation from aqueous solutions by nano-alumina: characterization and sorption studies." J. Hazard. Mater. 186(2): 1042-1049.

Liu, R., Gong, W., Lan, H., Gao, Y., Liu, H. and Qu, J. (2011). “Defluoridation by freshly prepared aluminum hydroxides." Chem. Eng. J. 175: 144-149.

Liu, Y., Ma, D., Han, X., Bao, X., Frandsen, W., Wang, D. and Su, D. (2008). “Hydrothermal synthesis of microscale boehmite and gamma nanoleaves alumina." Mater. Lett. 62: 5.

Luo, F. and Inoue, K. (2004). “The removal of fluoride ion by using metal(III)-loaded amberlite resins." Solvent Extr. Ion Exc. 22(2): 305-322.

Lv, L. (2007). “Defluoridation of drinking water by calcined MgAl-CO_3 layered double hydroxides." Desalination 208(1-3): 125-133.

Maliyekkal, S. M., Sharma, A. K. and Philip, L. (2006). “Manganese-oxide-coated alumina: A promising sorbent for defluoridation of water." Water Rese. 40(19): 3497-3506.

Maliyekkal, S. M., Shukla, S., Philip, L. and Nambi, I. M. (2008). “Enhanced fluoride removal from drinking water by magnesia-amended activated alumina granules." Chem. Eng. J. 140(1-3): 183-192.

Martínez, C. E. and McBride, M. B. (2000). “Aging of coprecipitated Cu in alumina: changes in structural location, chemical form, and solubility." Geochim. Cosmochim. Ac. 64(10): 1729-1736.

Maheshwari and Maheshwari R. C. (2006). “Fluoride in drinking water and its removal." J. Hazard. Mater. 137(1): 456-463.

Mohapatra, M., Anand, S., Mishra, B., Giles, D. and Singh, P. (2009). “Review of fluoride removal from drinking water." J. Environ. Manage. 91: 67-77.

Onyango, M. S., Kojima, Y., Aoyi, O., Bernardo, E. C. and Matsuda, H. (2004). “Adsorption equilibrium modeling and solution chemistry dependence of fluoride removal from water by trivalent-cation-exchanged zeolite F-9." J. Colloid Interf. Sci. 279(2): 341-350.

Ozsvath, D. (2009). “Fluoride and environmental health: a review." Rev. Environ. Sci. Biotechnol. 8(1): 59-79.

Panias, D., Asimidis, P. and Paspaliaris, I. (2001). “Solubility of boehmite in concentrated sodium hydroxide solutions: model development and assessment." Hydrometallurgy 59(1): 15-29.

Pietrelli, L. (2005). “Fluoride wastewater treatment by adsorption onto metallurgical grade alumina." Ann. Chim.-Rome 95(5): 303-312.

Phillips, B. L., Casey, W. H. and Crawford, S. N. (1997). “Solvent exchange in $AlF_x(H_2O)_{6-x}^{3-x}$ (aq) complexes: Ligand-directed labilization of water as an analogue for ligand-induced dissolution of oxide minerals." Geochim. Cosmochim. Ac. 61(15): 3041-3049.

Ramos, R. L., Ovalle-Turrubiartes, J. and Sanchez-Castillo, M. A. (1999). “Adsorption of fluoride from aqueous solution on aluminum-impregnated carbon." Carbon 37: 609-617.

Rango, T., Bianchini, G., Beccaluva, L. and Tassinari, R. (2010). “Geochemistry and water quality assessment of central Main Ethiopian Rift natural waters with emphasis on source and occurrence of fluoride and arsenic." J. Afr. Earth Sci. 57(5): 479-491.

Saravanan, S., Kalyani, C., Vijayarani, M. P., Jayakodi, P., Felix, A. J. W., Nagarajan, S., Arunmozhi, P. and Krishnan, V. (2008). “Prevalence of dental fluorosis among primary school children in rural areas of Chidambaram Taluk, Cuddalore District, Tamil Nadu, India." Indian Journal of Community Medicine 33(3): 146-150.

Shimelis, B., Zewge, F. and Chandravanshi, B. S. (2006). “Removal of excess fluoride from water by aluminum hydroxide." B. Chem. Soc. Ethiopia 20(1): 17-34.

Smith R. M. and Martell A. E. (2004). "NIST Critically Selected Stability Constants of Metal Complexes Databases" in NIST Chemistry WebBook, NIST Standard Reference Database Number 46, Eds. P.J. Linstrom and W.G. Mallard, National Institute of Standards and Technology, Gaithersburg MD, 20899, http://webbook.nist.gov, (retrieved April 19, 2016).

Stephens, B., Novoselac, A. and Siegel, J. A. (2010). “The effects of filtration on pressure drop and energy consumption in residential HVAC systems (RP-1299)." HVAC&R Res. 16(3): 273-294.

Sujana, M. G., Thakur, R. S. and Rao, S. B. (1998). “Removal of fluoride from aqueous solution by using alum sludge." J. Colloid Interf. Sci. 206(1): 94-101.

Sun, Z.-X., Zheng, T.-T., Bo, Q.-B., Du, M. and Forsling, W. (2008). “Effects of calcination temperature on the pore size and wall crystalline structure of mesoporous alumina." J. Colloid Interf. Sci. 319(1): 247-251.

Suthar, S., Garg, V. K., Jangir, S., Kaur, S., Goswami, N. and Singh, S. (2008). “Fluoride contamination in drinking water in rural habitations of Northern Rajasthan, India." Environ. Monit. Assess. 145(1-3): 1-6.

Tang, Y., Guan, X., Su, T., Gao, N. and Wang, J. (2009). “Fluoride adsorption onto activated alumina: Modeling the effects of pH and some competing ions." Colloid Surfaces A 337(1-3): 33-38.

Tchomgui-Kamga, E., Alonzo, V., Nanseu-Njiki, C. P., Audebrand, N., Ngameni, E. and Darchen, A. (2010). “Preparation and characterization of charcoals that contain dispersed aluminum oxide as adsorbents for removal of fluoride from drinking water." Carbon 48(2): 333-343.

Tekle-Haimanot, R., Melaku, Z., Kloos, H., Reimann, C., Fantaye, W., Zerihun, L. and Bjorvatn, K. (2006). “The geographic distribution of fluoride in surface and groundwater in Ethiopia with an emphasis on the Rift Valley." Sci. Total Environ. 367(1): 182-190.

Tomar, V. and Kumar, D. (2013). “A critical study on efficiency of different materials for fluoride removal from aqueous media." Chem. Cent. J. 7(1): 51.

Tripathy, S., Bersillon, J. and Gopal, K. (2006). “Removal of fluoride from drinking water by adsorption onto alum-impregnated activated alumina." Sep. Purif. Technol. 50: 310-317.

UNICEF (2015). The State of The World's Children 2015 Country Statistics.

Violante, A. and Huang, P. M. (1984). “Nature and properties of pseudoboehmites formed in the presence of organic and inorganic ligands." Soil Sci. Am. J. 48(5): 9.

Violante, A. and Huang, P. M. (1993). “Formation mechanism of aluminum hydroxide polymorphs." Clay Clay Miner. 41(5): 590-597.

Wang, S. G., Ma, Y., Shi, Y. J. and Gong, W. X. (2009). “Defluoridation performance and mechanism of nano-scale aluminum oxide hydroxide in aqueous solution." J. Chem. Technol. Biot. 84(7): 1043-1050.

Wasay, S. A., Haran, M. J. and Tokunaga, S. (1996). “Adsorption of fluoride, phosphate, and arsenate ions on lanthanum-impregnated silica gel." Water Environ. Res. 68(3): 295-300.

Watanabe, Y., Yamada, H., Kasama, T., Tanaka, J., Komatsu, Y. and Moriyoshi, Y. (2002). "Adsorption behavior of phosphorus on synthetic boehmites." Proceedings of The 19th International Japan-Korea Seminar on Ceramics 80-84.

Wefers, K. and Misra, C. (1987). “Oxides and hydroxides of aluminum." Alcoa Laboratories

Wondwossen, F., Åstrøm, A. N., Bjorvatn, K. and Bårdsen, A. (2006). “Sociodemographic and behavioural correlates of severe dental fluorosis." Int. J. Paediatr. Dent. 16(2): 95-103.

World Health Organization (2004). Guidelines for drinking-water quality: recommendations (Vol. 1). World Health Organization.

Wu, X., Zhang, Y., Dou, X. and Yang, M. (2007). “Fluoride removal performance of a novel Fe-Al-Ce trimetal oxide adsorbent." Chemosphere 69(11): 1758-1764.

Xie, Z. M., Ye, Z. H. and Wong, M. H. (2001). “Distribution characteristics of fluoride and aluminum in soil profiles of an abandoned tea plantation and their uptake by six woody species." Environ. Int. 26(5-6): 341-346.

Yirdaw, E. (2001). “Diversity of naturally-regenerated native woody species in forest plantations in the Ethiopian highlands." New Forest. 22(3): 159-177.

Yokoi, T., Tatsumi, T. and Yoshitake, H. (2004). "Fe^{3+} coordinated to amino-functionalized MCM-41: an adsorbent for the toxic oxyanions with high capacity, resistibility to inhibiting anions, and reusability after a simple treatment." J. Colloid Interf. Sci. 274(2): 451-457.

Chapter 2 : Synthesis, characterization, and evaluation of simple aluminum-based adsorbents for fluoride removal from drinking water[1]

Introduction

Fluoride in drinking water is a pressing global issue as it can cause dental and skeletal fluorosis when present at levels above the World Health Organization (WHO) drinking water guideline of 1.5 mg/L (World Health Organization). As a result, there is a need for efficient fluoride removal technologies that can be applied in drinking water systems around the world. Among candidate technologies, adsorption is efficient, economical, and suitable for household use (Ayoob et al. 2008), and activated alumina is a widely used adsorbent for this purpose (Fawell et al. 2006, Onyango et al. 2006). However, the high cost of activated alumina, due primarily to the significant energy required for its manufacture from bauxite ore (Kasprzyk-Hordern 2004), limits its application in less developed countries. Aluminum (hydr)oxide-based sorbents that can be synthesized under lower energy conditions may be promising for treatment of fluoride contaminated water (Gong et al. 2012, Jain and Jayaram 2009, Jiménez-Becerril et al. 2012, Liu et al. 2011, Shimelis et al. 2006). In some cases, amendment of these sorbents with the (hydr)oxides of iron (Dhiman and Chaudhuri 2007, Kuriakose et al. 2004), magnesium (Maliyekkal et al. 2008), or manganese (Dhiman and Chaudhuri 2007, Maliyekkal et al. 2006, Teng et al. 2009) has been shown to increase fluoride (Maliyekkal et al. 2006, Maliyekkal et al. 2008) and arsenic (Kuriakose et al. 2004) adsorption capacities under favorable pH conditions (Maliyekkal et al. 2006), perhaps due to small increases in the

[1] This chapter is published in Chemosphere (Du, J., Sabatini, D. A. and Butler, E. C., 2014. Synthesis, characterization, and evaluation of simple aluminum-based adsorbents for fluoride removal from drinking water. Chemosphere, 101, 21-27.). Copyright (2014) Elsevier. Reuse with permission from Elsevier.

pH point of zero charge (pH_{pzc}) (Dhiman and Chaudhuri 2007) and/or adsorption affinity (Kuriakose et al. 2004, Maliyekkal et al. 2006). Layered double hydroxides (LDHs), consisting of alternating layers of hydroxides of mixed metals (e.g., Mg-Al and Zn-Al), intercalated with exchangeable anions (including carbonate and chloride), have also shown promise for fluoride adsorption (Lv 2007, Mandal and Mayadevi 2008)

The specific aluminum (hydr)oxide phase(s) that precipitate from dissolved aluminum salts depend on the pH, the ligand(s) present in solution, and aging time and temperature. Pseudoboehmite (poorly or finely crystalline boehmite (γ-AlOOH)) may form upon aging of an initial amorphous $Al(OH)_3$ precipitate at room temperature (Aldcroft et al. 1969). The presence of ligands that complex strongly with Al(III) in competition with OH^- can hinder formation of crystalline $Al(OH)_3$ phases and stabilize pseudoboehmite, which has a lower pH_{pzc} (Violante and Huang 1984). Pseudoboehmite aging at temperatures up to 300 ^oC increases crystallite size and lowers specific surface area (SSA), but does not promote phase changes (Gong et al. 2012, Tottenhorst and Hofmann 1980); calcination temperatures of 500 to 700 ^oC are required for transformation of pseudoboehmite to γ-Al_2O_3 (Gong et al. 2012, Lippens and de Boer 1964, Repelin and Husson 1990, Chary et al. 2008).

The overall objective of this study was to compare the fluoride adsorption performance of a series of aluminum based adsorbents that could be synthesized using common chemicals, such as water treatment coagulants, and heating equipment, such as kilns, that are readily available in rural areas of developing countries. Specific objectives were to synthesize adsorbents with a range of mineral phases, crystallinities, and surface properties (e.g., SSA and pH_{pzc}), by varying synthesis temperature,

concentrations of extra ligands, and metal oxide amendments, then to test these sorbents for fluoride adsorption efficiency.

Methods

Adsorbent synthesis

A series of aluminum (hydr)oxides was prepared by hydrolysis of $AlCl_3$ (Sigma-Aldrich), sometimes with addition of sulfate (as sodium sulfate (Acros)) or citrate (as sodium citrate (Sigma-Aldrich)), as well as temperature and pH adjustment (Violante and Huang 1984, Violante and Huang 1994, Watanabe et al. 2002). The overall approach is illustrated in Fig. 2-1. Briefly, 50 mM $AlCl_3$ was titrated with 5 M NaOH (Acros) to pH 8.2 (Violante and Huang 1984) for three sets of conditions: (1) no ligands other than the chloride present in the $AlCl_3$ were added, (2) 0.5 M sulfate was added, and (3) 5×10^{-4} M citrate was added. These concentrations of sulfate and citrate were based on the aluminum: ligand ratios in Violante and Huang (1984), and were intended to produce a similar extent of complexation of aluminum by either sulfate or citrate. (Less citrate was required because citrate is a much stronger complexing agent than sulfate (Violante and Huang 1984). The precipitated solids were then aged at either 25 ^{o}C (to yield lower crystallity pseudoboehmite) or 200 °C (to yield higher crystallinity pseudoboehmite) for 1 day, decanted and transferred to dialysis tubing (Fisher, Seamless cellulose dialysis tubing, 12000 Da) and dialyzed for 6 days, during which time deionized water was replaced daily. Next, the solids were centrifuged, air-dried,

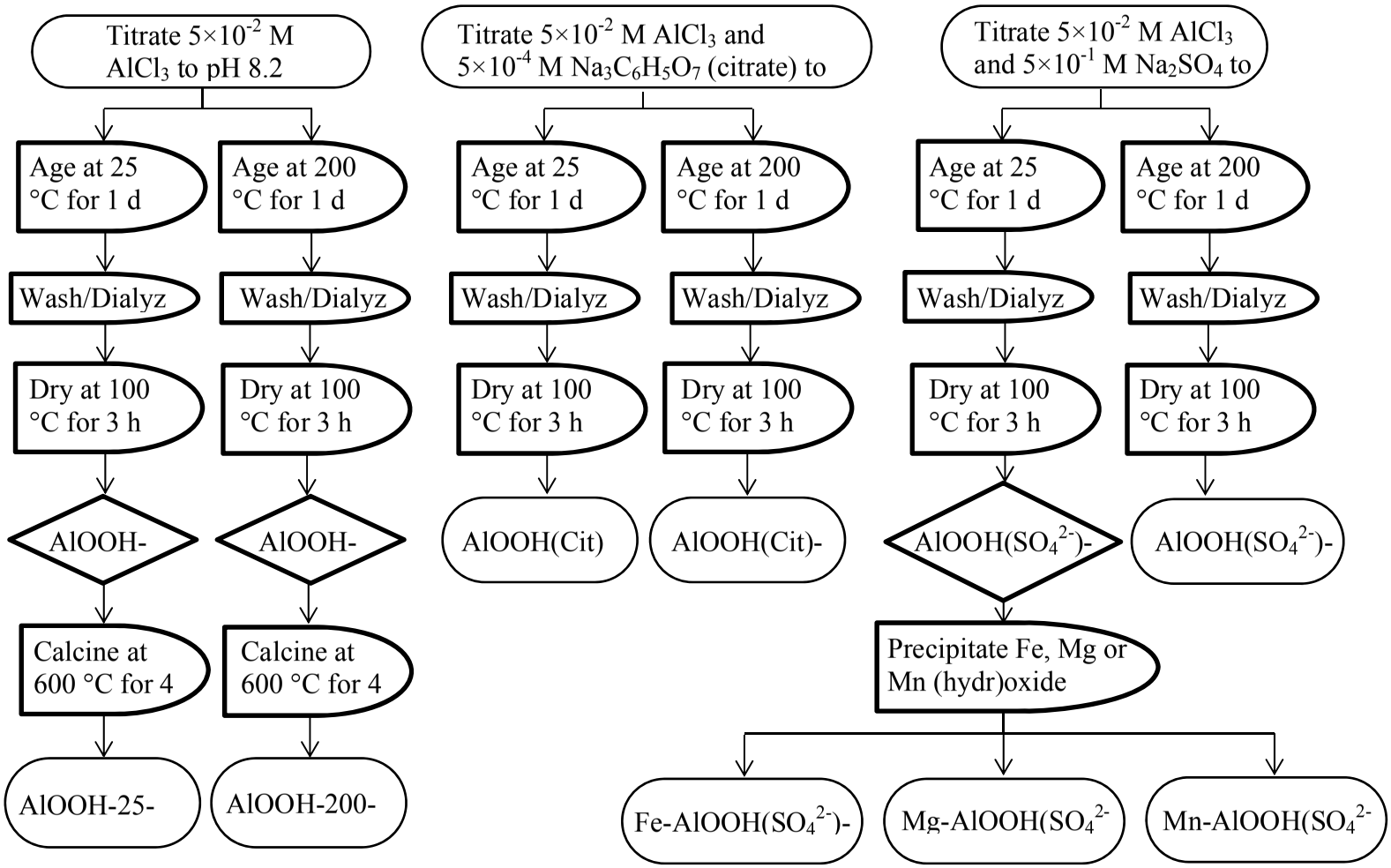

Figure 2-1Aluminum (hydr)oxide synthesis procedures.

ground with a mortar and pestle, dried in the oven at 100 °C for 3 h to remove water, and stored in a desiccator. A subset of the solids was then further heated to 600 °C for 4 h to promote the phase transition from pseudoboehmite to γ-Al_2O_3 (Fig. 2-1). Some aluminum (hydr)oxide adsorbents were further amended by precipitating (hydr)oxides of iron, magnesium, or manganese on their surfaces (Dhiman and Chaudhuri 2007, Kuriakose et al. 2004, Maliyekkal et al. 2006, Maliyekkal et al. 2008, Teng et al. 2006). These precipitates were generated by mixing a slurry of aluminum (hydr)oxide with 0.747 M $Fe(NO_3)_3 \cdot 9H_2O$ (Arcos), 1 M $MgCl_2$ (Arcos), or 1.5 M $(CH_3COOH)_2Mn$ (Arcos) followed by heating at 200 ^oC for 4 hours. After being washed, dried, and dialyzed as before, the metal amended aluminum (hydr)oxides were stored in a desiccator. All aluminum (hydr)oxides are hereafter referenced using the abbreviations in Fig. 2-1.

A series of LDHs, including Mg-Al-Cl^-, Mg-Al-CO_3^{2-}, Mg-Al-PO_4^{3-}, and Zn-Al-Cl^- was prepared by co-precipitation. Mg-Al LDHs were prepared according to Carriazo et al. (2007). Zn-Al-Cl^- LDH was prepared the same way as Mg-Al-Cl^- LDH, except $ZnCl_2 \cdot 6H_2O$ (Fisher) was used instead of $MgCl_2$. Like some of the aluminum (hydr)oxides, Mg-Al-Cl^- LDH was amended by precipitation of an iron (hydr)oxide on its surface by adding 10 g LDH to 7 mL 0.747 M $Fe(NO_3)_3 \cdot 9H_2O$, gentle mixing, and drying at 130 °C for 4 h. This sample is called Fe-Mg-Al-Cl^- LDH. One sample of Mg-Al-Cl^- LDH was heated at 500 °C for 4 h, and is denoted Mg-Al-Cl^- LDH-500.

Batch adsorption experiments

Polyethylene bottles containing 0.1 g adsorbent and 50 mL Nanopure water (18.2 MΩ, Barnstead D8961) with initial fluoride concentrations ranging from 20 to 100 mg/L were agitated on a reciprocal shaker at 300 rounds per minute for 24 h. Each sample was prepared in triplicate. The initial pH was approximately 6.0 and ranged from 7.3-8.6 after equilibration with fluoride. After equilibration, each sample was filtered (Whatman, Qualitative filter paper, 150 mm diameter) and the fluoride concentration was determined by ion selective electrode (Electrodesdirect). Prior to analysis, both standards and samples were diluted with total ionic strength adjustment buffer (TISAB) on a 1:1 basis to reduce interferences and maintain a constant pH and ionic strength during analysis. TISAB contains 60 g/L acetic acid/sodium acetate buffer, 58.5 g/L NaCl, and 4 g/L 1, 2-cyclohexylenedinitrilotetraacetic acid. A four point external calibration curve was prepared daily. Standard solutions were stored in a refrigerator at approximately 4 ^{o}C and replaced monthly (pHoenix Electrode Co. 1997). Blanks were prepared daily from equal volumes of nanopure water and TISAB. Mean and standard deviations of triplicate measurements were calculated for each value of C_e. Error propagation was used to calculate the standard deviations in Q_e using the experimental errors associated with sample weighing, volume measuring, and fluoride determination.

Experimental data were fit to the Langmuir isotherm by nonlinear regression using Sigma Plot 12.0 (Systat Software Inc., Chicago, IL), yielding estimates of the Langmuir parameters Q_m (the maximum adsorption capacity, in mg/g) and b (the affinity parameter, in L/mg). These estimated values were used to calculate $Q_{1.5\ mg/L}$ (in mg/g), which is the adsorbed fluoride concentration in equilibrium with a dissolved

fluoride concentration at the WHO guideline value of 1.5 mg/L. When more than one batch of a given adsorbent was prepared, selected measurements were repeated and Q_m values compared to confirm similar adsorbent properties between the batches. Properties such as SSA and pH_{pzc} were also confirmed to be the same within experimental uncertainties.

Adsorbent characterization

SSA and pH_{pzc} were determined for the adsorbents, except for those that showed only limited promise for fluoride removal. SSA was determined using two methods: (1) BET analysis using a Quantachrome Autosorb Automated Gas Sorption System with a Beckman Coulter SA-3100 Surface Area Analyzer and N_2 adsorption (SSA_{BET}), and (2) the ethylene glycol monoethyl ether (EGME) method (SSA_{EGME}) (Cerato and Luteneggar 2002). The EGME method is a gravimetric assessment based on the retention of highly volatile EGME molecules on the samples. The EGME molecules are assumed to quickly attach to the surface and form monolayer coverage (Carter et al. 1965) with the excess EGME volatilizing. The difference in the weight of samples before and after EGME coverage was documented to calculate surface area. EGME analysis was done to get a more complete assessment of adsorbent surface area, because the BET method may measure only the external surface area of certain minerals (Rives 2001, Yukselen and Kaya 2006). Both SSA_{BET} and SSA_{EGME} were measured in duplicate. The pH_{pzc} was measured using the "drift" method (Brunson and Sabatini 2009), in which a set of 0.1 g of samples for each adsorbent was immersed in 10 mL of 0.02 M KNO_3 with initial pH varying from 2.2 to 11.6. After shaking the mixture for 1

day, the final pH of each sample was measured under N_2 atmosphere and then plotted against initial pH. The pH_{pzc} was the value of final pH corresponding to the plateau in the plot. The pH_{pzc} for a subset of adsorbents was also determined by a potentiometric method (Vakros et al. 2002) for comparison to the drift method. These pH_{pzc} values were found to be within one pH unit of the values determined from the drift method.

X-ray diffraction (XRD) analysis of adsorbents was done with a Rigaku Ultima IV powder X-ray diffractometer with Cu Kα radiation and Bragg-Brentano optics. Jade 5.0 (Materials Data Inc., Livermore, CA) was used for data analysis and phase was assigned by comparison to the powder diffraction file (PDF) of the International Center for Diffraction Data (ICDD) (PDF databases, ICDD, Newtown Square, PA, U.S.). Samples were characterized by scanning electron microscopy with energy dispersive X-ray spectroscopy (SEM/EDS) using a Zeiss Neon SEM operating at 10 kV after sputter coating with gold and palladium.

Results and discussion

Effect of temperature during synthesis

Increasing the aging temperature for the aluminum (hydr)oxides from 25 to 200 ^oC decreased the adsorption isotherm plateaus (Fig. 2-2) and the corresponding Langmuir Q_m values (Table 2-1) in all cases. The $Q_{1.5\ mg/L}$ value (Table 2-1) was also lower for the 200 ^oC aged aluminum (hydr)oxide prepared with sulfate ($AlOOH(SO_4^{2-})$-200) versus the corresponding 25 ^oC aged aluminum (hydr)oxide ($AlOOH(SO_4^{2-})$-25), but there was no significant difference between $Q_{1.5\ mg/L}$ values for the 25 and 200 ^oC-aged aluminum (hydr)oxides containing citrate or no extra ligands (Table 2-1).

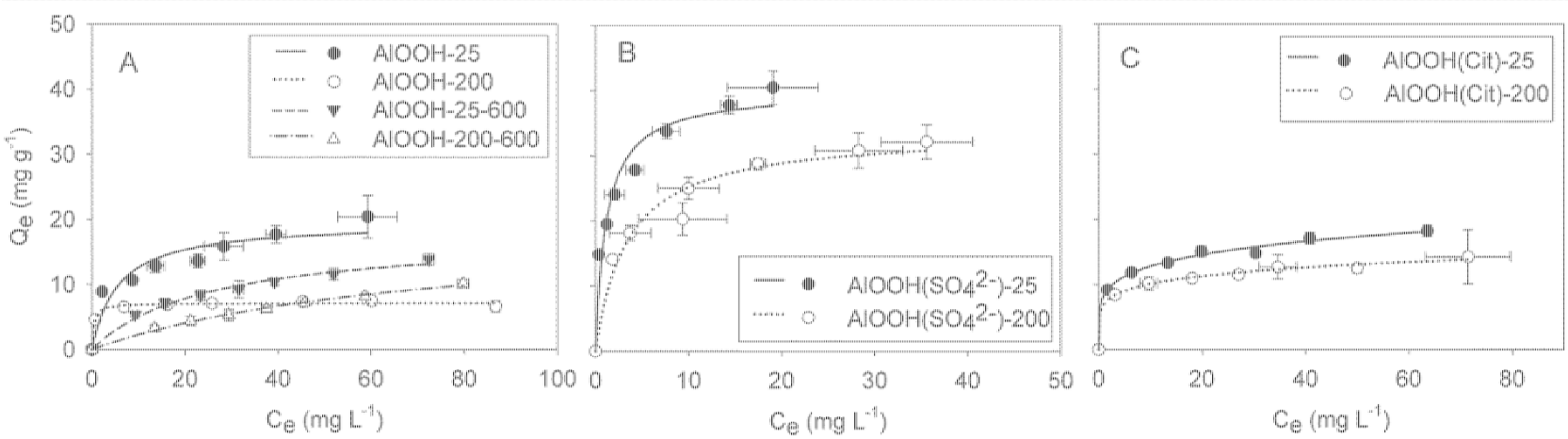

Figure 2-2 Fluoride adsorption to aluminum (hydr)oxides with Langmuir isotherm fits. Vertical and horizontal error bars represent the standard deviations of Q_e and C_e, respectively, calculated from triplicate measurements for each sample.

Table 2-1 Properties of synthesized adsorbents

Adsorbent	Q_m (mg g^{-1})[a]	b (L mg^{-1})[a]	$Q_{1.5\ mg\ L^{-1}}$ (mg g^{-1})[b]	SSA_{BET} (m^2 g^{-1})[c]	SSA_{EGME} (m^2 g^{-1})[c]	pH_{pzc}	Notes	Reference
Aluminum (hydr)oxides								
AlOOH-25	20±2.	0.18±0.08	4±2	(24±1)×10	(2.4±1)×100	4.5	pH 6	This study
AlOOH-200	7±0.1	2.5±0.5	6±1	124±4	(2±1)×100	5.5	pH 6	This study
AlOOH(SO_4^{2-})-25	40±2	0.8±0.2	22±7	103±2	(20±6)×10	5.4	pH 6	This study
AlOOH(SO_4^{2-})-200	34±2	0.30±0.07	10±3	6.6±0.6	147±3	4.5	pH 6	This study
AlOOH(Cit)-25	16.9±0.8	0.5±0.2	7±2	234±5	(32±1)×10	5.4	pH 6	This study
AlOOH(Cit)-200	13.2±0.5	0.4±0.1	5±2	280±5	(31±2)×10	5.1	pH 6	This study
AlOOH-25-600	18±1	0.040±0.007	1.0±0.2	(21±4)×10	(21±6)×10	4.9	pH 6	This study
AlOOH-200-600	19±1	0.014±0.002	0.38±0.06	(14±1)×10	(2±1)×100	5.6	pH 6	This study
Pseudoboehmite	83.3	2.0	62.5	NR	NR	NR	pH 6	Gong et al. (2012)
Boehmite	2.057	0.2806	0.61	NR	NR	NR	pH 7.3-8	Jiménez-Becerril et al. (2012)
Heat treated hydrated alumina	NR[d]	NR	26.7	NR	NR	NR	pH 7±0.3	Shimelis et al. (2006)
In-situ $Al_2O_3 \cdot xH_2O$	>110	NR	NR	118.24	NR	NR	pH 6	Liu et al. (2011)
Metal amended aluminum (hydr)oxides								
Fe-AlOOH(SO_4^{2-})-25	43±2	0.8±0.2	24±8	74±1	160±4	4.7	pH 6	This study
Mg-AlOOH(SO_4^{2-})-25	34±2	0.020±0.002	19±5	NM[e]	NM	NM	pH 6	This study
Mn-AlOOH(SO_4^{2-})-25	36±2	0.43±0.08	22±7	NM	NM	NM	pH 6	This study
LDHs								
Mg-Al-Cl^--LDH	78±7	0.006±0.001	0.7±0.1	36±1	123±2	7.7	pH 6	This study
Mg-Al-CO_3^{2-}-LDH	6.2±0.7	0.012±0.002	0.11±0.02	NM	NM	NM	pH 6	This study
Mg-Al-PO_4^{3-}-LDH	NA[f]	NA	0.08±0.02	NM	NM	NM	pH 6	This study
Mg-Al-Cl^--LDH-500	43±4	0.0069±0.0009	0.44±0.07	NM	NM	NM	pH 6	This study
Zn-Al-Cl^--LDH	55±7	0.006±0.001	0.5±0.1	NM	NM	NM	pH 6	This study
Fe-Mg-Al-Cl^--LDH	18.9±0.8	0.027±0.002	0.75±0.08	NM	NM	NM	pH 6	This study

[a] The uncertainties in Q_m and b values represent standard deviations determined from nonlinear regression using SigmaPlot version 12.0.
[b] The uncertainties in $Q_{1.5\ mg\ L^{-1}}$ values represent standard deviations determined from error propagation.
[c] The uncertainties in SSA represent standard deviations calculated from duplicate measurements for SSA.
[d] Not reported.
[e] Not measured.
[f] Not applicable. These data could not be fit to the Langmuir isotherm. Freundlich parameters (K=0.05±0.01 and n=1.04±0.05, where $q_e=KC_e^n$) were used to calculate $Q_{1.5\ mg\ L^{-1}}$.

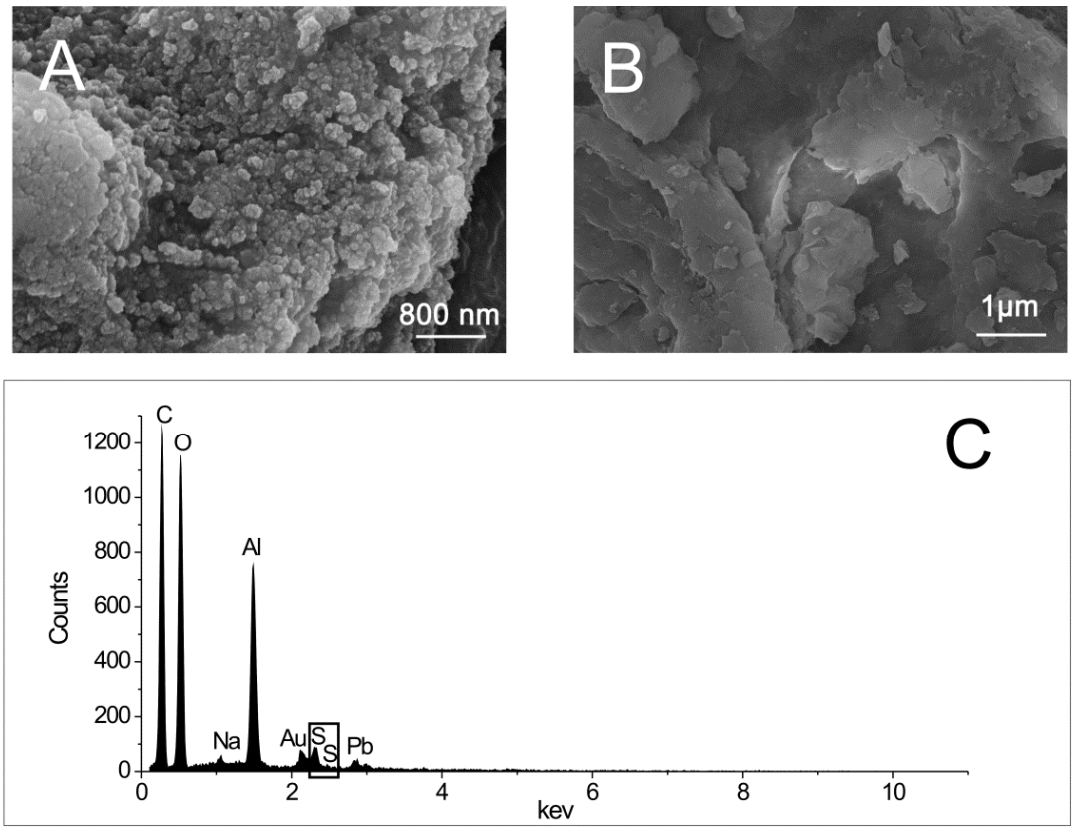

Figure 2-3 SEM images of AlOOH(SO_4^{2-})-25 (A), AlOOH(SO_4^{2-})-200 (B), and EDS spectrum of AlOOH(SO_4^{2-})-25 showing sulfur peak (C).

The decrease in the Langmuir maximum adsorption capacity (Q_m) for the sorbents aged at 200 ^oC versus 25 ^oC can in some cases be explained by a corresponding decrease in either SSA_{BET} or SSA_{EGME} for these sorbents (Table 2-1). For AlOOH(SO_4^{2-}), raising the aging temperature from 25 to 200 ^oC caused changes in surface morphology (Figs. 2-3A and 2-3B) that may be responsible for the reduced SSA_{BET} of the material aged at 200 ^oC. Specifically, AlOOH(SO_4^{2-}) aged at 25 ^oC consisted of particles with dimensions on the order of 100 nm (estimated from SEM image in Fig. 2-3A) that appear to be grouped in aggregates of micrometer dimensions (images not shown), while the same material aged at 200 ^oC consisted of smooth particles (Fig. 2-3B) of

micrometer dimensions (images not shown). There was also an increase in the height of XRD peaks associated with pseudoboehmite (PDF 49-0133, ICDD) upon aging at 200 ^{o}C versus 25 ^{o}C (Fig. 2-4), suggesting increased crystallinity. Previous reports have shown that higher aging temperatures result in increased pseudoboehmite crystallinity and/or reduced SSA_{BET} (Tottenhorst and Hofmann 1980, Violante and Huang 1984, Watanabe et al. 2002), as well as reduced fluoride adsorption capacity for aluminum (hydr)oxides (Gong et al. 2012, Lee et al. 2006, Shimelis et al. 2012).

Further treatment of AlOOH-25 and AlOOH-200 by heating at 600 °C for four hours resulted in significant decreases in $Q_{1.5\ mg/L}$ (Fig. 2-2A, Table 2-1). This temperature change did not cause a significant change in SSA (Table 2-1), but rather caused a phase change from pseudoboehmite to γ-Al_2O_3 (PDF 46-1131, ICDD) (Fig. 2-4), in agreement with previous studies (Chary et al. 2008, Gong et al. 2012, Lippens and de Boer 1964, Repelin and Husson 1990).

The Q_m and $Q_{1.5\ mg/L}$ values for the aluminum hydr(oxide) sorbents synthesized in this study are within the range of several previously reported values (see rows 9-12 in Table 2-1). For example, Gong et al. (2008) reported Langmuir adsorption parameters for a virtually amorphous aluminum (hydr)oxide synthesized at pH 5 and aged at 60 ^{o}C. The $Q_{1.5\ mg/L}$ value calculated from those adsorption parameters (Table 2-1) is exceptionally high, consistent with the trend reported here that lower aging temperatures lead to amorphous aluminum (hydr)oxides with high fluoride adsorption capacities. In addition, Liu et al. (2011) reported a Q_e greater than 110 mg/g at pH 6, an adsorbent dose of 27 mg/L as Al, and an initial fluoride concentration of 4 mg/L for Al_2O_3 prepared by immediately mixing $AlCl_3$ and NaOH at ambient temperatures. This

high Q_e is in line with the high fluoride adsorption capacity displayed by the low temperature adsorbent AlOOH(SO_4^{2-})-25 reported here (Table 2-1).

Effect of added sulfate and citrate

For 25 ^oC-aged aluminum (hydr)oxides, addition of sulfate and citrate did not lead to significant differences in crystallinity of the resulting aluminum (hydr)oxide sorbents (Fig. 2-4), nor were there any systematic differences in pH_{pzc} values for adsorbents formed in the presence of these ligands (Table 2-1). Comparison of the XRD patterns of AlOOH(SO_4^{2-})-200 and AlOOH(SO_4^{2-})-25 (Fig. 2-4), however, suggests the formation of a phase distinct from or in addition to pseudoboehmite in AlOOH(SO_4^{2-})-200. Instead of the distinct pseudoboehmite (020) peak at $2\theta \approx 14^o$, the XRD pattern of AlOOH(SO_4^{2-})-200 had a broad hump centered at $2\theta \approx 11°$, which may be the superposition of the (020) peak of pseudoboehmite and the (002) peak ($2\theta = 9.4°$) of basaluminite ($Al_4SO_4(OH)_{10}\cdot 4H_2O$) (PDF 42-0556, ICDD) (Fig. 2-4). Poorly crystalline basaluminite may also be present in AlOOH(SO_4^{2-})-25, since EDS results indicated the presence of sulfur at approximately 2% by mass in this solid (Fig. 2-3C) as well as AlOOH(SO_4^{2-})-200 (not shown). Violante and Huang (1984) also reported 6.2% sulfate by mass in pseudoboehmite prepared with excess sulfate. These percentages exceed the amount of sulfur that could be attributed to adsorbed sulfate based on calculations considering SSA and sulfate bond distances from Chiu and Genshaw (1969). Basaluminite and amorphous aluminum (hydr)oxide have been found to coexist elsewhere in natural systems (Jones et al. 2011).

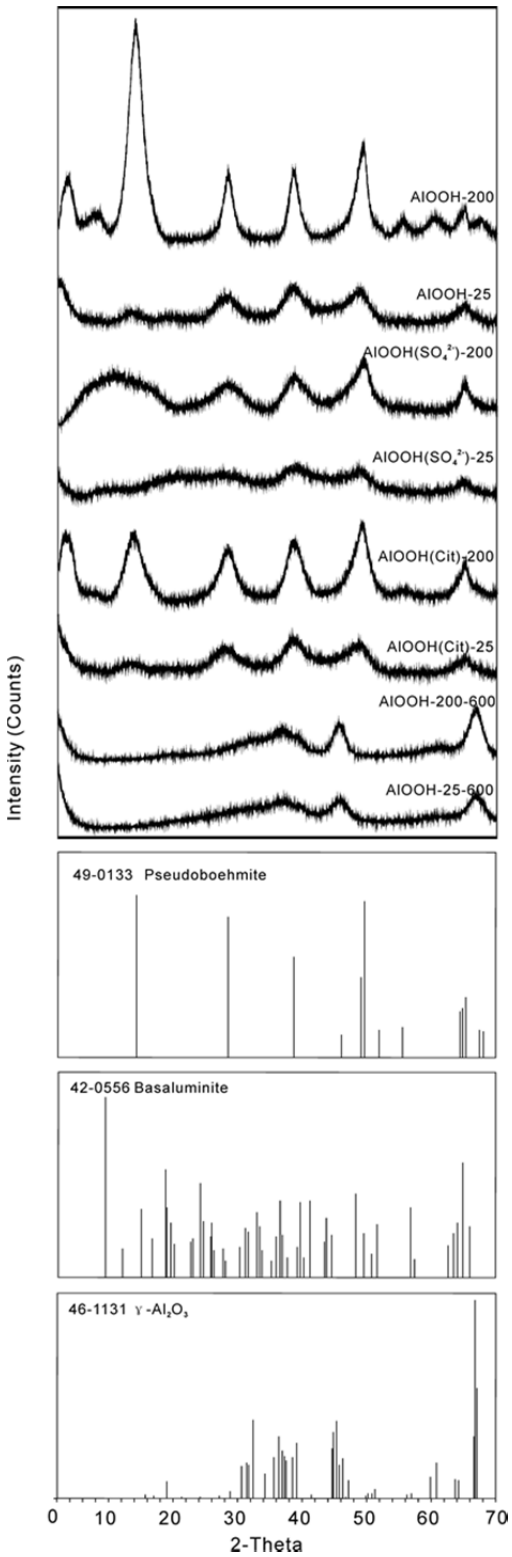

Figure 2-4 XRD patterns of aluminum (hydr)oxides.

The aluminum (hydr)oxides synthesized with extra sulfate showed significantly higher Q_m and $Q_{1.5\ mg/L}$ values compared to those synthesized with extra citrate or no extra ligands (Fig. 2-2, Table 2-1). These differences cannot be attributed to higher SSA values (Table 2-1). In a similar finding, pseudoboehmite prepared with extra sulfate had a higher phosphate adsorption capacity than pseudoboehmite prepared in the presence of other ligands, despite its lower SSA (Violante and Huang 1984). Also, Shimellis et al. (Shimelis et al. 2006) studied adsorption of fluoride to hydrated alumina prepared from aluminum sulfate that was heated to 300 ^{o}C for one hour. Their experimental pH was pH 7±0.3. Their reported Freundlich adsorption parameters were used to calculate a $Q_{1.5\ mg/L}$ value for fluoride adsorption (26.7 mg/g) that is comparable to that for AlOOH(SO_4^{2-})-25 (Table 2-1). The sulfur content of that aluminum (hydr)oxide was not reported (Shimelis et al. 2006).

Treatment of the best performing aluminum (hydr)oxide adsorbent (AlOOH(SO_4^{2-})-25) with the salts of iron, magnesium, or manganese had either a negative impact (for manganese) or no significant impact (for iron and magnesium) on Q_m (Table 2-1). Differences in $Q_{1.5\ mg/L}$ values were not statistically significant. While SEM/EDS was not able to detect or identify discrete particles of iron (hyr)oxides on the aluminum (hydr)oxide surface, iron was detected in the Fe-AlOOH(SO_4^{2-})-25 sample by EDS at mass concentrations of approximately 3 to 10 percent (not shown).

Layered double hydroxides

While several LDHs had relatively high Q_m values (Table 2-1), these maxima—estimated by best fit of the Langmuir isotherm equation to the experimental data—

corresponded to C_e values far above those measured in this study (Fig. 2-5), and therefore far above concentrations of dissolved fluoride generally relevant to drinking water treatment. However, comparing $Q_{1.5\ mg/L}$ values, which are relevant for water treatment, the best performing aluminum (hydr)oxide adsorbents outperformed the best performing LDHs (Table 2-1). Addition of iron salts during synthesis of the best performing LDH (Mg-Al-Cl^-) had no significant impact on $Q_{1.5\ mg/L}$ values (Table 2-1).

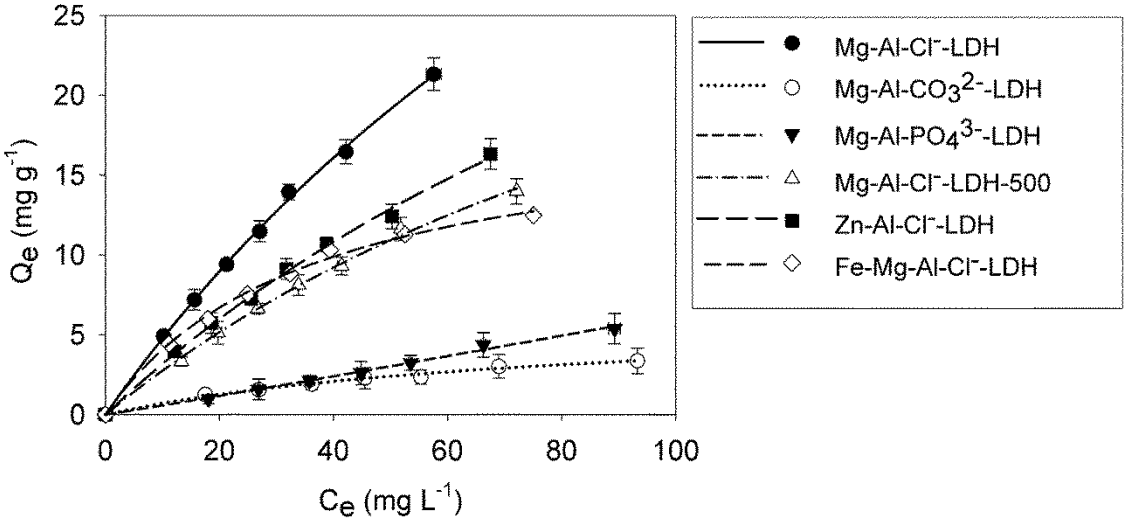

Figure 2-5 Fluoride adsorption to layered double hydroxides with Langmuir isotherm fits, or, for Mg-Al-PO_4^{3-}-LDH, a Freundlich isotherm fit.

Conclusions

Increases in aluminum (hydr)oxide synthesis temperatures, either during aging of aqueous slurries or calcination of dried powders, generally led to reduced fluoride adsorption efficiencies. Increasing the aging temperature from 25 ^oC to 200 ^oC produced pseudoboehmite with a higher degree of crystallinity, but a lower adsorption efficiency. Calcination of aluminum (hydr)oxides at 600 ^oC led to formation of γ-Al_2O_3

and further reductions in adsorption efficiencies. Modification of aluminum (hydr)oxide adsorbents by addition of salts of iron, manganese, and magnesium did not significantly change adsorption efficiencies at fluoride concentrations near the WHO guideline of 1.5 mg/L, although significant iron was detected in Fe-Al(SO_4^{2-})-25 by SEM/EDS. Addition of extra citrate during aluminum hydrolysis at pH 8.2 did not change adsorption efficiency, but addition of extra sulfate significantly improved fluoride adsorption efficiency, perhaps due to formation of basaluminite along with pseudoboehmite. While some LDHs had high Langmuir Q_m values, their $Q_{1.5\ mg/L}$ values were not competitive with the best performing aluminum (hydr)oxide adsorbent, which was AlOOH(SO_4^{2-})-25. Thus, aluminum (hydr)oxides synthesized at low temperatures with extra sulfate show promise for fluoride adsorption and merit further investigation.

References

Aldcroft, D., Bye, G. C. and Hughes, C. A. (1969) "Crystallization processes in aluminum hydroxide gels, IV. Factors influencing the formation of the crystalline trihydroxides." J. Appl. Chem. 19: 167-172.

Ayoob, S., Gupta, A. K. and Bhat, V. T. (2008) "A conceptual overview on sustainable technologies for the defluoridation of drinking water." Crit. Rev. Env. Sci. Tec. 38: 401-470.

Brunson, L. R. and Sabatini, D. A. (2009) "An evaluation of fish bone char as an appropriate arsenic and fluoride removal technology for emerging regions." Environ. Eng. Sci. 26, 1777-1784.

Carter, D. L., Heilman, M. D. and Gonzalez, C. L. (1965) "Ethylene glycol monoethyl ether for determining surface area of silicate minerals." Soil Sci. 100: 356-360.

Carriazo, D., del Arco, M., Martín, C. and Rives, V. (2007) "A comparative study between chloride and calcined carbonate hydrotalcites as adsorbents for Cr(VI)." Appl. Clay Sci. 37: 231-239.

Cerato, A. B. and Lutenegger, A. J. (2002) "Determination of surface area of fine-grained soils by the ethylene glycol monoethyl ether (EGME) method." Geotech. Test J. 25: 315-321.

Chary, K. V. R., Rao, P. V. R. and Rao, V. V. (2008) "Catalytic functionalities of nickel supported on different polymorphs of alumina." Catal. Commun. 9 : 886-893.

Chiu, Y. C. and Genshaw, M. A. (1969) "A study of anion adsorption on platinum by ellipsometry." J. Phys. Chem. 73: 3571-3577.

Dhiman, A. J. and Chaudhuri, M. (2007) "Iron and manganese amended activated alumina—A medium for adsorption/oxidation of arsenic from water." J. Water Supply Res. T. 56, 69-74.

Fawell, J., Bailey, K., Chilton, J., Dahi, E., Fewtrell, L. and Magara, Y. (2006) Chapter 5: Removal of excessive fluoride. In: *Fluoride in Drinking-water*, World Health Organization 41-83.

Gong, W., Qu, J., Liu, R. and Lan, H. (2012) "Adsorption of fluoride onto different types of aluminas." Chem. Eng. J. 189-190: 126-133.

Jain, S. and Jayaram, R. V. (2009) "Removal of fluoride from contaminated drinking water using unmodified and aluminum hydroxide impregnated blue lime stone waste." Separ. Sci. Technol. 44: 1436-1451.

Jiménez-Becerril, J., Solache-Ríos, M. and García-Sosa, I. (2012) "Fluoride removal from aqueous solutions by boehmite." Water Air Soil Poll. 223: 1073-1078.

Jones, A. M., Collins, R. N. and Waite, T. D. (2011) "Mineral species control of aluminum solubility in sulfate-rich acidic waters." Geochim. Cosmochim. Ac. 75: 965-977.

Kasprzyk-Hordern, B. (2004) "Chemistry of alumina, reactions in aqueous solution and its application in water environment." Adv. Colloid Interfac. 110: 19-48.

Kuriakose, S., Singh, T. S. and Pant, K. K. (2004) "Adsorption of As(III) from aqueous solution onto iron oxide impregnated activated alumina." Water Qual. Res. J. Canada 39: 258-266.

Lee, H. W., Park, B. K., Tian, M. Y. and Lee, J. M. (2006) "Relationship between properties of pseudoboehmite and its synthetic conditions." J. Ind. Eng. Chem. 12: 295-300.

Lippens, B. C. and de Boer, B. H. (1964) “Study of phase transformations during calcination of aluminum hydroxides by selected area electron diffraction.” Acta Crystallogr. 17 : 1312-1321.

Liu, R., Gong, W., Lan, H., Gao, Y., Liu, H. and Qu, J. (2011) “Defluoridation by freshly prepared aluminum hydroxides.” Chem. Eng. J. 175: 144-149.

Lv, L. (2007) “Defluoridation of drinking water by calcined MgAl-CO_3 layered double hydroxides.” Desalination 208, 125-133.

Maliyekkal, S. M., Sharma, A. K and Philip, L. (2006) “Manganese-oxide-coated alumina: A promising sorbent for defluoridation of water.” Water Res. 40: 3497-3506.

Maliyekkal, S. M., Shukla, S., Philip, L. and Nambi, I. M. (2008) “Enhanced fluoride removal from drinking water by magnesia-amended activated alumina granules.” Chem. Eng. J. 140: 183-192.

Mandal, S. and Mayadevi, S. (2008) “Adsorption of fluoride ions by Zn-Al layered double hydroxides.” Appl. Clay Sci. 40: 54-62.

Onyango, M. S., Matsuda, H. (2006) Chapter 1: Fluoride removal from water using adsorption technique. In: *Fluorine and the Environment—Agrochemicals, Archaeology, Green chemistry and Water*, Advances in Fluorine Science, 2: 1-48.

pHoenix Electrode Co. (1997) Fluoride ion selective electrodes instruction manual.

Repelin, Y. and Husson, E. (1990) “Etudes structurales d'alumines de transition: 1-alumines gamma et delta.” Mater. Res. Bull. 25: 611-621.

Rives, V. (2001) Layered Double Hydroxides: Present and Future. Nova Science Publishers Inc., New York, 230-231.

Shimelis, B., Zewge, F. and Chandravanshi, B. S. (2006) “Removal of excess fluoride from water by aluminum hydroxide.” Bull. Chem. Soc. Ethiop. 20: 17-34.

Teng, S. X., Wang, S. G., Gong, W. X., Liu, X. W. and Gao B. Y. (2009) “Removal of fluoride by hydrous manganese oxide-coated alumina: Performance and mechanism.” J. Hazard. Mater. 168: 1004-1011.

Tottenhorst, R. and Hofmann, D. A. (1980) “Crystal chemistry of boehmite.” Clay Clay Miner. 28: 373-380.

Vakros, J., Kordulis, C. and Lycourghiotis, A. (2002) “Potentiometric mass titrations: A quick scan for determining the point of zero charge.” Chem. Commun. 17: 1980-1981.

Violante, A. and Huang, P. M. (1984) “Nature and properties of pseudoboehmites formed in the presence of organic and inorganic ligands.” Soil Sci. Soc. Am. J. 48: 1193-1201.

Violante, A. and Huang, P. M. (1993) “Formation mechanism of aluminum hydroxide polymorphs.” Clay Clay Miner. 41: 590-597.

Watanabe, Y., Yamada, H., Kasama, T., Tanaka, J., Komatsu, Y. and Moriyoshi, Y. (2002) “Adsorption behavior of phosphorus on synthetic boehmites.” Proceedings of The 19th International Japan-Korea Seminar on Ceramics 80-84.

World Health Organization (WHO) (2008) Safe Water, Better Health. WHO Press, Geneva, Switzerland.

Yukselen, Y. and Kaya, A. (2006) “Comparison of methods for determining specific surface area of soils.” J. Geotech. Geoenviron. 132: 931-936.

Chapter 3 : Preparation, characterization, and regeneration of aluminum (hydr)oxide amended molecular sieves for fluoride removal from drinking water[2]

Introduction

Consuming water with a fluoride concentration above 1.5 mg/L (WHO 2008) causes fluorosis and poses a threat to human health (Edmunds and Smedley 2013, Johnson and Bretzler 2015). To mitigate these impacts, various materials have been utilized to remove fluoride from drinking water. Aluminum (hydr)oxide amended materials constitute a group of adsorbents prepared by treating substrate matrices (Jagtap et al. 2012, Tomar and Kumar 2013) such as wood char (Brunson and Sabatini 2015), resins (Luo and Inoue 2004), and clay (Agarwal et al. 2003) with aluminum salts. They are designed to incorporate aggregated nanoscale aluminum (hydr)oxide particles with high fluoride adsorption affinities (Gong et al. 2012a, Shimelis et al. 2006) into porous substrate materials that have low adsorption capacities (Daifullah et al. 2007, Kau et al. 1998, Meenakshi and Viswanathan 2007), but that are suitable for application in a flow through column setup (Sperry and Peirce 1995) due to their larger particle size.

To date, numerous efforts have attempted to integrate aluminum (hydr)oxides and different types of simple substrate materials (Mohapatra et al. 2009, Loganathan et al. 2013) that can be applied in low-income regions of the world. These efforts, however, are constrained by low fluoride adsorption capacities (Agarwal et al. 2003, Brunson and Sabatini 2015) and limited available substrate materials, e.g., ion-exchange

[2] This chapter is published in the Journal of Environmental Engineering (Du, J., Sabatini, D. A. and Butler, E. C., 2016. Preparation, Characterization, and Regeneration of Aluminum (Hydr) Oxide–Amended Molecular Sieves for Fluoride Removal from Drinking Water. Journal of Environmental Engineering, p.04016043). Copyright (2016) American Society of Civil Engineers. Reuse with permission from ASCE.

resins (Luo and Inoue 2004). Molecular sieves or their natural counterparts—zeolites—are widespread minerals with their primary occurrence in volcanic areas, e.g., stilbite in the Rift Valley in Ethiopia (Gómez-Hortigüela et al. 2013) and the Birbhum district in West Bengal, India (Majumdar et al. 2009, Mondal et al. 2014) , and sodalite in the Serra do Mar Alkaline Province, Southeast Brazil (Thompson et al. 1998) and the Huarina Belt in Bolivia (Jiménez and López-Velásquez, 2008). The volcanic areas where molecular sieves mainly occur often overlap with or are close to endemic fluorosis areas, such as the Rift Valley in Ethiopia and the Chacopampean plain in Argentina (Gomez et al. 2008); thus zeolites are available in these areas for fluoride treatment.

By definition, molecular sieves consist of a hollow cage framework containing microporous (alumino)silicate tetrahedral units and extra-framework counter ions for charge balance (Davis and Lobo 1992). In pure silicon molecular sieves, counter ions do not exist due to the absence of framework charge. Owing to their porous structure, molecular sieves have large surface areas (Vyas and Kumar 2004) for precipitation of aluminum (hydr)oxide. Preliminary experiments showed that aluminum (hydr)oxide amended molecular sieves exhibited higher fluoride adsorption capacities than similarly treated fibrous materials (cellulose, steel wool, glass wool and wood char), and resins (Supplemental Information (SI) Fig. S1 and Tables S1 and S2). The objective of this study was to develop low-cost and efficient fluoride adsorbents using molecular sieves that represent the natural zeolites abundant in low-income fluoride impacted regions. We speculated that the pore size, counter ions, and point of zero charge (pH_{PZC}) of the molecular sieves might influence the properties of these materials after aluminum

(hydr)oxide amendment, and thus the extent of fluoride adsorption, and so chose a series of molecular sieves and zeolites with various pore sizes and compositions for study. In addition, since reusability plays a vital role in evaluating the performance of adsorbents (Yami et al. 2015, Yokoi et al. 2004), the fluoride adsorption capacities of aluminum (hydr)oxide amended molecular sieves after multiple adsorption and regeneration cycles were measured.

Materials and Methods

Materials

Molecular sieves with pore sizes ranging from 0.3 to 4.7 nm, differing pH_{PZC} values, and sodium, calcium, or potassium as counter ions were selected for study (Table 3-1). Molecular sieves 3A, 4A, 5A and 13X were obtained from Sigma-Aldrich and molecular sieve Y was from Strem Chemicals Inc. All purchased molecular sieves were used directly without purification. Molecular sieves Si-MS1.5, Si-MS3.2, and Si-MS4.7—which are pure silica molecular sieves with pore sizes of 1.5, 3.2 and 4.7 nm, respectively—were prepared according to Sierra and Guth (1999). Sodalite, a naturally occurring zeolite, was also included to test the applicability of the aluminum (hydr)oxide amendment method for modifying natural zeolites for fluoride removal. The sodalite used in this study was originally from Ayopaya, Bolivia and was purchased from Ward's Science. Sodalite pieces were crushed with a mortar and pestle and then sieved with No. 40 and 80 mesh sieves to retain the 180-425 μm fraction.

Aluminum (Hydr)oxide Amendment

Molecular sieves and sodalite were mixed with 0.6 M aluminum chloride (Sigma-Aldrich)—a concentration determined to be optimum in a preliminary study—at a solid-to-liquid ratio of 60 g/L. After mixing, the pH was immediately raised to 5.3 to maximize the precipitation of aluminum (hydr)oxide at slightly acidic pH while at the same time preventing the dissolution of molecular sieves at lower pH. Preliminary tests showed that molecular sieves and aluminum (hydr)oxide could be recovered at pH 5.3 without loss of mass due to dissolution. All the aluminum in the 0.6 M aluminum chloride solution was anticipated to precipitate at pH 5.3 based on the pH of minimum solubility (Cerqueira and da Costa Marques 2012), and most likely formed amorphous aluminum (hydr)oxide (Du et al. 2009), i.e., $Al^{3+} + 3\ OH^{-} = AlOOH_{am}(s) + H_2O$, on the surface and inside the pores of the molecular sieves.

After preparation, the mixture was agitated on a reciprocal shaker (Cole Palmer Ping-pong ™#51504) at 200 rounds per minute for five days. The solid was then filtered and repeatedly washed on the filter paper (Whatman, Qualitative filter paper, 150 mm diameter) with about four liters of nanopure water (18.2 MΩ-cm, Barnstead D8961). Next, samples were dried at 100 °C overnight and crushed with a mortar and pestle. The resulting aluminum (hydr)oxide amended molecular sieves are denoted Al-MS- (3A, 4A, 5A, 13X, or Y) for the purchased molecular sieves, and Al-Si-MS- (1.5, 3.2, or 4.7) for the synthesized molecular sieves. Likewise, the amended sodalite is denoted Al-sodalite. Pure aluminum (hydr)oxide without zeolite (AlOOH) was also prepared with procedures identical to those described above.

Fluoride Adsorption and Regeneration

The fluoride adsorption capacities of unamended and amended molecular sieves or zeolites as well as pure AlOOH (19 samples in total, Table 3-1) were determined via batch tests with solution fluoride concentrations ranging from 10 to 100 mg/L (10, 20, 30, 50, 60, 75, and 100 mg/L) (NaF, Fisher) and a 0.1 g/50 mL solid-to-solution ratio. The results were fit with Freundlich adsorption isotherms, and the adsorption capacity at an equilibrium dissolved fluoride concentration of 1.5 mg/L ($Q_{1.5}$, mg/g) was calculated from the Freundlich isotherm parameters. The pH of the batch adsorption experiments was maintained at 7 using 50 mM HEPES (4-(2-hydroxyethyl)-1-piperazineethanesulfonic acid, Sigma) buffer to simulate the pH of natural groundwater. Preliminary adsorption tests showed that there was no difference in the amount of fluoride adsorbed from a 50 mg/L fluoride solution at pH 7, whether or not 50 mM HEPES buffer was present, indicating that HEPES did not hinder or enhance fluoride adsorption. The duration of the batch experiments was 48 hours based on a preliminary kinetic study that showed a negligible change in fluoride concentration after 24 hours (SI Fig. S2). After 48-hours agitation at 200 rounds per minute on the reciprocal shaker, the solids were removed by filtration and the fluoride concentration in the solution measured by ion selective electrode. Duplicates were evaluated for each initial fluoride concentration.

Standard fluoride solutions (0.4, 1, 10, and 100 mg F^-/L) were measured to prepare a calibration curve; blanks were also measured to ensure fluoride measurement free of contamination. Before measurement, samples, standards, and blanks were

diluted with an equal volume of total ionic strength adjustment buffer (TISAB) to reduce interferences and maintain a constant pH and ionic strength during analysis (Frant and Ross 1968).

Table 3-1 Matrix of materials (unamended and amended molecular sieves (and zeolite) and pure AlOOH) tested in fluoride adsorption experiments

Adsorbent	Largest pore dimension (nm)[a]	pH_{PZC}	Counter ions	Al content (%)[b]
Unamended				
MS-3A	0.3	9.4	K^+ and Na^+	17.8
MS-4A	0.4	10.1	Na^+	19.0
MS-5A	0.5	8.0	Ca^{2+} and Na^+	19.5
MS-13X	1.0	8.2	Na^+	15.7
MS-Y	1.12	8.4	Na^+	0.2-15.7
Si-MS1.5	1.5	4.8	Not applicable (NA)	0
Si-MS3.2	3.2	5.7	NA	0
Si-MS4.7	4.7	8.3	NA	0
Sodalite	Not measured (NM)	NM	Na^+	16.7
Amended				
Al-MS-3A	NM	3.3	K^+ and Na^+	28
Al-MS-4A	NM	4.1	Na^+	28.8
Al-MS-5A	NM	4.5	Ca^{2+} and Na^+	28.9
Al-MS-13X	NM	4.5	Na^+	26.2
Al-MS-Y	NM	4.3	Na^+	24
Al-Si-MS1.5	NM	4.6	NA	16.9
Al-Si-MS3.2	NM	4.8	NA	16.9
Al-Si-MS4.7	NM	4.8	NA	16.9
Al-Sodalite	NM	NM	Na^+	27.3
Pure AlOOH	NM	NM	NA	45

[a] Wijntje et al. (2007) (MS-Y), Sierra and Guth (1999) (pure silicon molecular sieves), Sigma-Aldrich (MS-3A, 4A, 5A and 13X).

[b] The aluminum content was calculated by dividing the amount of aluminum, consisting of that from the molecular sieves (estimated from their formulas) and from the added aluminum (as AlOOH), by the total mass of the amended material. It was assumed that all the aluminum precipitated as AlOOH on the substrates and that no aluminum was lost during the amendment process.

Solutions of sodium hydroxide (Acros) at three concentrations (10^{-6}, 10^{-4}, and 0.1 M) were used to regenerate the adsorbents. Prior to regeneration, samples from adsorption experiments (the whole bottle containing 0.1 g adsorbent and 50 mL fluoride solution) were centrifuged for five minutes at 3,661 × g (Thermo Scientific IEC CL10) to remove the supernatant. Then, the remaining solids of about 0.1 g were mixed with 50 mL sodium hydroxide solution for one day to promote fluoride desorption and sorbent regeneration. Preliminary tests showed equal recoveries of fluoride adsorption capacity for regeneration times of one day and longer. After regeneration, the solution was again separated from the solids by centrifugation for 5 minutes at 3,661 × g. Then, a second (and sometimes third or fourth) fluoride adsorption batch experiment was performed as above. At each solid/solution separation, the actual weight of the solid adsorbent was measured after drying the solid at 105 ^{o}C overnight.

Adsorbent Characterization

The pH_{PZC} of amended and unamended molecular sieves was analyzed using the drift method (Herczynska 1964) by adding the solid sample to a series of potassium nitrate (EMD) solutions with initial pH values from 2 to 12, and equilibrating for 24 hours. The pH_{PZC} was considered to be the plateau in a plot of final versus initial pH. The specific surface area (SSA) of virgin and regenerated Al-MS-13X was measured with a Quantachrome Autosorb Automated Gas Sorption System with a Beckman Coulter SA-3100 Surface Area Analyzer and N_2 adsorption.

X-ray diffraction (XRD) characterization of materials was performed with a Rigaku Ultima IV powder X-ray diffractometer with Cu Kα radiation and Bragg-

Brentano optics. Mineral phases were identified using the Jade 6 software (Materials Data, Livermore, CA), and the powder diffraction file (PDF) of the International Center for Diffraction Data (ICDD) (PDF databases, ICDD, Newtown Square, PA, US). The scanning electron microscopy characterization along with the energy dispersive X-ray spectroscopy (SEM/EDS) was done on a Zeiss Neon SEM instrument operating at 5 kV or 10 kV of accelerating voltage after sputter coating with iridium.

Results and Discussion

Fluoride Adsorption

The Freundlich isotherm provided a good fit of the adsorption data (Fig. 3-1). The fluoride adsorption capacity at an equilibrium fluoride concentration of 1.5 mg/L, i.e., $Q_{1.5}$, was also calculated using the Freundlich parameters (Table 3-2). $Q_{1.5}$ is the most suitable indicator of the ability of adsorbents to lower the fluoride concentration in treated water to the World Health Organization (WHO) recommended level of 1.5 mg/L.

While most unamended molecular sieves had negligible adsorption (not shown), MS-3A, MS-4A, MS-5A, and sodalite had measurable adsorption capacities even without aluminum amendment (Table 3-2, Fig. 3-1C), suggesting that, in some situations, they might be favorable fluoride adsorbents even without amendment. These molecular sieves all possess the same sodalite framework structure, characterized by the arrangement of aluminosilicate tetrahetra with a cubo-octahedral cavity at center (Hussan and Grundy 1984). The higher fluoride adsorption of unamended molecular sieves A and sodalite compared to the others (Table 3-2) could be due to their high

aluminum content or high pH_{PZC} values (Table 3-1), both of which would favor fluoride adsorption.

Table 3-2 Values of $Q_{1.5}$ and normalized $Q_{1.5}$ of fluoride adsorbents. $Q_{1.5}$ values were calculated from Freundlich isotherm parameters unless otherwise specified. Values of normalized $Q_{1.5}$ were equal to the $Q_{1.5}$ divided by the mass fraction of aluminum (hydr)oxide loaded on the molecular sieves.

Adsorbent	$Q_{1.5}$ (mg/g)[f]	Normalized $Q_{1.5}$ (mg/g AlOOH)[f]
Unamended		
MS-3A	0.214±0.026	Not applicable (NA)
MS-4A	0.068±0.061	NA
MS-5A	0.118±0.067	NA
MS-13X	Negligible	NA
MS-Y	Negligible	NA
Si-MS1.5	Negligible	NA
Si-MS3.2	Negligible	NA
Si-MS4.7	Negligible	NA
Sodalite	0.0255±0.0066	NA
Amended		
Al-MS-3A	7.33±0.71	19.6±1.9
Al-MS-4A	7.70±0.88	20.5±2.4
Al-MS-5A	4.16±0.44	11.1±1.2
Al-MS-13X	11.8±0.6	31.4±1.7
Al-MS-Y	14.5±1.3	38.6±3.5
Al-Si-MS1.5	10.6±1.0	28.2±2.7
Al-Si-MS3.2	17.4±1.3	46.3±3.4
Al-Si-MS4.7	14.8±0.9	39.3±2.5
Al-Sodalite	23.7±2.0	63.2±5.3
Pure AlOOH	44.6±2.3	44.6±2.3
Regenerated		
Al-MS-13X (1 regeneration cycle)	3.63±0.49	12.2±1.6
Al-MS-13X (2 regeneration cycles)	1.42±0.07	5.90±0.29
Al-MS-13X (3 regeneration cycles)	0.048±0.039	0.25±0.20
Other studies		
Aluminum exchanged zeolite F-9[a]	4.66	—
Aluminum loaded natural zeolite[b]	0.92	—
Heat treated hydrated alumina[c]	27 (Langmuir)	27
Boehmite[d]	0.61 (Langmuir)	0.61
Aluminum (hydr)oxide[e]	22±7 (Langmuir)	22±7

[a] Onyango et al. (2004)

[b] Samatya et al. (2007)

[c] Shimelis et al. (2006)

[d] Jiménez-Becerril et al. (2012)

[e] Du et al. (2014)

[f] The uncertainties in $Q_{1.5}$ and normalized $Q_{1.5}$ values represent standard errors determined from error propagation.

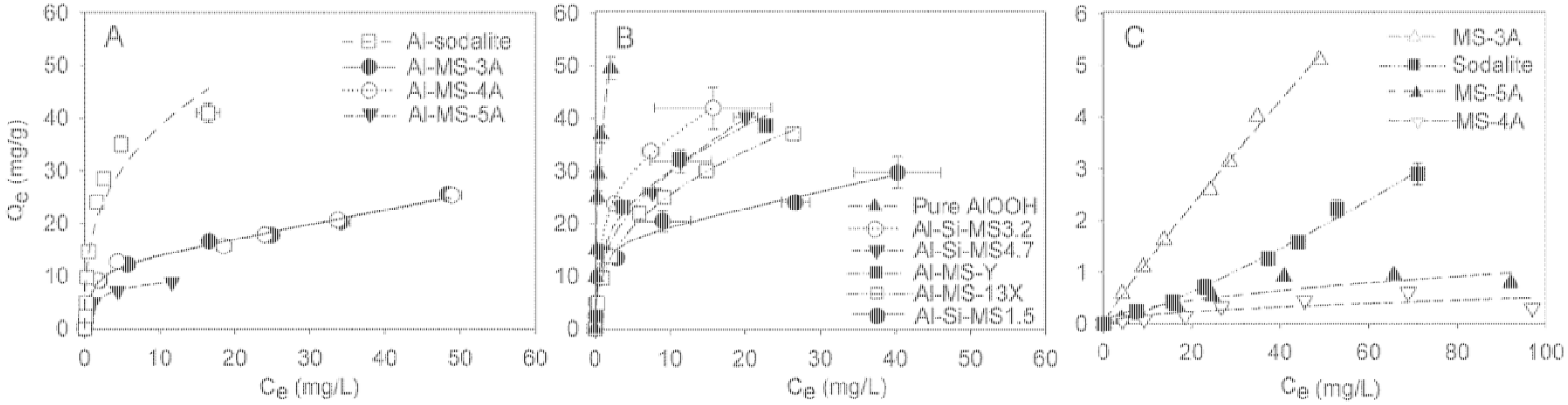

Figure 3-1 Fluoride adsorption to pure AlOOH, and to unamended and AlOOH-amended molecular sieves or zeolites (from Table 3-1) with Freundlich isotherm fits. Unamended molecular sieves with $Q_{1.5}$ values below 0.01 mg/g are not shown. The isotherms were divided into three panels for clarity. Vertical and horizontal error bars represent the standard deviations of Q_e (equilibrium fluoride adsorption densities) and C_e (equilibrium fluoride concentrations), respectively.

Amendment of all the molecular sieves and sodalite with aluminum (hydr)oxide resulted in significant improvement in fluoride adsorption capacity, with $Q_{1.5}$ values of up to 23.7 mg/g for Al-sodalite (Fig. 3-1, Table 3-2). These $Q_{1.5}$ values exceed those of other aluminum amended zeolites prepared by ion exchange (Onyango et al. 2004; Samatya et al. 2007) and are on par with synthesized aluminum (hydr)oxides (Du et al. 2014, Shimelis et al. 2006) in terms of fluoride adsorption (see Table 3-2). The comparatively high adsorption capacities of our amended molecular sieves as compared from others can be attributed to two factors. First, while the molecular sieves in this study were treated with $AlCl_3$ at pH 5.3, which is the minimum solubility of aluminum (hydr)oxide and thus expected to yield the most precipitated aluminum, other studies used molecular sieves treated with aluminum salts at very low pH values (Onyango et al. 2004, Samatya et al. 2007), resulting in only limited aluminum loaded on the zeolites, e.g., 0.24% (Samatya et al. 2007). And second, the aluminum (hydr)oxide formed in this study was amorphous as indicated by the absence of peaks in the XRD pattern that could be ascribed to crystalline aluminum (hydr)oxides (SI Fig. S3), unlike the aluminum (hydr)oxides prepared at pH 8-8.5 in Samatya et al. (2007), which were possibly boehmite (AlOOH) or bayerite ($Al(OH)_3$) (Du et al. 2009). Amorphous aluminum (hydr)oxide formed under acidic conditions has been found to have greater fluoride adsorption capacity than boehmite or bayerite prepared at basic pH values (Gong et al. 2012a).

Next, the $Q_{1.5}$ values of the amended molecular sieves and sodalite were normalized (divided) by the mass fraction of aluminum (hydr)oxide (37.5% by weight assuming that all the added aluminum precipitated as AlOOH) in the amended

molecular sieves (Table 3-1). Many normalized $Q_{1.5}$ values were less than or equal to the $Q_{1.5}$ of pure AlOOH (Table 3-2), meaning that in these cases, there was less fluoride adsorption to the same mass of aluminum (hydr)oxide when it had precipitated into the pores of the molecular sieve compared to aluminum (hydr)oxide precipitated without the molecular sieve, perhaps due to loss of accessible surface area. This trend, i.e., lower fluoride adsorption to some aluminum treated molecular sieves than to pure aluminum (hydr)oxide synthesized with the same mass of aluminum salt, is also apparent from Fig. 3-1. This effect (i.e., a lowering of the aluminum (hydr)oxide normalized $Q_{1.5}$ value in the presence of molecular sieves), was noted for all molecular sieves with pore sizes less than 1 nm (Table 3-1). On the other hand, Si-MS3.2 and Si-MS4.7, with pore sizes of 3.2 and 4.7 nm, respectively, had aluminum (hydr)oxide normalized $Q_{1.5}$ values similar to that for pure AlOOH (Table 3-2), perhaps because fluoride could access the aluminum (hydr)oxide precipitated in the larger pores. In fact, there was a slight correlation between values of normalized $Q_{1.5}$ and the pore size of the unamended molecular sieves (Fig. 3-2). While the slope of the regression line was statistically different from zero at the 95% confidence level, the coefficient of determination (0.546) indicates that pore size can explain only about 55% of the variance in $Q_{1.5}$, and those additional parameters, such as specific surface area, also influence adsorption capacity. Nonetheless, the limited data reported here suggest that the anticipated benefits of Al amended molecular sieves (i.e., better hydraulic performance in a column setup compared to pure AlOOH) are more likely to be achieved when using molecular sieves with larger pores.

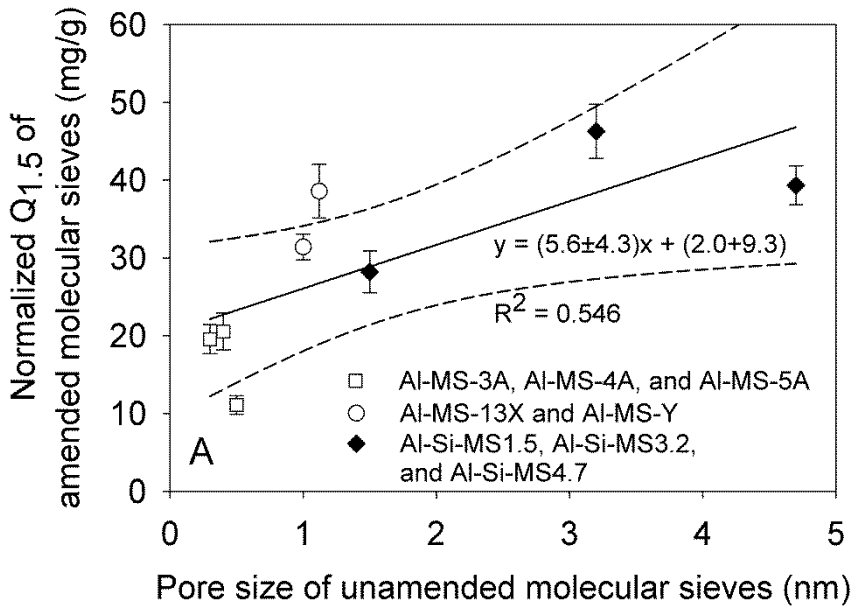

Figure 3-2 Correlation between the normalized $Q_{1.5}$ of amended molecular sieves and the pore size of the unamended molecular sieves. An linear regression equation (solid line) and 95% confidence intervals (indicated by the area enclosed by the dashed lines) are shown. The uncertainties associated with the slope and intercept correspond to the breadth of the 95% confidence interval band, which were calculated using the mean and standard errors of the slope and the intercept given by the linear regression equation. The 95% confidence interval band means that there is a 95% probability that the linear regression line describing the correlation of normalized $Q_{1.5}$ versus pore size of unamended molecular sieves falls within the band.

Monolayer adsorption of fluoride to the amended molecular sieves cannot by itself explain the high normalized adsorption capacities reported in Table 3-2. For example, assuming a diameter for hydrated fluoride of 0.52 nm (Emsley et al. 1990) and using the measured specific surface area for Al-MS-13X (40.1 m^2/g), the maximum fluoride adsorption capacity assuming monolayer coverage would equal approximately 6 mg/g. This is much less than the aluminum (hydr)oxide normalized $Q_{1.5}$ value of Al-MS-13X (31.4±1.7 mg/g, Table 3-2). Formation of an aluminum hydroxide-fluoride co-precipitate, in which fluoride is thought to enter the aluminum (hydr)oxide structure

by substituting for hydroxyl groups (Alfredo 2012), may account for the fluoride removal beyond monolayer coverage (Alfredo 2012, Gong et al. 2012b).

Concurrent with the change in fluoride adsorption capacity, a change in surface morphology was noted for the representative molecular sieve Al-MS-13X after amendment with $AlCl_3$. Specifically, the surface of unamended MS-13X (Fig. 3-3A) increased in roughness after amendment (Fig. 3-3B, circle), with the appearance of fine particles (Fig. 3-3B, arrows), that could be aluminum (hydr)oxide (Wang et al. 2014). In addition, the aluminum content of the molecular sieve increased from 12% to 15% after amendment, while the silicon and sodium contents decreased (Fig. 3-4).

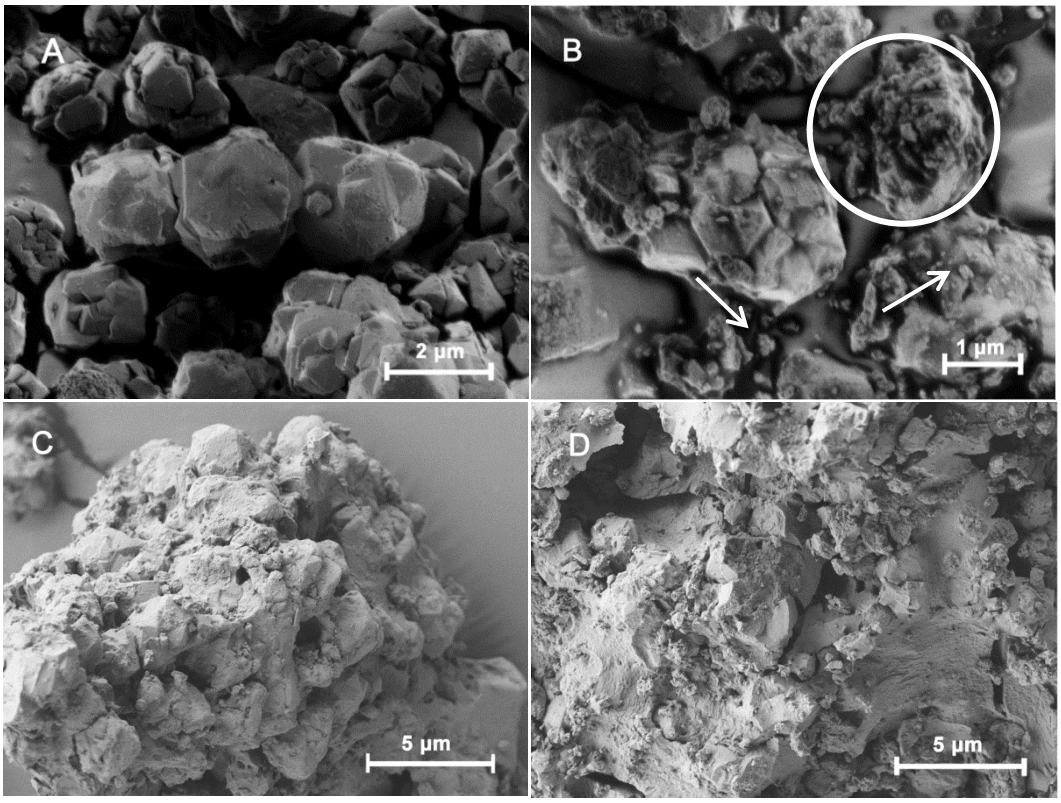

Figure 3-3 SEM images of MS-13X (A) before aluminum amendment, (B) after aluminum amendment, (C) after the second adsorption batch experiment and one regeneration cycle, and (D) after the fourth adsorption batch experiment and three regeneration cycles. The concentration of sodium hydroxide regenerant was 10^{-4} M.

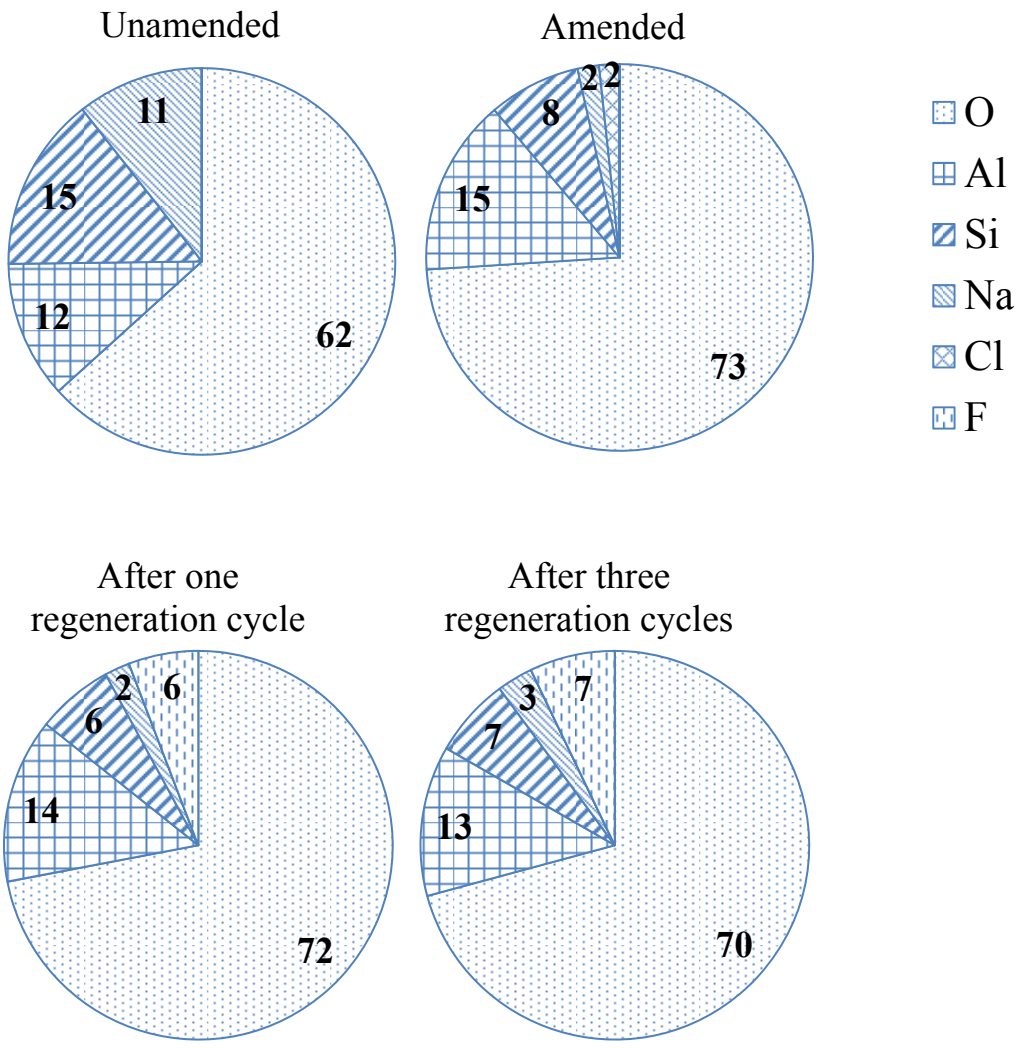

Figure 3-4 Elemental composition (by molar percent) of MS-13X: before aluminum (hydr)oxide amendment (corresponding to Fig. 3-3A), after amendment (corresponding to Fig. 3-3B), after one regeneration cycle (corresponding to Fig. 3-3C), and after three regeneration cycles.

XRD characterization was conducted for two samples, Al-MS-4A and Al-MS-13X, chosen since they represent two common molecular sieve groups: sodalite (Al-MS-4A), in which aluminosilicate tetrahedra enclose a cubo-octahedral cavity with square openings, and faujasite (Al-MS-13X), in which aluminosilicate tetrahedral units are stacked to generate a pore with a 12-membered ring opening. No diffraction peaks associated with aluminum (hydr)oxide were found in either sample (SI Fig. S3), indicating that the precipitated aluminum (hydr)oxide was amorphous, consistent with the findings of Li et al. (2001), Tchomgui-Kamga et al. (2010), and Ganvir and Das (2011). The estimated proportion of aluminum (hydr)oxide in the amended materials (37.5% wt.) greatly exceeds the XRD detection limit, estimated to be 2% wt. (Smith 1999), so the lack of aluminum (hydr)oxide peaks in the XRD pattern is not due to concentrations below detection limits. The XRD pattern of Al-MS-4A was best matched by Zeolite A (Na) (PDF 31-1261), while that for Al-MS-13X best matched Faujasite-Na (PDF 12-0228).

Experiments were conducted in which the fluoride adsorption capacities were measured after each regeneration cycle. Unlike other reports (Liao and Shi 2005, Maliyekkal et al. 2008, Zhang et al. 2012), use of 0.1 M sodium hydroxide as the regenerant led to poor fluoride removal efficiency in subsequent adsorption experiments (Fig. 3-5). This was most likely due to dissolution and loss of molecular sieves at high pH, since the mass of molecular sieves went from 0.1 g to less than 0.04 g after regeneration with 0.1 M sodium hydroxide. By contrast 60-80% of the original fluoride removal efficiency was recovered after regeneration when using 10^{-4} M (pH 9.6) or 10^{-6} M (pH 6.8) sodium hydroxide solutions (Fig. 3-5).

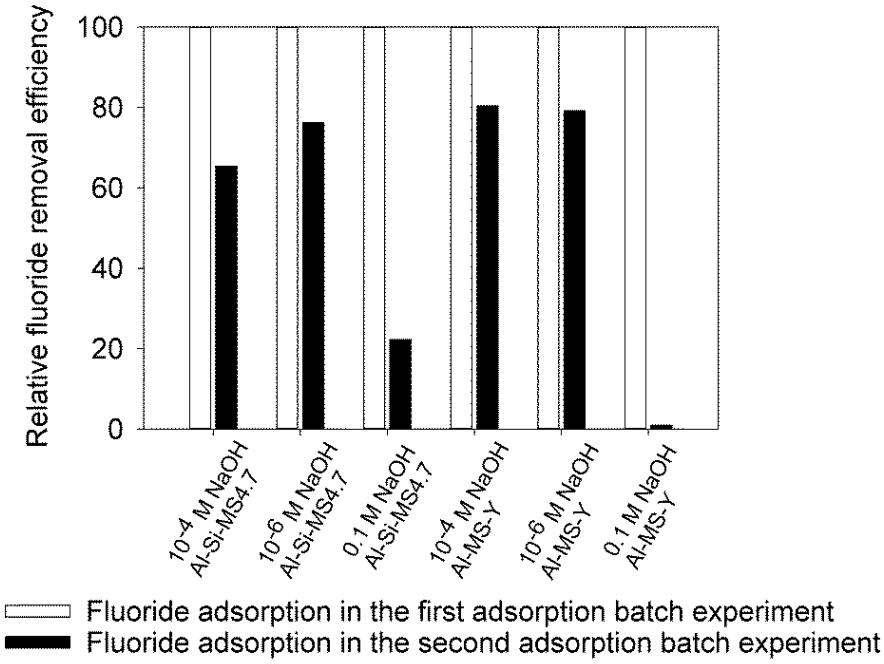

Figure 3-5 Relative fluoride removal efficiency, expressed as the fluoride adsorption capacity divided by that before regeneration (as %) for Al-Si-MS4.7 and Al-MS-Y. The initial fluoride concentration was 100 mg/L for all the tests.

Regeneration Performance of Aluminum (Hydr)oxide Amended Molecular Sieves

With 10^{-4} M sodium hydroxide solution, Al-MS-13X showed the highest recovery in fluoride adsorption capacity among all the amended materials after one regeneration cycle (SI Fig. S4). Thus, Al-MS-13X, which is the most promising of the amended molecular sieves when considering repeated-use, was selected for the following multiple-regeneration tests. For multiple regenerations of Al-MS-13X using 10^{-4} M sodium hydroxide, there was a decrease in $Q_{1.5}$ after each regeneration cycle (Fig. 3-6 and Table 3-2). Despite a progressive decline, however, Al-MS-13X still exhibited a $Q_{1.5}$ of 2.21 ± 0.11 mg/g after two regeneration cycles. The use of this material may not

be justified after further regeneration cycles, however, due to the quite low $Q_{1.5}$ value (0.094±0.076 mg/g) measured in the fourth adsorption batch experiment.

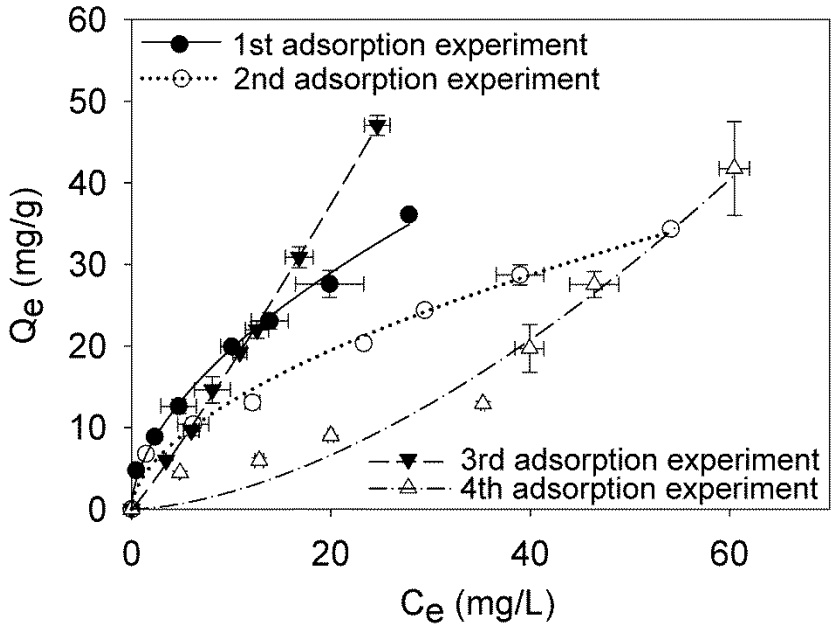

Figure 3-6 Fluoride adsorption to Al-MS-13X before and after regeneration with Freundlich isotherm fits. Vertical and horizontal error bars represent the standard deviations of Q_e (equilibrium fluoride adsorption densities) and C_e (equilibrium fluoride concentrations), respectively.

A close inspection of SEM results showed that particles of regenerated Al-MS-13X (Fig. 3-3C and D) were distinct from those before adsorption (Fig. 3-3B). In contrast with the initial grain size of approximately 2 μm (Fig. 3-3B), after regeneration and further adsorption, particles grew to large grains of more than 20 μm (Fig. 3-3C and D). These large grains seemed to be composed of small particles resembling those before adsorption and regeneration (Fig. 3-3B). Despite this apparent particle aggregation, however, there was a slight increase in surface area (from 40.1 m^2/g for

Al-MS-13X (shown in Fig. 3-3B) to 73.8 m^2/g after three regeneration cycles (shown in Fig. 3-3D).

In addition to the changes seen by SEM, there was a downward trend in the aluminum content from 15% (by molar fraction) in Al-MS-13X before any fluoride adsorption to 13% after multiple regeneration-adsorption cycles (Fig. 3-4), coinciding with a decrease in $Q_{1.5}$ (Table 3-2). In addition, up to 7% fluorine was detected in the regenerated Al-MS-13X (Fig. 3-4). The high fluorine content is consistent with fluoride removal by more than monolayer adsorption, which in theory would yield only approximately 0.6% (by molar fraction) fluoride in the solid. The high fluorine content in the regenerated adsorbent might be explained by formation of a fluoride-containing precipitate such as aluminum trifluoride (AlF_3) or cryolite (Na_3AlF_6). However, the lack of new peaks in the XRD pattern of Al-MS-13X after three regeneration cycles (not shown) means that any fluorine-containing mineral products that may have formed in the adsorbents were amorphous or below the XRD detection limits. The disappearance of chlorine from the solid (Fig. 3-4) could be due to the exchange of chloride with fluoride (Gong et al. 2012a), or to the dissociation of loosely bound chloride from the surface during adsorption and regeneration.

Conclusions

Several molecular sieves that possessed the sodalite structure and that had relatively high aluminum contents and pH_{PZC} values (MS-3A, MS-4A, MS-5A, and sodalite) showed moderate adsorption of fluoride without any aluminum amendment. All the molecular sieves had a significant improvement in fluoride adsorption capacity when

amended with aluminum chloride in order to precipitate aluminum (hydr)oxide. In some cases, the mass-normalized adsorption capacities of the aluminum amended molecular sieves were less than that of an equivalent mass of pure AlOOH, perhaps because aluminum (hydr)oxide precipitated in small pores that were then not accessible for fluoride adsorption. For several molecular sieves with pores of one to several nanometers, however, the mass-normalized fluoride adsorption capacities were similar to that of pure AlOOH. These materials (Al-MS-Y, Al-Si-MS3.2, Al-Si-MS4.7, and Al-sodalite) are the best candidates for column applications, since they possess the high adsorption capacity of nanoparticulate aluminum (hydr)oxide, but the larger bulk particle size of the molecular sieves.

The normalized adsorption capacities of most aluminum (hydr)oxide amended molecular sieves exceeded the maximum theoretical fluoride adsorption capacity assuming monolayer coverage, suggesting that in addition to adsorption, other processes, such as co-precipitation, were responsible for fluoride removal. The amended molecular sieves showed the ability to be regenerated and to partially recover fluoride adsorption capacities. However, the continuous decrease in $Q_{1.5}$ upon regeneration, most likely due a loss in aluminum, made the amended molecular sieves less effective after repeated uses.

References

Agarwal, M., Rai, K., Shrivastav, R. and Dass, S. (2003). “Deflouridation of water using amended clay." J. Clean. Prod., 11(4): 439-444.

Alfredo, K. A. (2012). Drinking water treatment by alum coagulation: competition among fluoride, natural organic matter, and aluminum. Ph.D. dissertation. The University of Texas at Austin.

Brunson, L. R. and Sabatini, D. A. (2015). “Role of Surface Area and Surface Chemistry during an Investigation of Eucalyptus Wood Char for Fluoride Adsorption from Drinking Water." J. Environ. Eng., 141(2): 04014060.

Cerqueira, A. A., and da Costa Marques, M. R. (2012). Electrolytic Treatment of Wastewater in the Oil Industry. In: Gomes, J. S. (Eds.), *New Technologies in the Oil and Gas Industry*, INTECH Open Access Publisher, 1-28.

Daifullah, A. A. M., Yakout, S. M. and Elreefy, S. A. (2007). “Adsorption of fluoride in aqueous solutions using $KMnO_4$-modified activated carbon derived from steam pyrolysis of rice straw." J. Hazard. Mater. 147(1-2): 633-643.

Davis, M. E. and Lobo, R. F. (1992). “Zeolite and molecular sieve synthesis." Chem. Mater. 4(4): 756-768.

Du, J., Sabatini, D. A. and Butler, E. C. (2014). “Synthesis, characterization, and evaluation of simple aluminum-based adsorbents for fluoride removal from drinking water." Chemosphere 101(0): 21-27.

Du, X., Wang, Y., Su, X., and Li, J. (2009). “Influences of pH value on the microstructure and phase transformation of aluminum hydroxide”. Powder Technol. 192(1): 40-46.

Edmunds, W. M. and Smedley, P. (2013). Fluoride in Natural Waters. In: O. Selinus (Eds.), *Essentials of Medical Geology*, Springer, Netherlands, 311-336.

Emsley, J., Arif, M., Bates, P. A. and Hursthouse, M. B. (1990). “Hydrogen bonding between free fluoride ions and water molecules: two X-ray structures." J. Mol. Struct. 220(0): 1-12.

Frant, M and Ross, Jr. J. W. (1968) Use of a total ionic strength adjustment buffer for electrode determination of fluroide in water supplies. Anal. Chem. 40(7): 1169-1171.

Ganvir, V. and Das, K. (2011). “Removal of fluoride from drinking water using aluminum hydroxide coated rice husk ash." J. Hazard. Mater. 185(2-3): 1287-1294.

Gomez, M. L., Blarasin, M. T. and Martínez D. E. (2009). “Arsenic and fluoride in a loess aquifer in the central area of Argentina." Environ. Geol. 57(1): 143-155.

Gómez-Hortigüela, L., Pérez-Pariente, J., García R., Chebude Y. and Díaz I. (2013). “Natural zeolites from Ethiopia for elimination of fluoride from drinking water." Sep. Purif. Technol. 120(0): 224-229.

Gong, W.-X., Qu, J.-H., Liu, R.-P. and Lan, H.-C. (2012a). “Adsorption of fluoride onto different types of aluminas." Chem. Eng. J. 189-190(0): 126-133.

Gong, W.-X., Qu, J.-H., Liu, R.-P. and Lan, H.-C. (2012b). “Effect of aluminum fluoride complexation on fluoride removal by coagulation." Colloid. Surface. A 395(0): 88-93.

Herczynska, E. (1964). “Adsorption isotherms of potential determining ions." J. Inorg. Nucl. Chem. 26(12): 2127-2133.

Jagtap, S., Yenkie, M. K., Labhsetwar N. and Rayalu S. (2012). “Fluoride in drinking water and defluoridation of water." Chem. Rev.: 112(4), 2454-2466.

Jiménez-Becerril, J., Solache-Ríos, N. and García-Sosa, I. (2012), "Fluoride removal from aqueous solutions by boehmite." Water Air Soil Poll. 223: 1073-1078.

Jiménez, N. and López-Velásquez, S. (2008). “Magmatism in the Huarina belt, Bolivia, and its geotectonic implications." Tectonophysics 459(1-4): 85-106.

Johnson, C. A. and Bretzler, A. (2015). Geogenic Contamination Handbook. Dübendorf, Eawag: Swiss Federal Institute of Aquatic Science and Technology.

Kau, P. M. H., Smith, D. W. and Binning, P. (1998). “Experimental sorption of fluoride by kaolinite and bentonite." Geoderma 84(1-3): 89-108.

Li, Y.-H., Wang, S., Cao, A., Zhao, D., Zhang, X., Xu, C., Luan, Z., Ruan, D., Liang, J., Wu, D. and Wei, B. (2001). “Adsorption of fluoride from water by amorphous alumina supported on carbon nanotubes." Chem. Phys. Lett. 350(5-6): 412-416.

Liao, X.-p. and Shi, B. (2005). “Adsorption of fluoride on zirconium(IV)-impregnated collagen fiber." Environ. Sci. Technol. 39(12): 4628-4632.

Loganathan, P., Vigneswaran, S., Kandasamy, J. and Naidu, R. (2013). “Defluoridation of drinking water using adsorption processes." J. Hazard. Mater. 248-249(0): 1-19.

Luo, F. and Inoue, K. (2004). “The removal of fluoride ion by using metal(III)-loaded amberlite resins." Solvent Extr. Ion Exc. 22(2): 305-322.

Majumdar, N., Mukherjee, A. L. and Majumdar, R. K. (2009). “Mixing hydrology and chemical equilibria in Bakreswar geothermal area, Eastern India." J. Volcanol. Geoth. Res. 183(3-4): 201-212.

Maliyekkal, S. M., Shukla, S., Philip, L. and Nambi, I. M. (2008). “Enhanced fluoride removal from drinking water by magnesia-amended activated alumina granules." Chem. Eng. J. 140(1-3): 183-192.

Meenakshi, S. and Viswanathan, N. (2007). “Identification of selective ion-exchange resin for fluoride sorption." J. Colloid Interf. Sci. 308(2): 438-450.

Mohapatra, M., Anand, S., Mishra, B., Giles, D. and Singh, P. (2009). “Review of fluoride removal from drinking water." J. Environ. Manage. 91: 67-77.

Mondal, D., Gupta, S., Reddy, D. V. and Nagabhushanam, P. (2014). “Geochemical controls on fluoride concentrations in groundwater from alluvial aquifers of the Birbhum district, West Bengal, India." J. Geochem. Explor. 145(0): 190-206.

Onyango, M. S., Kojima, Y., Aoyi, O., Bernardo, E. C. and Matsuda, H. (2004). “Adsorption equilibrium modeling and solution chemistry dependence of fluoride removal from water by trivalent-cation-exchanged zeolite F-9." J. Colloid Interf. Sci. 279(2): 341-350.

Samatya, S., Yüksel, Ü., Yüksel, M. and Kabay, N. (2007). “Removal of Fluoride from Water by Metal Ions (Al^{3+}, La^{3+} and ZrO^{2+}) Loaded Natural Zeolite." Sep. Sci. Technol. 42(9): 2033-2047.

Shimelis, B., Zewge, F. and Chandravanshi, B. S. (2006). “Removal of excess fluoride from water by aluminum hydroxide." Chem. Soc. Ethiopia 20(1): 17-34.

Sierra, L. and Guth, J. L. (1999). “Synthesis of mesoporous silica with tunable pore size from sodium silicate solutions and a polyethylene oxide surfactant." Micropor. Mesopor. Mat. 27(2-3): 243-253.

Smith, F. (Ed.) (1999). Industrial applications of X-ray diffraction. CRC Press. pp. 394.

Sperry, J. M. and Peirce, J. J. (1995). "A model for estimating the hydraulic conductivity of granular material based on grain shape, grain size, and porosity." Groundwater 33(6): 892-898.

Tchomgui-Kamga, E., Alonzo, V., Nanseu-Njiki, C. P, Audebrand, N., Ngameni, E. and Darchen, A. (2010). “Preparation and characterization of charcoals that contain dispersed aluminum oxide as adsorbents for removal of fluoride from drinking water." Carbon 48(2): 333-343.

Thompson, R. N., Gibson, S. A., Mitchell, J. G., Dickin, A. P., Leonardos, O. H., Brod, J. A. and Greenwood, J. C. (1998). “Migrating cretaceous–eocene ,agmatismin the Serra do Mar Alkaline Province, SE Brazil: Melts from the deflected trindade mantle plume?" J. Petrol. 39(8): 1493-1526.

Tomar, V. and Kumar, D. (2013). “A critical study on efficiency of different materials for fluoride removal from aqueous media." Chem. Cent. J. 7(1): 51.

Vyas, R. K. and Kumar, S. (2004). “Determination of micropore volume and surface area of zeolite molecular sieves by DR and DA equations: A comparative study." Indian J. Chem. Technol. 11: 704-709.

Wang, N., Fu, Y., Liu, Y., Yu, H. and Liu, Y. (2014). “Synthesis of aluminum hydroxide thin coating and its influence on the thermomechanical and fire-resistant properties of wood." Holzforschung 68(7): 781-789.

WHO (2008). Safe water, better health. WHO, Geneva.

Wijntje, R., Bosch, H., de Haan, A. B. and Bussmann, P. J. T. (2007). “Influencing the selectivity of zeolite Y for triglycine adsorption." J. Chromatogr. A 1142(1): 39-47.

Yami, S., Du, J., Brunson, L. R., Chamberlain, J. C., Butler, E. C. and Sabatini, D. A. (2015). “Life cycle assessment of adsorbents for fluoride removal from drinking water in East Africa." Int. J. Life Cycle Ass. 20: 1277-1286.

Yokoi, T., Tatsumi, T. and Yoshitake, H. (2004). “Fe^{3+} coordinated to amino-functionalized MCM-41: an adsorbent for the toxic oxyanions with high capacity, resistibility to inhibiting anions, and reusability after a simple treatment." J. Colloid Interf. Sci. 274(2): 451-457.

Zhang, G., He, Z. and Xu, W. (2012). “A low-cost and high efficient zirconium-modified-Na-attapulgite adsorbent for fluoride removal from aqueous solutions." Chem. Eng. J. 183(0): 315-324.

Chapter 4 : Evaluation of aluminum (hydr)oxide and aluminum (hydr)oxide-amended zeolites for drinking-water fluoride filtration

Introduction

Although the health impacts (dental and skeletal fluorosis) of excessive fluoride intake from drinking-water have been recognized for decades (Largent 1961, Krishnamachari 1986, Edmunds and Smedley 2013), the challenge of removing fluoride from drinking-water is still formidable. Currently, endemic fluorosis is prevalent in at least 25 countries (UNICEF 2003) and affects over 200 million people in the world (UNICEF 1999), a majority of whom live in developing countries. Every year dozens of novel materials are developed for fluoride treatment (Ayoob et al. 2008, Jagtap et al. 2012, Tomar and Kumar 2013). Among them, aluminum (hydr)oxide (AlOOH) and AlOOH-amended zeolites were promising candidates due to their high fluoride removal capacity determined in batch adsorption studies (Shimelis e al. 2006, Gong et al. 2012, Du et al. 2014, Du et al. 2016). Nevertheless, column fluoride removal studies are needed for these AlOOH-based materials to help bridge the gap between batch experiments and practical implementation (Maji et al. 2007).

Aluminum (hydr)oxides are precipitated AlOOH colloids produced by mixing aluminum salt with base (Shimelis et al. 2006, Gong et al. 2012). The synthesis of aluminum (hydr)oxides can be achieved in a simple system with common chemicals (e.g., aluminum chloride and sodium hydroxide), and at room temperature and ambient pressure (Du et al. 2014). Owing to the low crystallinity, the prepared AlOOH exhibited very high fluoride removal capacity (Du et al. 2014, Du et al. 2016). Aluminum (hydr)oxides can also be loaded on zeolites (Onyango et al. 2004, Samatya

et al. 2007, Du et al. 2016). Zeolites are widely-distributed naturally occurring minerals available in many areas where endemic fluorosis prevails, e.g., stilbite in the Rift Valley in Ethiopia (Gómez-Hortigüela et al. 2013) and sodalite in the Chacopampean plain in Argentina (Gomez et al. 2009). Zeolites such as sodalite and MS-13X have a porous structure and large surface areas which allow for amendment with high loading of aluminum (hydr)oxides (Vyas and Kumar 2004). Through coupling AlOOH with substrate zeolites, the fluoride removal capacity of raw zeolites was significantly improved (Du et al. 2016).

During preparation of AlOOH-amended zeolites, parameters such as substrate zeolite size, aluminum concentration, and pH levels used during AlOOH precipitation might affect column performance. While the aluminum concentration used in the amendment can alter the amount of precipitated AlOOH, the pH in material preparation can affect the crystallinity and fluoride removal capacity of AlOOH as the basic pH (e.g., 9) facilitated the formation of crystalline boehmite (AlOOH) which is unfavorable to fluoride adsorption (Gong et al. 2012, Du et al. 2016). Hence, the first objective was to investigate the effects of pH and aluminum loading on the column performance of studied materials.

Aluminum leaching is a potential risk of using aluminum-based materials (Doshi et al. 2008) as elevated aluminum in drinking-water might damage human neural system and bones (Boegman and Bates 1984). Because of the susceptibility of AlOOH to fluoride-induced dissolution (Roberson and Hem 1969), the second objective was to monitor the aluminum concentration in the column effluent and understand the aluminum release pattern during column operation when using pure AlOOH and

AlOOH-amended zeolites. Currently, there is no agreed on maximum acceptable toxicant concentration of aluminum in drinking-water (Flaten 2001, Soni et al. 2001) for the formulation of compulsory standard. In the absence of enforceable standards, the World Health Organization drinking-water standard (WHO 2004) of 0.2 mg/L, which takes into account the potential health risk of aluminum, is used as a reference.

In addition, the adsorption capacity of some fluoride adsorbents was reported to decrease in the presence of natural solutes, e.g., phosphate and silicate, in groundwater, particularly when these solutes occur at high concentrations (Sujana et al. 1998, Cai et al. 2012). Due to their high concentrations and valence, phosphate and silicate may occupy a portion of adsorption sites of AlOOH and make them inaccessible to fluoride (Cai et al. 2012, Sujana et al. 1998). For example, the competition between phosphate and fluoride reduced the removal capacity of alum sludge by 60 percent compared to the control without competing solutes (Sujana et al. 1998). And natural organic matter was able to compete with fluoride over surface bonding sites on aluminum-based coagulants (Alfredo 2012). Thus, the third objective was to examine the potential competitive adsorption effect between fluoride and several common solutes in the groundwater (sulfate, bicarbonate, silicate, and pyromellitic acid as a surrogate for natural organic matter) for pure AlOOH and AlOOH-amended zeolites.

Considering limited access to energy and the low-income level in many endemic fluorosis areas, the use of fluoride removal materials must be affordable by local communities with respect to energy consumption and material production cost (Freenstra et al. 2007). As a means to reduce the production cost, regeneration is usually conducted to release the adsorbed fluoride for repeated use of adsorbents

(Ghorai and Pant 2004). The last objective was thus to determine the energy consumption in column operation and the regenerability of pure AlOOH or AlOOH-amended zeolite in fluoride removal. For brevity, the term "zeolite" is used below to refer to both natural and synthetic (molecular sieves) zeolites.

Materials and Methods

Preparation of pure AlOOH and AlOOH-amended zeolites

For the preparation of pure AlOOH, methods in Du et al. (2014) for the materials used in competitive adsorption tests and Du et al. (2016) for the materials used in column experiments were used. Although the procedure in Du et al. (2014) is slightly different from that in Du et al. (2016) as extra sulfate was added to the synthesis solution to reduce the crystallization of AlOOH in the former method, both AlOOH minerals formed with two methods were amorphous and presented comparable fluoride removal capacity (Du et al. 2014, Du et al. 2016). Pure AlOOH was dried at 70 °C overnight and then sieved with No. 40 and 80 mesh sieves to retain the 180-425 μm fraction.

For AlOOH-amended zeolites, two different sizes of sodalite (Ward's Science) (average size 0.3 and 1 mm) or two types of molecular sieve 13X (Sigma-Aldrich) (2 μm powder and 2 mm beads) were mixed with aluminum chloride (Sigma-Aldrich) of varying concentrations (0.05, 0.2, or 0.6 M) at a solid-to-liquid ratio of 60 g/L. After addition of aluminum chloride to the zeolites, the pH of the mixture was adjusted to 5.3 or 8.2 immediately with 5 M sodium hydroxide (Acros) to precipitate AlOOH. For a pH value between 3 and 11, almost all the aluminum in the solution of 0.6 M aluminum is expected to precipitate (Cerqueira and da Costa Marques 2012). After pH

adjustment, the mixture was agitated on a reciprocal shaker (Cole Palmer Ping-pong ™#51504) at 200 rounds per minute for five days at room temperature. Next, the AlOOH-amended zeolites were separated with filter paper (Whatman Grade 1) and washed thoroughly with 4 L of nanopure water (18.2 MΩ-cm, Barnstead D8961). Afterwards, samples were dried at 70 °C overnight and sieved to retain the fraction of target sizes (> 1.4 mm, 0.6-1.4 mm, or 0.180-0.425 mm). Abbreviations of AlOOH-amended zeolites are denoted in Table 4-1 along with their preparation procedures; for example, 0.6Al-sodalite-5.3-0.3 denotes that 0.6 M AlOOH was precipitated at pH 5.3 on sodalite with an average size of 0.3 mm.

Column Adsorption and Regeneration

A small column was employed in this study as a model for large scale filters that are used in the field. According to Crittenden et al. (1986), results of the small scale column test can provide similar fluoride removal capacity to those of large scale filters but with reduced time and cost. With the small column, fluoride removal materials were evaluated in terms of service time, energy consumption, and cost of materials. The service time is the duration of column operation before breakthrough when the effluent fluoride concentration reaches 1.5 mg/L (WHO recommended level) at an initial concentration of 10 mg/L.

Table 4-1 Adsorbent materials used in the column fluoride adsorption experiments

Adsorbent abbreviations	Zeolite particle size used to support precipitating AlOOH (mm)	Average particle size of zeolite (mm)	Aluminum concentration used in AlOOH precipitation (M)	pH used in AlOOH precipitation
0.6Al-sodalite-5.3-0.3	0.180 – 0.425	0.3	0.6	5.3
0.6Al-sodalite-5.3-1	0.60 – 1.40	1	0.6	5.3
0.6Al-sodalite-8.2	0.180 – 0.425	0.3	0.6	8.2
0.2Al-sodalite-5.3	0.180 – 0.425	0.3	0.2	5.3
0.05Al-sodalite-5.3	0.180 – 0.425	0.3	0.05	5.3
0.6Al-MS-13X-2μm	0.002	0.3	0.6	5.3
0.6Al-MS-13X-2mm	1 – 3	2	0.6	5.3
Pure AlOOH	0.180 – 0.425	0.3	0.6	5.3

Glass columns were used to conduct fluoride adsorption experiments (1 cm diameter, Ace-Glass Adjusta-Chroma) with their inlet and outlet ends connected to a peristaltic pump (Cole-Palmer Masterflex) and a fraction collector (Pharmacia LKB-Frac-100), respectively, via silicone tubing (inner diameter of 0.3175 cm) (SI Fig. S5). For each experiment, five centimeters of adsorbent were filled into the column which resulted in an empty bed volume of 3.93 mL (determined from the height of packed material and diameter of the column). A constant upflow of fluoride-spiked water at 0.6 mL/min was pumped through the column continuously and the resulting empty bed contact time was 6.5 minutes. A 10 mg/L fluoride solution was prepared by adding sodium fluoride (Fisher) to deionized water (conductivity of 6 μS/cm) and used throughout the study. The influent pH was fixed at 7 with 50 mM HEPES buffer (4-(2-hydroxyethyl)-1-piperazineethanesulfonic acid, Sigma). The pH of effluent was constant at pH 7 after about 30 bed volumes until column exhaustion (effluent concentration equals 10 mg/L) when using HEPES buffer. Effluent was collected by a fraction collector. In addition, a pressure gauge with a range of 0-41.4 kPa (0-6 psi) (Kodiak Controls, Inc., Illinois) or 0-206.8 kPa (0-30 psi) (Zenport Industries, Oregon) was connected to the tubing before entering the column to monitor the inlet pressure over the course of column operation.

In-situ column regeneration experiments were undertaken with the same flow rate (0.6 mL/min) and direction (upward) as column adsorption. The reason for using column instead of batch regeneration is to prevent the loss of adsorbents, which have fine particle size, during transferring adsorbents to and decanting regenerant from batch containers. The same flow direction as adsorption was adopted to minimize the

disturbance of materials. Before regeneration, column adsorption was run up to the breakthrough point. Afterwards, the influent was switched to a regenerant solution containing sodium hydroxide to desorb the fluoride from the adsorbent. Considering that fluoride can be desorbed at high pH (Sujana and Anand 2010), two concentration levels (10^{-4} and 0.01 M) of sodium hydroxide were used. Sodium hydroxide concentrations above 0.01 M were not attempted since AlOOH and zeolites were dissolved at pH greater than 12 in preliminary tests. After the first round of adsorption-regeneration, new cycles continued until it was not efficient to pursue further regeneration. Regeneration was discontinued if the volume of sodium hydroxide solution consumed during regeneration exceeded the volume of fluoride-safe water produced in the following adsorption stage.

Effluent Fluoride and Aluminum Analysis

The fluoride concentration in the effluent was determined by ion selective electrode (Thermo-scientific Orion). The fluoride electrode was calibrated daily by measuring the electro-potential of standard fluoride solutions (0.4, 1, 10, and 100 mg F^-/L). Blanks (deionized water) were also tested daily to ensure contamination-free measurement. Total ionic strength adjustment buffer (TISAB), which contains 1 M sodium hydroxide, 1 M acetic acid/sodium acetate buffer, and 4 g/L 1,2 cyclohexylenedinitrilotetraacetic acid, was used to dilute samples, standards and blanks with an equal volume ratio prior to measurement. The TISAB serves to maintain a constant pH and ionic strength during analysis, and to prevent the formation of metal-fluoride complex during the analysis (Frant and Ross 1968).

A number of effluent samples were collected at different times during column operation for aluminum analysis. In the first eight hours of column operation when the effluent contained visible suspended solids, aliquots of sampled effluent were filtered through 0.2 μm membrane (PTFE, Fisher). The filtered and unfiltered samples were subsequently acidified with concentrated nitric acid (two drops, Fisher trace metal grade) and preserved at 4°C. A control sample was also prepared by acidifying deionized water with concentrated nitric acid. Sample analysis was performed by the Ana-lab Corp. (Kilgore, Texas). The Environmental Protection Agency standard method EPA 200.8 (EPA 1994) was used for aluminum measurement. The actual aluminum concentration was obtained by subtracting the value in the control, which was 0.0117 mg/L, from those in the samples. Additionally, the aluminum content in four solid AlOOH-amended zeolites (sodalite or MS-13X) was analyzed by the Ana-lab Corp. (Kilgore, Texas) following the EPA standard method EPA 6020A (EPA 2004).

Competitive Adsorption

Fluoride removal capacity of pure AlOOH was determined via batch tests in the presence of competing solutes (sulfate (Na_2SO_4, Acros), bicarbonate ($NaHCO_3$, Fisher), silicate (Na_2SiO_3, Fluka), and pyromellitic aicd ($C_{10}H_6O_8$, Sigma-Aldrich)). These solutes represent common species in groundwater that are most likely to compete with fluoride adsorption (Rango et al. 2012). Pyromellitic acid is regarded as a good substitute for natural organic matter (NOM) in adsorption studies due to its similar adsorption behavior to NOM (Evanko and Dzombak 1998). In each batch experiment, one of four competing solutes with concentration of 5 mM was added to solution

containing 20 mg/L (1.05 mM) fluoride (pH maintained at 8.5 with Tris buffer (Tris(hydroxymethyl)aminomethane, Sigma-Aldrich)) at a 0.1 g/50 mL solid-to-solution ratio. Although the solute concentration of 5 mM surpasses that common in natural groundwater and the pH of 8.5 is close to the high-end of typical groundwater pH range (7-8.5) (Liao et al. 2011), these conditions were selected to amplify the possible competition effects and to simulate the worst scenario in the field (due to the strongest interference from hydroxide for fluoride adsorption at pH 8.5). Batch experiments lasted for 48 hours on the reciprocal shaker agitated at 200 rounds per minute as a negligible change in fluoride concentration was observed after 48 hours. Duplicate samples were tested for each competitive solute to calculate the uncertainties associated with fluoride removal capacity.

Energy Consumption and Production Cost Estimation

Household and community-scale columns are two common filtration approaches used for fluoride treatment in developing countries (Onyango and Matsuda 2006). When using these filters, energy consumption needs to be estimated for the design and selection of energy supply systems (e.g., pump station or elevated water tanks). Two scenarios were thus considered in energy consumption calculations including a household filter to provide 50 L water per day (10 people at 5 L per day) (length of 30 cm and diameter of 4.8 cm) and a community-scale filter to provide 500 L water per day (100 people at 5 L per day) (length of 70 cm and diameter of 10 cm). We simplified the analysis of energy consumption in filtration systems by assuming that all the required energy was supplied by one pump with 70% efficiency (typical range of

pump efficiencies is between 60% and 85% (Horowitz 2006)). The energy required by the column operation is comprised of kinetic, potential and pressure energy, and energy loss due to tubing and column friction (Schetz and Fuhs 1999). As a parameter frequently used to calculate the final energy consumption, the energy density (Pa or $kg/(m \cdot s^2)$) is the energy consumed per unit time (W or $kg \cdot m^2/s^3$) divided by the volumetric flow rate (m^3/s) (Baaquie and Willeboordse 2009). Expressions of kinetic and potential energy densities as well as energy density loss due to column friction can be seen in the SI section 3.

To accurately estimate the pressure energy density loss, both Ergun equation (Ergun 1952) and Darcy's law (Darcy 1856) were used for large-scale column calculations. The Ergun equation, which includes laminar flow and nonlinear flow terms, has been widely applied in the analysis of pressure drop in packed bed filters (Narayan et al. 1997, Propp et al. 2000, Arbat et al. 2013). The bed porosity as required by Ergun equation to calculate pressure energy density was obtained experimentally and assumed to be constant in small and large columns. Nevertheless, the Ergun equation fails to take into account the variation of particle shape (Macdonald et al. 1979) and wall effect (Mehta and Hawley 1969) and thus may underestimate the pressure drop across adsorbents (Mehta and Hawley 1969, Macdonald et al. 1979). On the other hand, Darcy's law is free of these problems as the particle shape and wall effects have been incorporated in the calculated intrinsic permeability, which was determined from the difference of column inlet and outlet pressure read off pressure gauges (in this case a second pressure gauge was mounted at the outlet of column). Intrinsic permeability, being an exclusive function of particle size distribution and packing structure

(Corrochano et al. 2015), is expected to be equal for small and large columns as long as the same adsorbent (same particle-size distribution) and bed porosity (identical packing structure) are used. Unfortunately, Darcy's law does not consider the contribution from nonlinear (non-laminar) flow to pressure drop which might become apparent when the bed porosity is large (Dukhan et al. 2014). Although nonlinear flow was unlikely to happen at the slow flow rate (0.6 mL/min) selected in this study, Ergun equation was still used to identify the nonlinear flow contribution to energy density loss as a complement to Darcy's law. Detailed calculations of energy consumption in large-scale filters using two approaches can be seen in the SI section 3. For the production cost of AlOOH-based adsorbents, details of calculations are given in the SI section 4.

Adsorbent Characterization

Scanning electron microscopy (SEM) was conducted using a Zeiss Neon SEM instrument operating at accelerating voltage of 10 kV or 15 kV. Before analysis, samples were mounted on carbon tape and sputter coated with iridium.

Results and Discussion

Column Fluoride Adsorption

Service time of pure AlOOH and AlOOH amended sodalite was compared to investigate the effects of amendment conditions on column fluoride adsorption. A much longer service time (time until column effluent fluoride concentration reaches 1.5 mg/L, the WHO recommended fluoride level) of AlOOH-amended sodalite (1370 bed volumes) was observed when using a sodalite size of 0.3 mm (Fig. 4-1A, open triangle)

compared to 32 bed volumes with 1 mm sodalite (Fig. 4-1A, solid triangle). A similar trend was noticed for AlOOH-amended MS-13X in that the service time increased from 20 to 1260 bed volumes by reducing the size of MS-13X from 2 mm (Fig. 4-1A, solid square) to 2 μm (Fig. 4-1A, open square). These results suggest that for AlOOH-amended zeolites (sodalite and MS-13X) an extended service time was more likely to be achieved when using a small-size substrate zeolite than that of a large size. This striking contrast of the service time between small and large-size zeolites (Fig. 4-1A) could be due to a greater mass of AlOOH contained in the amended materials prepared with fine-particle substrate zeolites (0.3 mm sodalite and 2 μm MS-13X) than those based on coarse particles (1 mm sodalite and 2 mm MS-13X). This was confirmed by higher measured aluminum contents in small-size amended zeolite than large-size amended zeolite, e.g., 166 g Al/kg in 0.6Al-sodalite-5.3-0.3 versus 121 g Al/kg in 0.6Al-sodalite-5.3-1 and 212 g Al/kg in 0.6Al-MS-13X-5.3-2μm versus 120 g Al/kg in 0.6Al-MS-13X-5.3-2mm. In the preparation with coarse-particle zeolites, e.g., sodalite (1 mm) amended with 0.6 M AlOOH at pH 5.3, in which 14-30 mesh sieves were used to retain the fraction of adsorbents between 0.6 and 1.4 mm, since the size of most AlOOH flocs formed at pH 5.3 do not exceed 450 μm (Wang et al. 2009), a large fraction of AlOOH may have been lost during sieving. In contrast, the use of fine mesh sieves in the preparation with fine-particle substrate zeolites, e.g., 40-80 mesh (0.180-0.425 mm) for sodalite (0.3 mm) amended with 0.6 M AlOOH at pH 5.3, might have significantly reduced the loss of AlOOH during sieving.

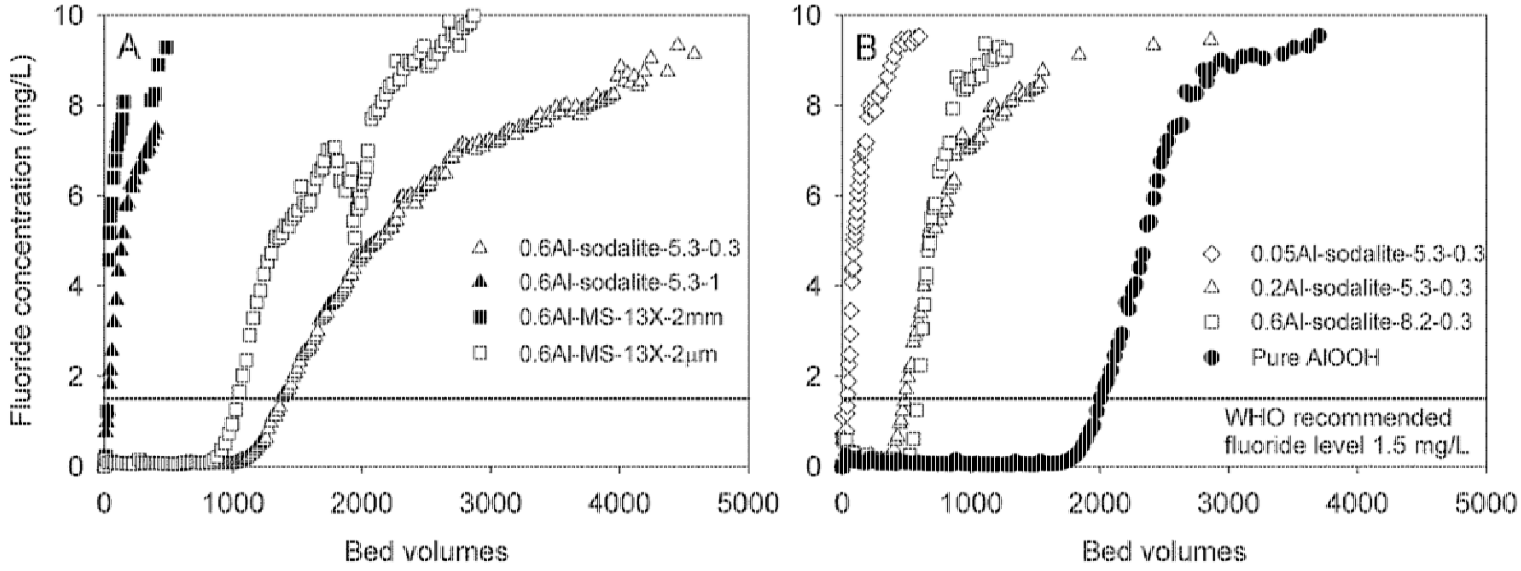

Figure 4-1 Breakthrough curves for AlOOH-amended zeolites. Adsorbents with different sizes of substrate zeolite (0.3 and 1 mm for sodalite, and 2 μm (particles) and 2 mm (beads) for MS-13X) (A), and prepared with various aluminum concentrations (0.05, 0.2, and 0.6 M) and pH values (5.3 and 8.2) (B). The interruption on the breakthrough curve of 0.6Al-MS-13X-2μm (panel A) (starting at about 1800 bed volumes) was due to the decreased flow rate caused by tubing leakage. After tubing replacement, the flow rate was recovered and the breakthrough curve returned to the original profile (at about 2100 bed volumes).

The dependency of service time on the mass loading of AlOOH in these amended materials can be also observed by comparing the fluoride removal results of sodalite (0.3 mm) amended with different amounts of AlOOH (Fig. 4-1). By tripling the aluminum concentration used in the amendment of sodalite (0.3 mm) (from 0.2 to 0.6 M) (and accordingly tripling the mass loading of AlOOH) the service time also increased by three times (485 bed volumes (Fig. 4-1B, open triangle) to 1370 bed volumes (Fig. 4-1A, open square)). Particularly with 100% AlOOH, the pure AlOOH exhibited the longest service time (2000 bed volumes (Fig. 4-1B, solid circle)). These findings in combination with the relatively low affinity of fluoride to sodalite (Batch Q_{10}=0.26 mg/g) versus fluoride affinity of AlOOH (Batch Q_{10} of pure AlOOH is 58.9 mg/g) (Du et al. 2016) suggest that AlOOH might be the main contributor to fluoride removal of AlOOH-amended zeolites. The dominant role of AlOOH loading in fluoride removal for amended zeolites is also consistent with the result that the column Q_{10} of 0.6Al-sodalite-5.3-0.3 and 0.6Al-MS-13X-5.3-2μm became close to that of pure AlOOH after normalizing the column Q_{10} by the aluminum content (Table 4-2).

In addition to zeolite size and aluminum concentration, the column fluoride adsorption is also a function of pH used when precipitating AlOOH on the zeolite. A slightly acidic pH value (pH 5.3) led to much longer service time (1370 versus 585 bed volumes for amended sodalite prepared with 0.6 M $AlCl_3$ at pH 5.3 (Fig. 4-1A, open triangle) versus pH 8.2 (Fig. 4-1B, open square)). In contrast to aluminum (hydr)oxides precipitated at pH 8.2, which were possibly boehmite (AlOOH) or bayerite ($Al(OH)_3$), the mineral phase formed under acidic conditions could have been amorphous AlOOH

Table 4-2 Column fluoride adsorption service time and fluoride removal capacity (column Q_{10}, aluminum content-normalized column Q_{10}, and batch Q_{10}) of AlOOH based materials

Materials	Column service time (number of bed volumes)	Column Q_{10} (mg F^-/g)[a]	Al-normalized column Q_{10} (mg F^-/g Al)[b]	Batch Q_{10} (mg F^-/g)[c]
0.6Al-sodalite-5.3-0.3	1370	22.2	133	38.9
0.6Al-sodalite-5.3-1	32	1.7[d]	14	Not determined
0.6Al-sodalite-8.2-0.3	585	11.1	Not determined	Not determined
0.2Al-sodalite-5.3-0.3	485	8.3	Not determined	Not determined
0.05Al-sodalite-5.3-0.3	40	1.4	Not determined	Not determined
0.6Al-MS-13X-2μm	1260	25.6	121	Not determined
0.6Al-MS-13X-2mm	20	2.0 [d]	17	Not determined
Pure AlOOH	2000	38.6	86	58.9
Regenerated 0.6Al-sodalite-5.3-0.3[e]				
After one cycle	560	Not determined	Not determined	Not determined
After two cycles	180	Not determined	Not determined	Not determined

[a] Column Q_{10} is equal to the total amount of fluoride removed until column exhaustion divided by the mass of materials packed into the column.

[b] Al-normalized column Q_{10} is the column Q_{10} divided by the measured aluminum content or the assumed aluminum content only for pure AlOOH (i.e., 450 g Al/kg AlOOH). For pure AlOOH, the composition of sample was assumed to be AlOOH and no sample was lost during preparation.

[c] Batch Q_{10} is the fluoride uptake density at the equilibrium fluoride concentration of 10 mg/L in batch experiments and calculated from the Langmuir isotherm parameters in Du et al. (2016).

[d] The mass of 0.6Al-sodalite-5.3-1 and 0.6Al-MS-13X-2mm packed in columns was not determined after column adsorption experiments. Instead, the measured weight of packing adsorbent 0.6Al-sodalite-5.3-0.3 (4.37 g) and 0.6Al-MS-13X-2μm (2.41 g) was used to calculate the column Q_{10} of 0.6Al-sodalite-5.3-1 and 0.6Al-MS-13X-2mm, respectively. The weight of 0.6Al-sodalite-5.3-0.3 and 0.6Al-MS-13X-2μm was measured after the column adsorption experiments.

[e] After fluoride adsorption, adsorbent was regenerated with 0.01 M NaOH. The adsorption-regeneration cycle was carried out twice.

(Du et al. 2009, Gong et al. 2012), which has greater fluoride removal capacity than boehmite or bayerite prepared at basic pH values (Gong et al. 2012).

With influent fluoride concentration of 10 mg/L, pure AlOOH and sodalite (0.3 mm) amended with 0.6 M AlOOH at pH 5.3 presented the longest service time (the period before the ratio of effluent fluoride concentration to influent fluoride concentration reaches 0.15) among all studied materials (2000 bed volumes for pure AlOOH and 1370 bed volumes for 0.6Al-sodalite-5.3-0.3, Table 4-2), which outperform conventional fluoride adsorbents (e.g., 70 bed volumes for activated alumina (Brunson and Sabatini 2014) and 380 bed volumes for Mn oxide coated alumina (Maliyekkal et al. 2006)), amended substrate materials (e.g., 27 bed volumes for iron loaded cotton cellulose (Zhao et al. 2008) and 4.7 bed volumes for acid-treated bentonite (Ma et al. 2011), and other metal (hydr)oxides (e.g., 53 bed volumes for cellulose supported Zn-Al layered double hydroxides (Mandal and Mayadevi 2008)). It is noteworthy that more favorable column operation conditions were usually employed in other studies compared to this study, i.e., empty bed contact time of 6.5 minutes and influent fluoride concentration of 10 mg/L. For example, longer empty bed contact time such as 11 minutes for iron loaded cotton cellulose (Zhao et al. 2008) and 29 minutes for acid-treated bentonite (Ma et al. 2011), and lower influent fluoride concentrations such as 8.6 mg/L for activated alumina (Brunson and Sabatini 2014) and 3.56 mg/L for Mn oxide coated alumina (Maliyekkal et al. 2006) were used. Thus if the adsorbents in this study (pure AlOOH and AlOOH-amended sodalite) were to be tested with longer empty bed contact time and lower influent fluoride concentrations, a prolonged service time would be expected.

The long service time of pure AlOOH and 0.6Al-sodalite-5.3-0.3 can be attributed to their ability to take up fluoride through processes other than adsorption (Alfredo 2012, Du et al. 2016). These additional processes, in contrast, might not happen when using other fluoride adsorbents. However, despite the occurrence of additional fluoride removal processes, these were still more than 40 percent of the batch fluoride removal capacity lost during column operation when using pure AlOOH and amended sodalite (e.g., batch Q_{10} of 38.8 mg/g versus column Q_{10} of 22.2 mg/g for 0.6Al-sodalite-5.3-0.3, Table 4-2), which probably resulted from slow mass transfer and insufficient intraparticle diffusion of fluoride within packed adsorbents in limited residence time (48 h in batch experiments versus 6.5 min in column experiments) (Al-Degs et al. 2009).

Effluent aluminum concentration

With their long column service time pure AlOOH and sodalite (0.3 mm) amended with 0.6 M AlOOH at pH 5.3 are most promising among all studied AlOOH-based materials for practical fluoride treatment. Thus, they were also subjected to effluent aluminum concentration measurement to ensure the quality of column effluent. At the beginning of column operation, with the outflow of a large amount of AlOOH particles the effluent aluminum started with very high concentrations, i.e., total aluminum concentration (unfiltered) 140 mg/L for pure AlOOH (Fig. 4-2A) and 20 mg/L for amended sodalite (prepared with 0.6 M $AlCl_3$ and at pH 5.3) (Fig. 4-2B). Afterwards, between 9 and 70 bed volumes, the effluent aluminum concentrations for both

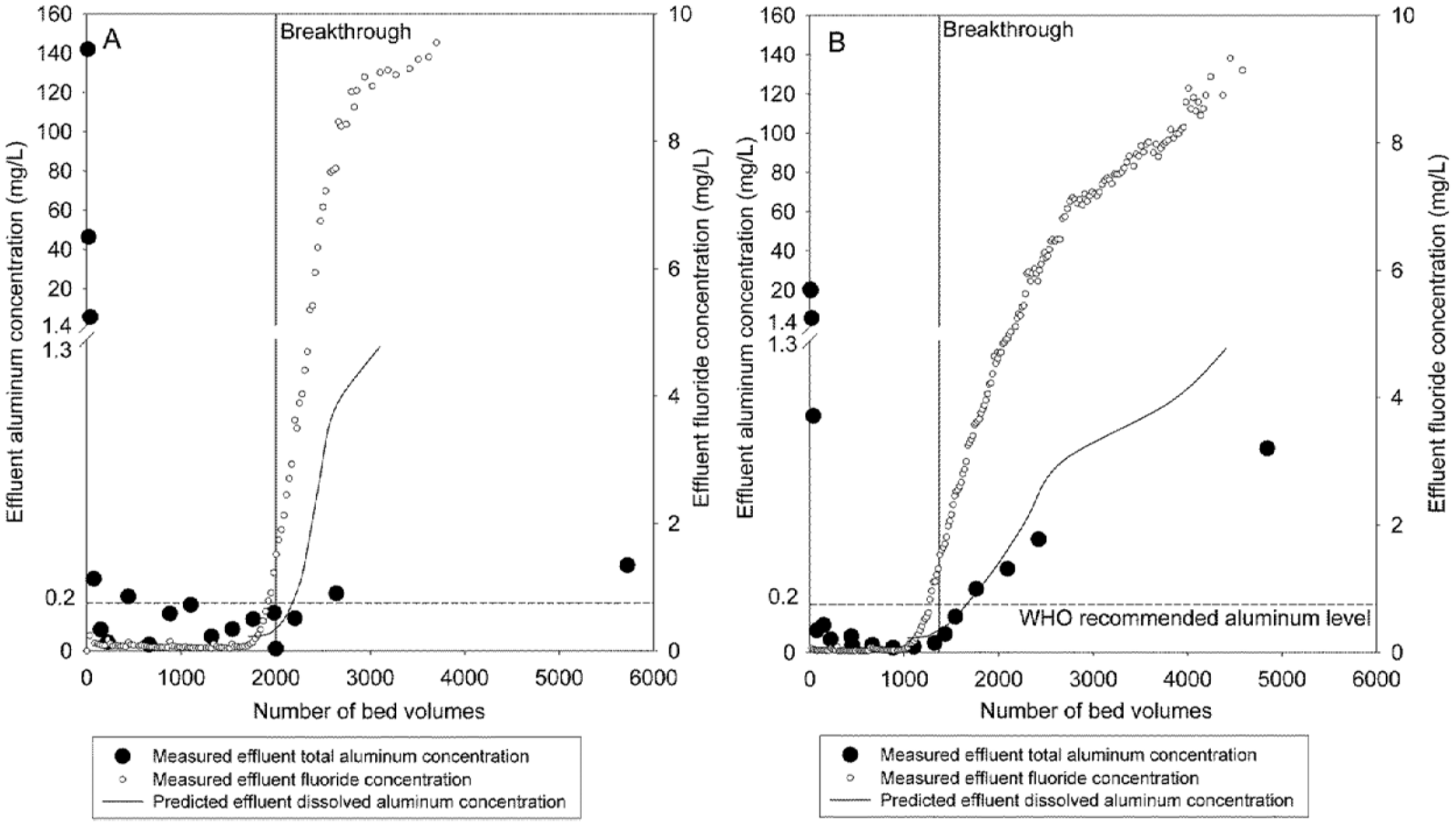

Figure 4-2 Effluent aluminum concentrations versus number of bed volumes: pure AlOOH (A) and 0.6Al-sodalite-5.3-0.3 (B). Solid vertical lines indicate the number of bed volumes at which column breakthrough happens; and dashed horizontal lines denote the WHO recommended level for drinking water aluminum. Solid curves represent the predicted equilibrium effluent dissolved aluminum pattern with respect to dissolved fluoride release.

Table 4-3 Effluent aluminum concentration in filtered and unfiltered samples

	Number of bed volumes	Effluent aluminum concentration (mg/L)	
		Unfiltered samples	0.2 μm Filtered samples
Pure AlOOH	9.2	140	91.9
	18.3	46.4	10.2
	36.7	5.63	0.31
	73.4	0.30	0.04
	5723	0.36	0.30
0.6Al-sodalite-5.3-0.3	4.6	20.4	11.2
	9.2	19.9	18.0
	18.3	5.85	5.39
	36.7	0.99	0.06
	73.4	0.09	0.03
	4843	0.85	0.82

adsorbents dropped remarkably to levels under 0.5 mg/L due to the depletion of small AlOOH particles in the column (as most small particles had been flushed out) (Fig. 4-2). Upon a separate analysis of filtered and unfiltered samples, high aluminum concentration above 5 mg/L was also detected in filtered samples, especially of those collected before 20 bed volumes (Table 4-3). The high aluminum concentration in filtered samples at the beginning of column operation cannot be explained by the solubility of AlOOH, which is approximately 0.05 mg/L as calculated by Visual Minteq ver. 3.1 (KTH, Stockholm) when the effluent fluoride was 0.1 mg/L. Since the value of 0.05 mg/L was obtained by assuming that the pK_{sp} of AlOOH equals that of freshly prepared amorphous pseudoboehmite (10.2), the value of 0.05 mg/L is likely to be an upper end of equilibrium dissolved aluminum concentration in the presence of 0.1 mg/L fluoride. Although there could be small uncertainties associated with the pK_{sp} of amorphous pseudoboehmite and dissolved aluminum concentration, e.g., 0.16 mg Al/L leached if a small amount of more soluble amorphous phase with pK_{sp} of 10.6 is in

equilibrium with 0.1 mg/L fluoride solution, the predicted equilibrium dissolved aluminum level is still much less than the measured effluent total aluminum concentration at the beginning of column operation (e.g., 5.63 mg/L at 36.7 bed volumes for pure AlOOH). Instead, it is possible that small particles less than 0.2 μm passed the filter membrane and made a significant contribution to a high aluminum level in the effluent. The lower effluent aluminum concentration in both unfiltered and filtered samples of amended sodalite than those of pure AlOOH before 73.4 bed volumes (Table 4-3) implies a favorable role of sodalite in alleviating aluminum release. There is greater extent of reduction in effluent aluminum for unfiltered samples than filtered samples by comparing pure AlOOH with amended sodalite at the same number of bed volume (Table 4-3). This might be due to the ability of sodalite to retain AlOOH particles, especially those greater than 0.2 μm, governed by physicochemical deposition (Xu et al. 2006) (including van der Waals, electrical double-layer, and steric interactions (Petosa et al. 2010)).

From 70 to 1500 bed volumes, for both pure AlOOH and amended sodalite, the aluminum concentration in the effluent was below 0.2 mg/L (a level recommended by the WHO). Their temporal variation of aluminum release during this period (70 to 1500 bed volumes) presented similar patterns in which the aluminum concentration stayed around 0.05 mg/L before breakthrough followed by an increase until column exhaustion (Fig. 4-2). Similar to the first 70 bed volumes, the use of amended sodalite also released less aluminum compared to using pure AlOOH between 70 bed volumes and breakthrough (Fig. 4-2), which still might be due to the retention of AlOOH particles by sodalite. For the aluminum concentration after 1500 bed volumes, its

increase was accompanied by the elevation of effluent fluoride concentration (Fig. 4-2). Because of fluoride-induced dissolution (see relevant reactions in the SI section 5), it is expected that a higher concentration of fluoride leads to more dissolution of aluminum based mineral (Roberson and Hem 1969).

Dissolved aluminum concentration in the effluent over the course of column fluoride adsorption was modelled using Visual Minteq ver. 3.1 (KTH, Stockholm) at conditions similar to column experiments (varying total fluoride concentration in the range of 0 and 10 mg/L, 0.05 M HEPES, freshly precipitated AlOOH as the infinite solid phase (unlimited amount of solid phase) with pK_{sp} of 10.2 (calculated based on results of Hem and Roberson (1967)); equilibrium constants of relevant reactions were from the Minteq database, Hem and Roberson (1967), Phillips et al. (1997), and Sanjuan and Michard (1987), see them in the SI Section 4). Fluoride adsorption was excluded in the simulation. Modeling results showed that the equilibrium aqueous aluminum concentration would increase from 0.06 mg/L with 1.9×10^{-4} mg/L (10^{-8} M) fluoride to 0.45 mg/L with 5 mg/L ($10^{-3.6}$ M) fluoride (Fig. 4-3). With the rise of fluoride concentration, the predicted total dissolved aluminum concentration also increases as a result of enhanced fluoride-induced dissolution of AlOOH and formation of aqueous species $AlF_3(aq)$ and AlF_2^+ (Fig. 4-3). Reactions controlling this process include $AlOOH(s) + 3\ H^+ + 3\ F^- = AlF_3(aq) + 2\ H_2O$ and $AlOOH(s) + 3\ H^+ + 2\ F^- = AlF_2^+ + 2\ H_2O$. The dissolved total aluminum concentration predicted by the model is in agreement with the experimental data for amended sodalite (about 0.05 mg Al/L ($10^{-5.7}$ M) with 1.5 mg F^-/L ($10^{-5.3}$ M) to about 0.5 mg Al/L ($10^{-4.7}$ M) with 5 mg F^-/L ($10^{-3.6}$

M)), which indicates that the majority of effluent aluminum column breakthrough was from aqueous species.

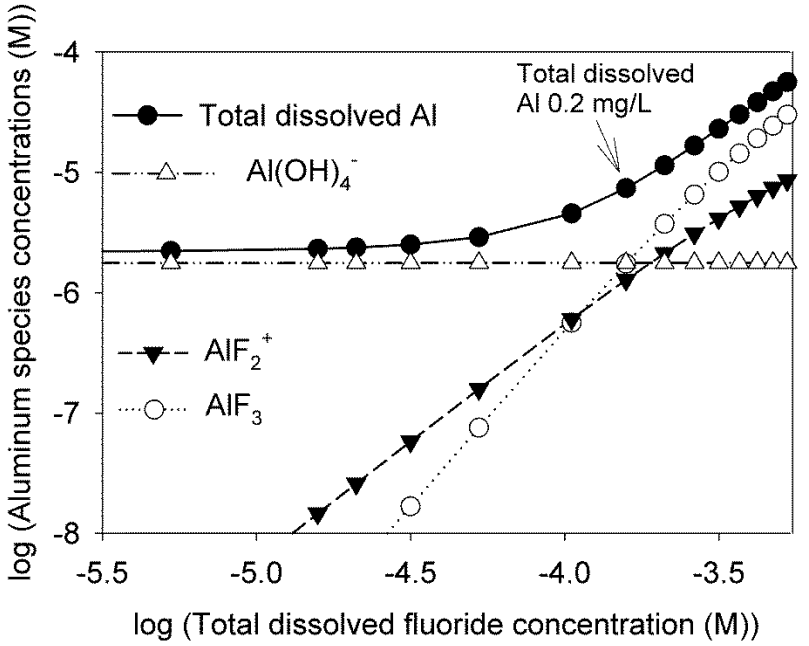

Figure 4-3 Concentrations of predicted total dissolved aluminum and major aqueous aluminum species versus the total dissolved fluoride concentration at pH 7

However, after about 2000 bed volumes, the effluent aluminum concentration of amended sodalite (Fig. 4-2B) became larger than that of pure AlOOH; and this trend continued until column exhaustion (Fig. 4-2). This finding is in contrast with the equilibrium modeling result that pure AlOOH is supposed to have larger effluent aluminum concentration than amended sodalite at any number of bed volume (after 1600 bed volumes) due to a more rapid rise in dissolved fluoride concentration after breakthrough (Fig. 4-2). In this period (2000 bed volumes to exhaustion), more aluminum was contributed by the portion of effluent passing through 0.2 μm filter (Table 4-3, pure AlOOH 5723 bed volumes compared to amended sodalite 4843 bed volumes) and could have been primarily aqueous species. Slow kinetics is unlikely to

be the limiting factor that causes the measured effluent aluminum concentrations to be lower than the predicted equilibrium dissolved aluminum levels, as the dissolution of boehmite (AlOOH) is a very fast process when a large amount of fluoride attaches to the surface of AlOOH, e.g., a dissolution rate greater than 0.01 mg/s at 20 mg adsorbed fluoride amount per gram of AlOOH (Nordin et al. 1999). The smaller increase in effluent aluminum concentration after 1600 bed volumes for pure AlOOH compared to amended sodalite might result from the adsorption of aqueous aluminum by AlOOH. As there is more mass of AlOOH in pure AlOOH than amended sodalite, a larger amount of aqueous aluminum was adsorbed by pure AlOOH. Aluminum adsorption to kaolinite has been reported in which aluminum ion could complex with surface aluminum hydroxide groups of kaolinite (Walker et al. 1988). Since pure AlOOH has the same surface aluminum hydroxide groups (and the same aluminum hydroxide octahedral structure) as kaolinite (Wefers and Misra 1987, Walker et al. 1988), adsorption of aluminum to pure AlOOH was also surmised to happen. Alternatively, the overestimated equilibrium model could be due to the uncertainties in the mineral phase of precipitated AlOOH and in the solubility product equilibrium constant (K_{sp}) of AlOOH. If the precipitated aluminum (hydr)oxide mineral has a smaller K_{sp}, a lower effluent dissolved aluminum concentration is expected.

The aluminum concentration could affect the selection of fluoride adsorbent from amended sodalite (0.6Al-sodalite-5.3-0.3) and pure AlOOH. Although there has not been a consensus on the toxicity of aluminum in drinking-water (Flaten 2001, Soni et al. 2001), a low concentration of effluent aluminum seems to be more desirable to minimize potential damages to human health. In this sense, 0.6Al-sodalite-5.3-0.3 is

preferred to pure AlOOH for drinking-water fluoride treatment with less aluminum leaching (due to less particles release) before breakthrough. Therefore, the water produced within the first 70 bed volumes and after breakthrough when using 0.6Al-sodalite-5.3-0.3 is recommended not be used or treated using a second-stage filter packed with iron oxides to reduce the potential health risks associated with elevated aluminum and fluoride concentrations. Additionally, the effluent aluminum concentration dissolved from AlOOH might be subject to changes in water pH values. Based on the equilibrium modeling, the minimum equilibrium dissolved aluminum concentration from AlOOH (pK_{sp} = 10.2) in the presence of 10 mg/L fluoride is predicted to be at pH 7.5 (close to the pH 7 used in this study) (SI Fig. S6). As the fluoride concentration decreased, the pH corresponding to the minimum equilibrium dissolved aluminum shifted to lower values (e.g., pH 7.2 for 1.5 mg/L fluoride, pH 7.0 for 0.5 mg/L fluoride, and pH 6.5 for 0 mg/L fluoride) (SI Fig. S6). The dissolved aluminum concentration would increase rapidly below pH 6.0.

Competitive adsorption

Competitive adsorption was evaluated by looking at sulfate, bicarbonate, silicate, and pyromellitic acid at 20 mg/L fluoride level. Unlike the reported competition between fluoride and sulfate (activated alumina (Tang et al. 2009) and aluminum amended bone char (Brunson and Sabatini 2014)), and bicarbonate (activated alumina (Tang et al. 2009))), fluoride adsorption to AlOOH was only slightly affected by studied competing solutes, with fluoride removal capacity decreasing by less than 12 percent (Fig. 4-4), indicating the selective adsorption of fluoride to AlOOH. This selective adsorption

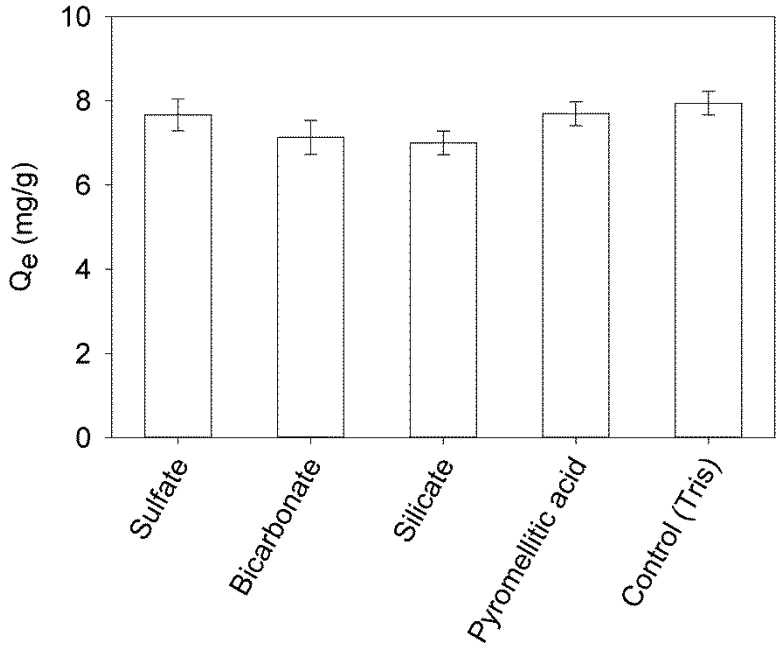

Figure 4-4 Competitive adsorption to AlOOH between fluoride and common solutes in natural groundwater. Fluoride concentration: 20 mg/L (~1 mM), Competing solutes concentration: 5 mM, pH: 8.5 (maintained with Tris buffer), solid-to-liquid ratio: 2 g/L. The uncertainties associated with each bar are the standard deviations of equilibrium fluoride adsorption density (Q_e).

might be due to the involvement of some special process during fluoride removal that only exists between fluoride and AlOOH. The process, which is likely to be the precipitation of aluminum-fluoride complex (Du et al. 2016), might not happen for activated alumina, activated carbon or modified bone char since their maximum fluoride removal capacity (~11 mg/g and 10.2 mg/g for activated alumina (Tang et al. 2009) and amended bone char (Brunson and Sabatini 2014)) are close to the calculated values of complete surface monolayer coverage (11.6 mg/g and 9.1 mg/g for activated alumina (surface area 363 m^2/g) and amended bone char (surface area 284 m^2/g)). Surface adsorption would rather dominate the fluoride removal of activated alumina, activated carbon or modified bone char. Therefore, solutes such as sulfate might compete with fluoride for the available surface of those adsorbents but not pure AlOOH, thus

resulting in a difference of fluoride removal capacity upon the addition of competing solutes. Considering the positive relationship between batch adsorption capacity and column adsorption performance (Naja and Volesky 2008), the unchanging fluoride removal capacity in the presence of competing solutes also suggests consistent column fluoride adsorption of AlOOH even in the presence of high concentrations of sulfate, bicarbonate, and natural organic matters. Nevertheless, the small decrease in fluoride adsorption (7.94±0.28 mg/g for control with uncertainties represent the standard deviation) with the addition of silicate (7.00±0.28 mg/g) needs to be noted (Fig. 4-4), for the reduction of fluoride removal capacity might become apparent in the case that the silicate concentration is abnormally high. Moreover, the fluoride removal capacity of AlOOH at pH 8.5, 7.94±0.28 mg/g, is lower than that at pH 7.0, i.e., 9.82±0.17 mg/g (Du et al. 2016), indicating a negative impact of basic pH values on fluoride adsorption.

Column Inlet Pressure and Energy Consumption

During fluoride adsorption, 0.6Al-sodalite-5.3-0.3 and pure AlOOH shared similar trend in the variation of column inlet pressure which remained constant in the first thousand bed volumes followed by a gradual elevation until 2800 bed volumes (Fig. 4-5 inset). Based on the Ergun equation, the increase in inlet pressure over time might be due to the reduction in particle size or column porosity (Ergun 1952). Since there was no confirmative evidence from SEM showing decreased particle size after fluoride adsorption (SI Fig. S7), the reduced column porosity might be a more plausible explanation. In contrast to fluoride adsorption, the flow of HEPES buffer without fluoride through the column did not result in the increased inlet pressure after 1000 bed

volumes (Fig. 4-5 inset, solid spheres). It was possible that the continuous adsorption of fluoride led to a reduction in column porosity. With elevated effluent fluoride concentration, the enhanced fluoride-induced dissolution (Fig. 4-3) might densify loose AlOOH particles (Shin and Santamarina 2009) and resulted in a porosity loss. For MS-13X (2 μm) amended with 0.6 M AlOOH at pH 5.3, despite its favorable service time, the high column inlet pressure (> 103.4 kPa, Fig. 4-5 0.6Al-MS-13X-2μm) will negatively affect its practical application in the field. This high inlet pressure might be caused by the very small particle size (2 μm) of MS-13X. Although these micrometer-scale particles of MS-13X are inclined to aggregate during AlOOH precipitation and remain agglomerated after sieving (with 40-80 mesh sieves) (Du et al. 2016), the MS-13X tiny particle clusters could have disaggregated during column fluoride adsorption and led to such a high inlet pressure (> 103.4 kPa).

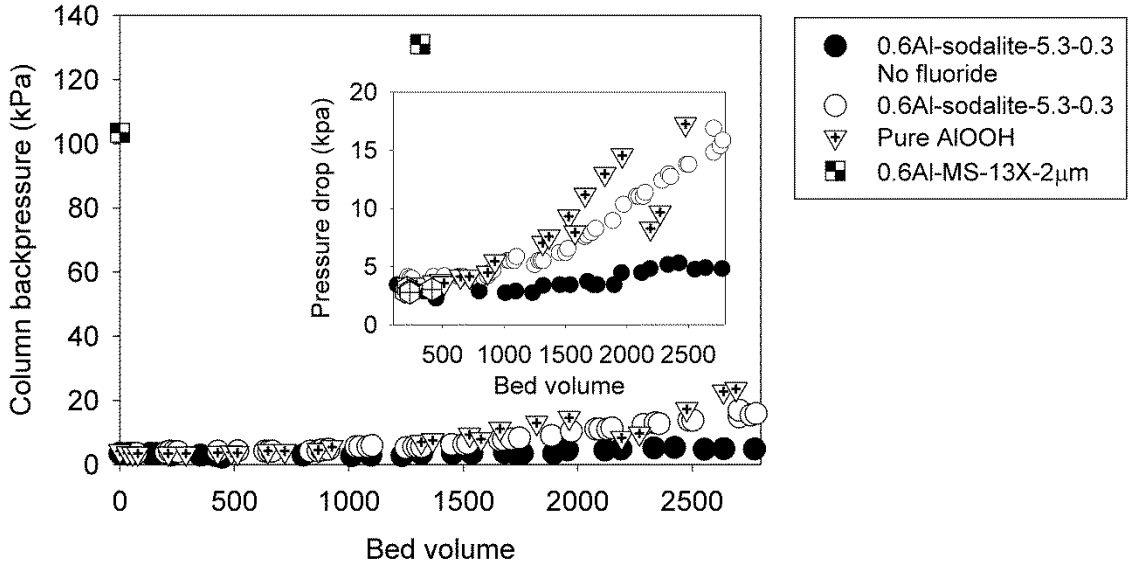

Figure 4-5 Column inlet pressure during column operation versus number of bed volumes. Column parameters are the same as given in the text. No fluoride in the legend means that only 50 mM HEPES was used.

Energy consumption when using AlOOH-amended sodalite (0.3 mm sodalite amended with 0.6 M AlOOH at pH 5.3) in fluoride treatment was estimated for household and community-scale filters with Ergun equation and Darcy's law (Table 4-4). It is worthwhile noting that there is only slight difference between the results calculated with Ergun equation and Darcy's law. For Darcy's law, an average inlet and outlet pressure difference of 124 Pa was used to calculate the intrinsic permeability. The 17% higher energy consumption calculated using Darcy's law than Ergun equation (24.3 versus 20.8 kPa) might come from the extra energy density loss caused by the irregular particle shape and wall effect. By using Darcy's law and experiment-based intrinsic permeability, this portion of energy density loss, embodied in the pressure difference between column inlet and outlet, had been accounted for. Also in the calculation with Ergun equation, the loss of energy density due to the nonlinear flow (0.2 kPa, the second term of Ergun equation (see the SI section 3)) is insignificant compared to that contributed by linear flow (20.6 kPa, first term of Ergun equation (see the SI section 3)). Darcy's law thus seems to present a better estimate of total energy consumption, or at least demarcates a range where the accurate value of energy requirement lies in together with Ergun equation. For household filters about 2.13×10^{-4} kWh was required per day; whereas energy consumption increased remarkably when scaling up to community-scale filters (0.011 kWh/day) due to the large dimensions (Table 4-4). Nonetheless, a community-scale filter (about 0.02 kWh/m^3 produced water corresponding to a flow rate of 0.0139 L/s) is still much more energy-efficient than electrocoagulation (10.8 kWh/m^3 (Ghosh et al. 2008)) and reverse osmosis (5 kWh/m^3

Table 4-4 Total energy density, hydraulic head, pump power, and energy consumption under two scenarios

Method	Scenario	Total energy density (kPa)	Hydraulic head (m H_2O)	Required pump power (W)	Energy consumption per day (kWh)
Ergun equation	Household filter	3.8	0.39	7.57×10^{-3}	1.82×10^{-4}
	Community-scale filter	20.8	2.12	0.42	0.010
Darcy's law	Household filter	4.47	0.46	8.89×10^{-3}	2.13×10^{-4}
	Community-scale filter	24.3	2.48	0.49	0.011

(Shannon et al. 2008)) in drinking-water treatment. Even in the absence of continuous electricity supply, the community -scale filter with AlOOH-amended sodalite can be operated with hydrostatic energy. By converting total energy density to hydraulic head, a water tank placed 2.5 meters above the column (i.e., approximately 4 m above the ground which is feasible in most communities) is found to provide enough energy for the operation of community-scale filter (Table 4-4).

Adsorbent Regeneration

Among all the tested adsorbents, sodalite (0.3 mm) amended with 0.6 M AlOOH at pH 5.3 and pure AlOOH were the most cost-effective per unit of treated water. Even though the production cost of these two materials ($2.10/kg on average) outstrips the price of commercial activated alumina ($0.63/kg), due to their high fluoride removal capacity, their cost on the treated-water volume basis is quite small ($1.01/$m^3$ of treated water on average, Table 4-5) and much less than the cost of fluoride treatment using activated alumina (about $2.94/$m^3$ of treated water (Onuoha 1983), see calculation in the SI section 4). Two strategies were proposed to further reduce its production cost, i.e., by decreasing the cost of aluminum salt used in the amendment with aluminum sulfate which price is about $0.35/kg compared to $0.45/kg for aluminum chloride, and by extending the life of materials via regeneration and reuse. It is found that were aluminum sulfate to be used, the production cost of amended sodalite and pure AlOOH could be lowered to $0.75 and $0.67 per cubic meters of treated water compared to $1.05 and $0.97 using aluminum chloride (Table 4-5), although the column fluoride removal of aluminum sulfate-based amended sodalite needs to be further evaluated.

Table 4-5 Production cost of AlOOH based materials

Materials	Regeneration with 0.01 M NaOH	Mass of materials packed in one bed volumes (g)	Estimated amount of AlOOH contained in one bed volumes of material (g)	Production cost of fluoride removal materials (dollars per kg)	Cost of fluoride removal materials (dollars per cubic meters fluoride-safe water)
0.6Al-sodalite-5.3-0.3	No	4.37	1.64	1.23	1.05
	One regeneration	4.37	1.64	1.23	0.84
	Two regenerations	4.37	1.64	1.23	0.86
Pure AlOOH	No	2.49	2.49	2.96	0.97
Activated alumina	No	Not available	Not available	0.63	2.94

Regeneration is a viable means to lower the cost of column operation as the estimated cost of fluoride removal materials, which took into account the consumption of sodium hydroxide and total column service time in multiple adsorption cycles, dropped by 20% by reusing the amended sodalite after one time of regeneration (Table 4-5). Fig. 4-6 illustrates that the column fluoride removal capacity could be partially

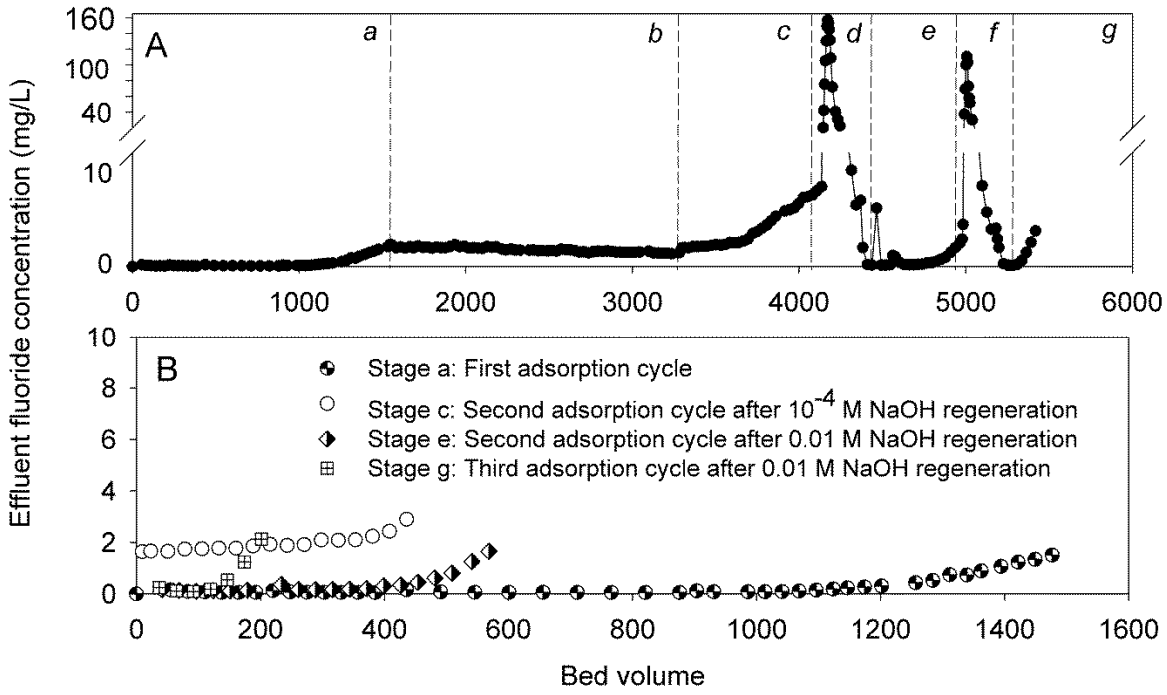

Figure 4-6 Column fluoride adsorption and desorption of AlOOH-amended sodalite (prepared with 0.6 M aluminum chloride and pH of 5.3) in multiple adsorption-regeneration cycles. The second and third adsorption cycles in the legend mean the column fluoride adsorption after one and two regenerations. Panel A shows the fluoride adsorption and desorption patterns in different adsorption and regeneration cycles, including seven stages (a) first adsorption cycle, (b) first regeneration cycle with 10^{-4} M NaOH, (c) second adsorption cycle after 10^{-4} M NaOH regeneration, (d) second regeneration cycle with 0.01 M NaOH, (e) second adsorption cycle after 0.01 M NaOH regeneration, (f) third regeneration cycle with 0.01 M NaOH, and (g) third adsorption cycle after 0.01 M NaOH regeneration. Panel B shows column fluoride adsorption curves before column breakthrough in different adsorption cycles.

recovered after regeneration using sodium hydroxide of relatively high concentration (e.g., 0.01 M versus 10^{-4} M NaOH, Fig. 4-6B). The release of fluoride, which was marked by a sharp peak of effluent fluoride concentration (maximum > 100 mg/L), was accomplished in approximately 200 bed volumes with 0.01 M sodium hydroxide; and 70% of adsorbed fluoride could be eluted in the first regeneration cycle (Fig. 4-6A stage d). The quick release of fluoride was also observed in Tor et al. (2009) where only 16 bed volumes of regenerant (0.2 M NaOH) was used to elute the fluoride adsorbed in 940 bed volumes. However, the service time in the second adsorption cycle (600 bed volumes, Fig. 4-6B) was inferior to that in the first adsorption cycle (about 1370 bed volumes, Fig. 4-6B). The loss in AlOOH loading during regeneration might be the reason for the decline of fluoride removal capacity in following adsorption cycles (Du et al. 2016). The trend of diminished service time was worse in the next adsorption cycle. There were merely 170 bed volumes of fluoride-safe water produced in the third adsorption cycle using 0.01 M sodium hydroxide (Fig. 4-6B), which were less than the volume of water required for regenerant preparation (200 bed volumes, Fig. 4-6A stages d and f). In this sense, the success to reduce the production cost with the strategy of adsorbent reuse is dependent on the number of regenerations. The strategy appears not to be effective after two adsorption cycles.

Conclusions

Among all the studied materials, pure AlOOH and AlOOH-amended sodalite (prepared with 0.6 M aluminum chloride and at pH 5.3) showed the most promising potential in drinking-water fluoride treatment based on their favorable column performance. For

pure AlOOH, slightly acidic pH (e.g., 5.3) increased the high fluoride removal capacity in column fluoride adsorption; while for AlOOH-amended zeolites, in addition to the slightly acidic pH, a relatively small substrate zeolite size (e.g., 0.3 mm) and considerable aluminum concentration were desirable to produce a long service time. The size of substrate zeolite as well as pure AlOOH, nonetheless, cannot be extremely small as the increased column pressure associated with tiny adsorbent particles will become adverse to the operation (water flow) of columns.

For the effluent aluminum concentration when using pure AlOOH and amended sodalite, although starting at very high values and above the WHO drinking-water standard level (0.2 mg/L) within the first 70 bed volumes, it could be maintained below 0.2 mg/L afterwards until column breakthrough. After breakthrough, effluent aluminum levels increased with the rise of effluent fluoride concentrations due to the fluoride-induced AlOOH dissolution. AlOOH-based materials were shown to provide consistent fluoride removal capacity (at pH 8.5 and initial fluoride concentration of 20 mg/L) even in the presence of 5 mM (five times the fluoride level) of sulfate, bicarbonate, silicate, and pyromellitic acid with less than 12 percent decrease in removal capacity.

The use of pure AlOOH and AlOOH-amended sodalite in household and community-scale filters is energy-efficient since a small amount of energy is required per day (about 2×10^{-4} and 0.01 kWh for household and community-scale filters). Because of the low energy consumption, the community-scale filter can be operated using hydrostatic energy provided by an elevated water tank about four meters above the ground.

AlOOH-amended zeolite could be regenerated once as the amount of produced safe water due to plummeted service time after two cycles fell short of the volume of water required to prepare regenerant. In spite of limited regenerability, the low production costs of amended sodalite and pure AlOOH ($1.05 and $0.97 per cubic meters of treated water for 0.6Al-sodalite-5.3-0.3 and pure AlOOH) were less than the expense that incurred in the drinking-water fluoride treatment using activated alumina ($2.94/$m^3$ of treated water, Onuoha (1983)). It could still be lowered by using aluminum sulfate in the AlOOH precipitation or reusing the material once after regeneration with 0.01 M sodium hydroxide.

References

Al-Degs, Y. S., Khraisheh, M. A. M., Allen, S. J. and Ahmad, M. N. (2009). "Adsorption characteristics of reactive dyes in columns of activated carbon." J. Hazard. Mater. 165(1-3): 944-949.

Alfredo, K. A. (2012). Drinking water treatment by alum coagulation: competition among fluoride, natural organic matter, and aluminum. Ph.D. dissertation. The University of Texas at Austin.

Arbat, G., Pujol, T., Puig-Bargués, J., Duran-Ros, M., Montoro, L., Barragán, J. and de Cartagena, F. R. (2013). "An experimental and analytical study to analyze hydraulic behavior of nozzle-type underdrains in porous media filters." Agr. Water Manage. 126, 64-74.

Ayoob, S., Gupta, A.K., Bhat, V.T., (2008). A conceptual overview on sustainable technologies for the defluoridation of drinking water. Crit. Rev. Env. Sci. Tec. 38, 401-470.

Baaquie, B. E. and Willeboordse, F. H. (2009). Exploring Integrated Science. CRC Press, pp. 133.

Boegman, R. J. and Bates, L. A. (1984). "Neurotoxicity of aluminum." Canadian Journal of Physiology and Pharmacology 62(8): 1010-1014.

Brunson, L. R. and Sabatini, D. A. (2014). "Practialuminum concentration considerations, column studies and natural organic material competition for fluoride removal with bone char and aluminum amended materials in the Main Ethiopian Rift Valley." Sci. Total Environ. 488-489: 580-587.

Cai, P., Zheng, H., Wang, C., Ma, H., Hu, J., Pu, Y. and Liang, P. (2012). "Competitive adsorption characteristics of fluoride and phosphate on calcined Mg-Al-CO_3 layered double hydroxides." J. Hazard. Mater. 213: 100-108.

Cerqueira, A. A. and da Costa Marques, M. R. (2012). Electrolytic Treatment of Wastewater in the Oil Industry. In: J. S. Gomes (Eds.), *New Technologies in the Oil and Gas Industry*, INTECH Open Access Publisher, 1-28.

Corrochano, B. R., Melrose, J. R., Bentley, A. C., Fryer, P. J. and Bakalis, S. (2015). "A new methodology to estimate the steady-state permeability of roast and ground coffee in packed beds." J. Food Eng. 150: 106-116.

Crittenden, J. C., Berrigan, J. K. and Hand, D. W. (1986). "Design of rapid small-scale adsorption tests for a constant diffusivity." J. Water Pollu. Con. F. 58(4): 312-319.

Darcy, H. (1856). Les fontaines publiques de la ville de Dijon: exposition et application. Victor Dalmont, Paris.

Doshi, R., Braida, W., Christodoulatos, C., Wazne, M. and O'Connor, G. (2008). "Nano-aluminum: Transport through sand columns and environmental effects on plants and soil communities." Environ. Res. 106(3): 296-303.

Du, J., Sabatini, D. and Butler, E. (in press). "Preparation, characterization, and regeneration of aluminum (hydroxide amended molecular sieves for fluoride removal from drinking water." J. Environ. Eng.

Du, J., Sabatini, D. A. and Butler, E. C. (2014). "Synthesis, characterization, and evaluation of simple aluminum-based adsorbents for fluoride removal from drinking water." Chemosphere 101(0): 21-27.

Du, X., Wang, Y., Su, X. and Li, J. (2009). "Influences of pH value on the microstructure and phase transformation of aluminum hydroxide." Powder Technol. 192(1): 40-46.

Dukhan, N., Bağcı, Ö. and Özdemir, M. (2014). "Metal foam hydrodynamics: Flow regimes from pre-Darcy to turbulent." Int. J. Heat Mass Tran. 77: 114-123.

Edmunds, W. M. and Smedley, P. (2013). Fluoride in Natural Waters. In: O. Selinus (Eds.), *Essentials of Medical Geology*, Springer, Netherlands, 311-336.

Emsley, J., Arif, M., Bates, P. A. and Hursthouse, M. B. (1990). "Hydrogen bonding between free fluoride ions and water molecules: two X-ray structures." J. Mol. Struct. 220(0): 1-12.

EPA (1994). Methods for the Determination of Metals in Environmental Samples, EPA.

EPA (2004). The Methods for Evaluating Solid Waste, Physical/Chemical Methods, EPA.

Ergun, S. (1952). "Fluid flow through packed columns." Chem. Eng. Prog. 48: 89-94.

Evanko, C. R. and Dzombak, D. A. (1998). "Influence of structural features on sorption of NOM-analogue organic acids to goethite." Environ. Scie. Technol. 32(19): 2846-2855.

Farrah, H., Slavek, J. and Pickering, W. (1987). "Fluoride interactions with hydrous aluminum oxides and alumina." Soil Res. 25(1): 55-69.

Feenstra, L., Vasak, L. and Griffioen, J. (2007). Fluoride in groundwater: Overview and evaluation of removal methods. Utrecht, Netherland, International Groundwater Resources Assessment Center.

Flaten, T. P. (2001). "Aluminium as a risk factor in Alzheimer's disease, with emphasis on drinking water." Brain Res. Bull. 55(2): 187-196.

Frant, M. and Ross, J. W. (1968). "Use of a total ionic strength adjustment buffer for electrode determination of fluoride in water supplies." Anal. Chem. 40(7): 1169-1171.

Ghorai, S. and Pant, K. (2004). "Investigations on the column performance of fluoride adsorption by activated alumina in a fixed-bed." Chem. Eng. J. 98: 165 - 173.

Ghosh, D., Medhi, C.R. and Purkait, M.K. (2008). "Treatment of fluoride containing drinking water by electrocoagulation using monopolar and bipolar electrode connections." Chemosphere 73(9): 1393-1400.

Gómez-Hortigüela, L., Pérez-Pariente, J., García, R., Chebude, Y. and Díaz, I. (2013). "Natural zeolites from Ethiopia for elimination of fluoride from drinking water." Sep. Purifi. Technol. 120(0): 224-229.

Gomez, M. L., Blarasin, M. T. and Martínez, D. E. (2009). "Arsenic and fluoride in a loess aquifer in the central area of Argentina." Environ. Geol. 57(1): 143-155.

Gong, W.-X., Qu, J.-H., Liu, R.-P. and Lan, H.-C. (2012). "Adsorption of fluoride onto different types of aluminas." Chem. Eng. J. 189-190(0): 126-133.

Haynes, W. M. ed. (2014). CRC Handbook of Chemistry and Physics. CRC press, pp. 6-7.

Hem, J. D. and Roberson, C. E. (1967). "Form and stability of aluminium hydroxide complexes in dilute solution." U.S. Geol. Surv. Water-Supply Pap. 1827-A.

Horowitz, F. B., Lipták, B.G. and Bain S. (2006). Pump controls. In: Lipták, B.G. (Eds.), *Instrument Engineers' Handbook: Process Control and Optimization*. CRC/Taylor and Francis, pp. 2088.

Jagtap, S., Yenkie, M. K., Labhsetwar, N. and Rayalu, S. (2012). "Fluoride in drinking water and defluoridation of water." Chemi. Rev. 112(4): 2454-2466.

Krishnamachari, K. A. (1986). "Skeletal fluorosis in humans: a review of recent progress in the understanding of the disease." Prog. Food Nutr. Sci. 10(3-4): 279-314.

Largent, E. J. (1961). Fluorosis: The Health Aspects of Fluorine Compounds. Ohio State University Press, Columbus.

Liao, Y., Liang, J. and Zhou, L. (2011). "Adsorptive removal of As(III) by biogenic schwertmannite from simulated As-contaminated groundwater." Chemosphere 83(3): 295-301.

Ma, Y., Shi, F., Zheng, X., Ma, J. and Gao, C. (2011). "Removal of fluoride from aqueous solution using granular acid-treated bentonite (GHB): Batch and column studies." J. Hazard. Mater. 185(2-3): 1073-1080.

Macdonald, I. F., El-Sayed, M. S., Mow, K. and Dullien, F. A. L. (1979). "Flow through porous media-the Ergun equation revisited." Ind. Eng. Chem. Fund. 18(3): 99-208.

Maji, S. K., Pal, A., Pal, T. and Adak, A. (2007). "Modeling and fixed bed column adsorption of As (III) on laterite soil." Sep. Purif. Technol. 56(3): 284-290.

Maliyekkal, S. M., Sharma, A. K. and Philip, L. (2006). "Manganese-oxide-coated alumina: A promising sorbent for defluoridation of water." Water Res. 40(19): 3497-3506.

Mandal, S. and Mayadevi, S. (2008). "Cellulose supported layered double hydroxides for the adsorption of fluoride from aqueous solution." Chemosphere 72(6): 995-998.

Mehta, D. and Hawley, M. C. (1969). "Wall effect in packed columns." Ind. Eng. Chem. Proc. DD. 8(2): 280-282.

Naja, G. and Volesky, B. (2008). "Optimization of a biosorption column performance." Environ. Sci. Technol. 42(15): 5622-5629.

Narayan, R., Coury, J. R., Masliyah, J. H. and Gray, M. R. (1997). "Particle capture and plugging in packed-bed reactors." Ind. Eng. Chem. Res. 36(11): 4620-4627.

Nordin, J. P., Sullivan, D. J., Phillips, B. L. and Casey, W. H. (1999). "Mechanisms for fluoride-promoted dissolution of bayerite [β-Al $(OH)_3$ (s)] and boehmite [γ-AlOOH]: ^{19}F-NMR spectroscopy and aqueous surface chemistry." Geochim. Cosmochim. Acta 63(21): 3513-3524.

Onuoha, U. O. (1983). "Evaluation of an activated alumina sorption system for removal of fluoride from water." Master Thesis, Texas Tech. University.

Onyango, M. S., Kojima, Y., Aoyi, O., Bernardo, E. C. and Matsuda, H. (2004). "Adsorption equilibrium modeling and solution chemistry dependence of fluoride removal from water by trivalent-cation-exchanged zeolite F-9." J. Colloid Interf. Sci. 279(2): 341-350.

Onyango, M. S. and Matsuda, H. (2006). "Fluoride removal from water using adsorption technique." Adv. Fluorine Sci. 2: 1-48.

Petosa, A. R., Jaisi, D. P., Quevedo, I. R., Elimelech, M. and Tufenkji, N. (2010). "Aggregation and deposition of engineered nanomaterials in aquatic environments: role of physicochemialuminum concentration interactions." Environ. Sci. Technol. 44(17): 6532-6549.

Phillips, B. L., Casey, W. H. and Crawford, S. N. (1997). "Solvent exchange in $AlF_x(H_2O)_{6-x}^{3-x}$ (aq) complexes: Ligand-directed labilization of water as an analogue for ligand-induced dissolution of oxide minerals." Geochim. Cosmochim. Ac. 61(15): 3041-3049.

Propp, R. M., Colella, P., Crutchfield, W. Y. and Day, M. S. (2000). "A numerical model for trickle bed reactors." J. Comput. Phys. 165(2): 311-333.

Rango, T., Kravchenko, J., Atlaw, B., McCornick, P. G., Jeuland, M., Merola, B. and Vengosh, A. (2012). "Groundwater quality and its health impact: An assessment of dental fluorosis in rural inhabitants of the Main Ethiopian Rift." Environ. Int. 43: 37-47.

Roberson, C. E. and Hem, J. D. (1969). "Solubility of aluminum in the presence of hydroxide, fluoride, and sulfate." U.S. Geol. Surv. Water-Supply Pap. 1827-A.

Samatya, S., Yüksel, Ü., Yüksel, M. and Kabay, N. (2007). "Removal of fluoride from water by metal ions (Al^{3+}, La^{3+} and ZrO^{2+}) loaded natural zeolite." Sep. Sci. Technol. 42(9): 2033-2047.

Sanjuan, B. and Michard, G. (1987). "Aluminum hydroxide solubility in aqueous solutions containing fluoride ions at 50°C." Geochim. Cosmochim. Ac. 51(7): 1823-1831.

Schetz J. A. and Fuhs A. E. (1999). Fundamentals of Fluid Mechanics, John Wiley and Sons, Inc., New York, pp. 9-14.

Shannon, M.A., Bohn, P.W., Elimelech, M., Georgiadis, J.G., Mariñas, B.J. and Mayes, A.M. (2008). "Science and technology for water purification in the coming decades." Nature 452(7185): 301-310.

Shimelis, B., Zewge, F. and Chandravanshi, B. S. (2006). "Removal of excess fluoride from water by aluminum hydroxide." B. Chem. Soc. Ethiopia 20(1): 17-34.

Shin, H. and Santamarina, J. C. (2009). "Mineral dissolution and the evolution of k_0." J. Geotech. Geoenviron. 135(8): 1141-1147.

Soni, M. G., White, S. M., Flamm, W. G. and Burdock, G. A. (2001). "Safety evaluation of dietary aluminum." Regul. Toxicol. Pharm. 33(1): 66-79.

Sujana, M.G. and Anand, S. (2010). "Iron and aluminium based mixed hydroxides: a novel sorbent for fluoride removal from aqueous solutions." Appl. Surf. Sci. 256(23): 6956-6962.

Sujana, M.G., Thakur, R.S. and Rao, S.B. (1998). "Removal of fluoride from aqueous solution by using alum sludge". J. Colloid Interf. Sci. 206(1): 94-101.

Tang, Y., Guan, X., Su, T., Gao, N. and Wang, J. (2009). "Fluoride adsorption onto activated alumina: Modeling the effects of pH and some competing ions." Colloid Surf. A 337(1-3): 33-38.

Tomar, V. and Kumar, D. (2013). "A critical study on efficiency of different materials for fluoride removal from aqueous media." Chem. Cent. J. 7(1): 1-15.

Tor, A., Danaoglu, N., Arslan, G. and Cengeloglu, Y. (2009). "Removal of fluoride from water by using granular red mud: batch and column studies." J. Hazard. Mater. 164(1): 271-278.

UNICEF (1999). States of the Art report on the extent of fluoride in drinking water and the resulting endemicity in Inida. New Delhi, India.

UNICEF. (2003). Water, environment and sanitation-Common water and sanitation-related diseases. Retrieved on Jan. 7, 2016, from http://www.unicef.org/wash/index_wes_related.html.

Virta, R. L. (2002). Zeolites. Unites States Geological Survey Publications 84: 1-3.

Vyas, R. K. and Kumar, S. (2004). "Determination of micropore volume and surface area of zeolite molecular sieves by DR and DA equations: A comparative study." Indian J. Chem. Technol. 11: 704-709.

Walker, W. J., Cronan, C. S. and Patterson, H. H. (1988). "A kinetic study of aluminum adsorption by aluminosilicate clay minerals." Geochim. Cosmochim. Ac. 52(1): 55-62.

Wang, Y., Gao, B.-Y., Xu, X.-M., Xu, W.-Y. and Xu, G.-Y. (2009). "Characterization of floc size, strength and structure in various aluminum coagulants treatment." J. Colloid Interf. Sci. 332(2): 354-359.

Wefers, K. and Misra, C. (1987). Oxides and hydroxides of aluminum. Alcoa Technical Paper No. 19, Alcoa Laboratories.

World Health Organization, 2004. Guidelines for drinking-water quality: recommendations (Vol. 1). World Health Organization.

Xu, S., Gao, B. and Saiers, J. E. (2006). "Straining of colloidal particles in saturated porous media." Water Resour. Res. 42(12): W12S16.

Zhao, Y., Li, X., Liu, L. and Chen, F. (2008). "Fluoride removal by Fe(III)-loaded ligand exchange cotton cellulose adsorbent from drinking water." Carbohyd. Polym. 72(1): 144-150.

Chapter 5 : Conclusions and Recommendations

Overall conclusions

Amorphous aluminum (hydr)oxides (AlOOH) and AlOOH-amended zeolites (including amended MS-13X, amended MS-Y, amended silicon molecular sieves, and amended sodalite) developed in this study showed high fluoride removal capacity superior to conventional fluoride adsorbents such as bone char, activated alumina and natural clays (Bhatnagar et al. 2011, Habuda-Stanić et al. 2014). The lower crystallinity of AlOOH and formation of new mineral phase, basaluminite, appear to be major factors responsible for the high fluoride adsorption. Further, the material preparation was using room-temperature synthesis using slightly acidic pH to precipitate AlOOH and with the addition of extra sulfate and citrate during preparation. In contrast, despite having the same basaluminite phase, AlOOH prepared at high temperature (200°C) was less effective in fluoride removal probably due to the loss of surface area during formation of larger AlOOH crystallites and improved crystallinity (Chapter Two). Loss of surface area is not the only factor that determines the decreased fluoride removal capacity since the variation in Q_m is not consistent with the change of surface area (Table 2-1). For example, after eliminating the effect of surface area (BET), AlOOH-25 (0.083 mg/m^2) still has higher surface area normalized Q_m than AlOOH-200 (0.056 mg/m^2), so does AlOOH(Cit)-25 (0.072 mg/m^2) compared to AlOOH(Cit)-200 (0.047 mg/m^2). Moreover, the conventional thermal treatment at 500 °C of AlOOH to produce activated alumina (γ-Al_2O_3) also resulted in a reduced fluoride removal capacity (Chapter Two).

When introducing extra metals to aluminum-based minerals through surface modification on synthesized AlOOH (e.g., iron oxide impregnated AlOOH) or co-

precipitation of aluminum-metal binary oxides (e.g., magnesium-aluminum layered double hydroxides), fluoride removal capacity declined compared to pure AlOOH. It was likely that some aluminum sites on AlOOH with high fluoride-affinity were replaced or covered by other metal (oxides). For practical applications in endemic fluorosis areas, AlOOH can be used on its own or in combination with low-cost zeolites which occur naturally in many areas of developing regions. Out of a variety of candidate materials, zeolites and their synthetic counterparts—molecular sieves—were found to be the most suitable substrates for amendment which showed high fluoride removal capacity after loaded with AlOOH. AlOOH and AlOOH-amended zeolites also demonstrated high specificity towards fluoride because a consistent fluoride removal capacity was observed in the presence of potential competing solutes (sulfate, silicate, bicarbonate, and pyromellitic acid with concentrations five times that of fluoride).

In addition to the high affinity and specificity to fluoride, lower energy consumption (~0.011 kWh/m^3) than electrocoagulation (10.8 kWh/m^3) and reverse osmosis (5 kWh/m^3), and lower production cost (~\$1.00/m^3) than activated alumina (\$2.94/m^3) per cubic meters of treated water were calculated for pure AlOOH and AlOOH-amended sodalite. The effluent from filters packed with pure AlOOH and AlOOH-amended zeolites showed a sign of aluminum leaching with the increase of effluent fluoride concentration after column breakthrough; nevertheless, after the initial flushing out of small AlOOH particles in the first 70 bed volumes, the aluminum concentration was maintained below 0.2 mg/L, a level recommended by the WHO drinking-water standard.

Based on the results, AlOOH-amended zeolite prepared with 0.6 M aluminum chloride and at pH 5.3 could be applied in developing countries for the following reasons. First, it has a promising batch fluoride removal capacity ($Q_{1.5}$ = 23.7±2.0 mg F^-/g) and impressive column service time (1370 bed volumes at influent fluoride concentration of 10 mg/L). Second, its operation only requires small amount of energy for household and community-scale filters (2.13×10^{-4} and 0.011 kWh per day, respectively). For areas without continuous electricity, hydrostatic energy (elevated storage tank) can be used for community-scale filter operation using a tank about 2.5 meters above the column. Third, it is an inexpensive material with the production cost of $1.05 to treat one cubic meter of fluoride-contaminated water. Lastly, its use shows less aluminum leaching (average 0.043 mg Al/L) than pure AlOOH (average 0.188 mg Al/L) before column breakthrough. The recipe of making AlOOH-amended zeolite can be modified depending on the availability of substrate zeolites and aluminum salts; but a large amount of aluminum concentration and slightly acidic pH are suggested to use during amendment.

Recommendations for Future Research

- *Fluoride removal mechanism of AlOOH*: Results in Chapter Three have shown that processes other than surface adsorption are primarily responsible for the fluoride removal by AlOOH, even at low fluoride concentrations (10 mg/L) (Chapters two and three). A typical explanation for enhanced adsorption was precipitation (of minerals consisting of adsorbate and elements from adsorbents) after initial surface adsorption or complexation (Wersin et al. 1989, Turner et al. 2005). This could be

used to account for the fluoride adsorption to AlOOH at high fluoride concentrations. In such a case, a large amount of aluminum ion was released with the dissolution of AlOOH, and might have precipitated with dissolved fluoride to form aluminum-fluoride complex minerals (e.g., cryolite (Na_3AlF_6)). Nevertheless, this explanation may not explain results for fluoride adsorption experiments (with AlOOH) conducted with low initial fluoride levels. The solution with low fluoride concentration (C_F^-) (e.g., 0.1 mg/L) and a low level of dissolved aluminum (e.g., 0.05 mg/L) is under-saturated with respect to two of the most likely formed aluminum-fluoride minerals (e.g., cryolite (Na_3AlF_6) or AlF_3). Hence, further research should seek to understand the type of the process dominating fluoride adsorption by AlOOH and to clarify the initiation, evolution and final products of this process in fluoride removal. Instead of dissolution-precipitation, the hypothesis is based on adsorption-phase-transformation. It is postulated that fluoride is first adsorbed to the surface sites of AlOOH followed by a phase-transformation process which produces a new mineral and incorporates those initially surface-attached fluoride into the bulk AlOOH mineral. Example of adsorption-induced phase-transformation can be found in Simmons et al. (1991) in which palladium lattice structure was reconstructed through the mediation of adsorbed-oxygen which stabilized the distorted surface sites with the increased palladium-oxygen bond strength. To test this hypothesis, surface-sensitive techniques such as X-ray photoelectron spectroscopy and X-ray absorption spectroscopy can be used to investigate the fluorine-aluminum bonding and speciation of fluorine.

- *Dominant fluoride adsorption crystal face:* When the aging temperature during AlOOH synthesis increased from 25°C to 200°C, the (020) peak on the XRD pattern (Fig. 5-1, AlOOH aged at 25°C versus AlOOH aged at 200°C, and AlOOH aged at 25°C and with extra citrate versus AlOOH aged at 25°C and with extra citrate) grew significantly from lowest-intensity to highest-intensity in contrast to (021), (130) and (150) peaks. However, the fluoride removal capacity of AlOOH showed a pronounced decline after the increase in aging temperature. As indicated by the results that the surface area normalized Q_m of AlOOH-25 (0.083 mg/m^2) and AlOOH(Cit)-25 (0.072 mg/m^2) are larger than those of AlOOH-200 (0.056 mg/m^2) and AlOOH(Cit)-200 (0.047 mg/m^2), respectively, factors other than surface area decrease might account for the decline in fluoride removal capacity with aging temperature. One hypothesis is that the enhanced development of (020) crystal face caused the reduced fluoride adsorption. The reasoning is that the (020) crystal face of AlOOH has lower affinity to fluoride compared to (021), (130), and (150) crystal faces and is inactive to fluoride adsorption. This proposal is based on the argument of McBride and Wesselink (1988) that an ideal (020) face of boehmite (AlOOH) is not reactive in surface ligand-exchange reactions. The reason could be that all hydroxyl groups on (020) face are coordinated to two aluminum atoms and are not readily available to protonate to form reactive $AlOH_2^+$ (McBride and Wesselink 1988). These reactive $AlOH_2^+$ groups could serve as Lewis acid sites (McBride and Wesselink 1988) that bond with fluoride ion.

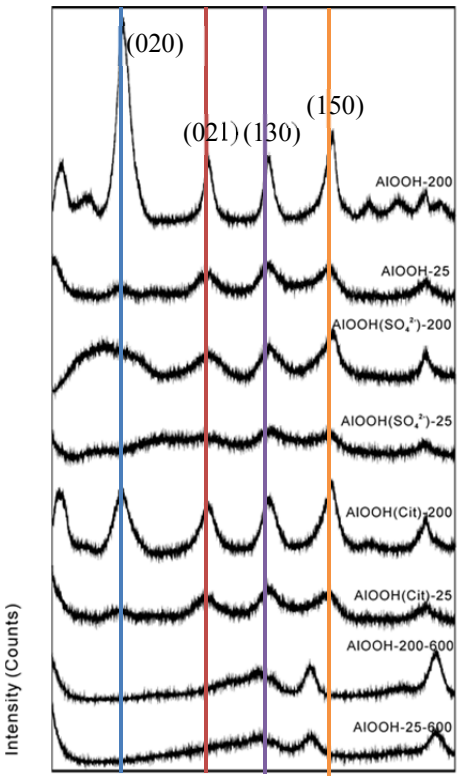

Figure 5-1 XRD patterns of aluminum (hydr)oxides prepared at different conditions (Chapter Two)

- *Effect of substrate material on the morphology of precipitated AlOOH:* As illustrated in Fig. 5-2, different substrate materials (sodalite (0.3 mm) versus molecular sieve 13X (2 μm)) presented distinct surface morphology after AlOOH precipitation. With different substrate materials, a rough surface of amended MS-13X with small particles on top (Fig. 5-2A open arrows) contrasted with a surface pattern showing flat terrace (Fig. 5-2B open arrows) mixed with cross-linked flake-like structure (Fig. 5-2B solid arrow) for amended sodalite (both amendment processes were conducted at exactly the same condition) (Fig. 5-2). It seems that substrate materials have an impact on the morphology of precipitated AlOOH.

Nevertheless, the morphological control mechanism of AlOOH remains unknown. Further research, therefore, should study the role of zeolites in the control of the morphology of precipitated AlOOH along with the determination of which property of zeolites is most critical in this process. A set of zeolites with different properties (e.g., roughness, particle size, and pore size) will be used to load AlOOH precipitates and effects of these properties on surface morphology will be investigated. To quantify properties, surface roughness (or root-mean square roughness) can be tested by atomic force microscope using silicon tip in the semi-contact mode (Asanithi 2014). Particle size and pore diameter can be measured by light scattering detector and BET pore analyzer, respectively.

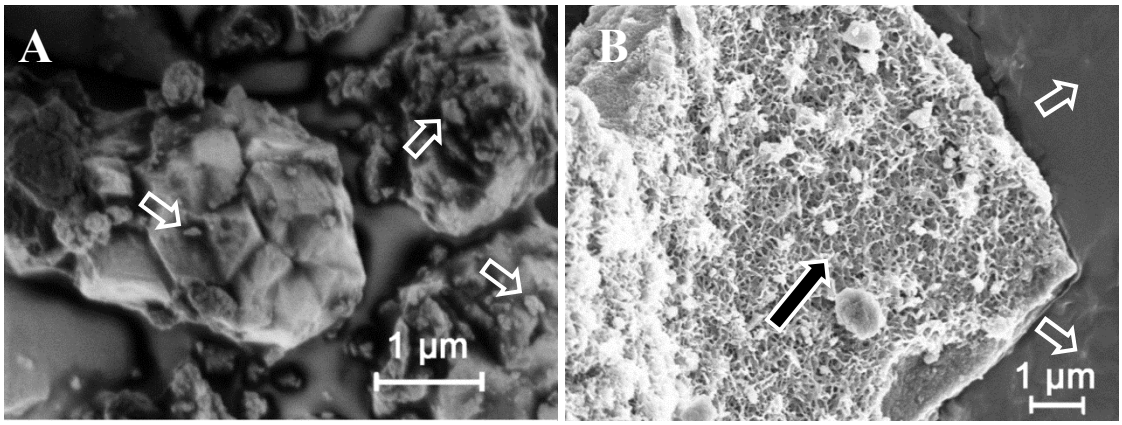

Figure 5-2 SEM images of Al-MS-13X (A) and Al-sodalite (B). Both materials were amended with 0.6 M $AlCl_3$ and prepared at pH 5.3

Recommendations for Practice

- *High-temperature granulation of AlOOH:* Based on energy consumption calculations, there is relatively high energy requirement (or requirement of relatively large hydrostatic pressure (2.48 m H_2O) to reach target flow rate)

associated with using small particle-size materials (0.3 mm) in community-scale filters (length of 70 cm and diameter of 10 cm) (Chapter Four). Although fine-particle (or powder) AlOOH can be directly used with coagulation techniques, it might require precise chemical weights and addition equipment and produce large amount of sludge during flocculation and coagulation (Phutdhawong et al. 2000). Moreover, the fine-particle material is difficult for storage and shipment and may cause health hazards related to dust emission during material shipment and use (Shanmugam 2015). Therefore, it might be desirable to increase the particle size of AlOOH based materials while maintaining high surface area when applying them in community-scale filters. For endemic fluorosis areas in developing countries, kiln firing is a readily available means for AlOOH granulation (without using pelletization equipment and binding agents) during which small particles coalesce to yield large granules (Liao and Huang 2011). However, evidence showed that the high-temperature treatment tends to deprive AlOOH of its high fluoride removal capacity, probably due to the improved crystallinity upon heating (Peri and Hannan 1960, Sun et al. 2008). Thus, the objective of this proposal work is to properly granulate AlOOH particles under thermal treatment without compromising their high fluoride removal capacity. An idea to circumvent the problem of fluoride removal capacity loss and to impede crystallization during heating is to attach some non-condensing groups (which do not join together during heating) to AlOOH particles before firing. For example, the increase in crystallinity of metal oxide during 500 °C thermal treatment were inhibited by bonding methyl siloxyl groups to the surface of metal oxide gels (Wu et al. 1999). Other material, such as starch,

might be an alternative option in impeding the crystallization or the growth of dominant crystal face of AlOOH. It was found by Nijhawan (manuscript in preparation) that hydroxyapatite fired at 1200 °C together with insoluble starch showed a less developed (211) face (as evidenced by a decreased peak intensity ratio of (211) reflection to (002), (112), (300) or (202) reflections in XRD patterns) and a higher fluoride removal capacity compared to the hydroxyapatite fired alone at 1200 °C (data not shown).

- *Practical issues for drinking-water fluoride treatment in developing countries:* To facilitate the implementation of AlOOH and AlOOH-amended zeolites in developing countries, the following steps are recommended. 1) Establish a method (e.g., plots of breakthrough curves under different conditions) that can help practitioners estimate the service time of a column under given inlet fluoride concentration and flow rate and replace spent adsorbents timely after column breakthrough. 2) Determine the fluoride removal performance of these materials at elevated temperature (e.g., 30°C) which may be encountered in summer and in tropic regions and at low temperature (e.g., 10°C) in winter. 3) Explore the possibility of using waste from alum production disposed of by alum manufacturing factories to prepare AlOOH adsorbent. There are currently huge amounts of alum waste discarded in open areas without treatment, e.g, Nigussie et al. (2007) indicated that about 4500-5000 tons of alum waste were accumulated in the outside of Awash Meklassa Aluminum Sulfate and Sulfuric Acid Factory, Ethiopia. Alum waste typically consists of quartz (silica) (~80%), clay minerals (~17.5%), alum (~3.5%), and aluminum hydroxide (~2%) (Nigussie et al. 2007). Aluminum can be

extracted from alum waste to produce AlOOH. Aluminum ion could be obtained by dissolving aluminum-based minerals contained in the waste and removing the major component, silica, at a low pH (e.g., pH 3) at which alum, aluminum hydroxide, and clay minerals readily dissolve (Siracusa and Somasundaran 1987, Cerqueira and da Cost Marques 2012) but silica not (Hamrouni and Dhahbi 2001). The use of alum waste could potentially reduce the production cost, although the effect of its contained impurity on fluoride adsorption should be assessed. 4) Evaluate the life cycle environmental impacts of AlOOH adsorbents in order to select the most environmental-friendly substrate materials and raw chemicals and to avoid heavy pollution-laden activities in procuring these raw materials. For instance, life cycle assessment can be conducted to facilitate the selection of aluminum-containing raw minerals for less resource-intensive aluminum chloride (or alum) production between bauxite and clay minerals.

References

Asanithi, P. (2014). "Surface porosity and roughness of micrographite film for nucleation of hydroxyapatite." J. Biomed. Mater. Res. A 102(8): 2590-2599.

Bhatnagar, A., Kumar, E. and Sillanpää, M. (2011). "Fluoride removal from water by adsorption—a review." Chem. Eng. J. 171(3): 811-840.

Haas, G., Menck, A., Brune, H., Barth, J. V., Venables, J.A. and Kern, K. (2000). "Nucleation and growth of supported clusters at defect sites: Pd/MgO (001)." Phys. Rev. B 61(16): 11105.

Habuda-Stanić, M., Ravančić, M. E. and Flanagan, A. (2014). "A review on adsorption of fluoride from aqueous solution." Materials 7(9): 6317-6366.

Hamrouni, B. and Dhahbi, M. (2001). "Analytical aspects of silica in saline water—application to desalination of brackish waters." Desalination 136(1): 225-232.

Liao, Y. C. and Huang, C. Y. (2011). "Effects of heat treatment on the physical properties of lightweight aggregate from water reservoir sediment." Ceram. Int. 37(8): 3723-3730.

McBride, M. B. and Wesselink, L. G. (1988). "Chemisorption of catechol on gibbsite, boehmite, and noncrystalline alumina surfaces." Environ. Sci. Technol. 22(6): 703-708.

Nigussie, W., Zewge, F. and Chandravanshi, B. S. (2007). "Removal of excess fluoride from water using waste residue from alum manufacturing process." J. Hazard. Mater. 147(3): 954-963.

Peri, J. B. and Hannan, R. B. (1960). "Surface hydroxyl groups on γ-alumina." J. Phys. Chem-US 64(10): 1526-1530.

Phutdhawong, W., Chowwanapoonpohn, S. and Buddhasukh, D. (2000). "Electrocoagulation and subsequent recovery of phenolic compounds." Anal. Sci. 16(10): 1083-1084.

Shanmugam, S. (2015). "Granulation techniques and technologies: recent progresses." BioImpacts: BI 5(1): 55-63.

Simmons, G. W., Wang, Y. N., Marcos, J. and Klier, K. (1991). "Oxygen adsorption on palladium (100) surface: phase transfomations and surface reconstruction." J. Phys. Chem. 95(11): 4522-4528.

Siracusa, P. A. and Somasundaran, P. (1987). "The role of mineral dissolution in the adsorption of dodecylbenzenesulfonate on kaolinite and alumina." Colloid. Surface. 26: 55-77.

Sun, Z. X., Zheng, T. T., Bo, Q. B., Du, M. and Forsling, W. (2008). "Effects of calcination temperature on the pore size and wall crystalline structure of mesoporous alumina." J. Colloid Interf. Sci. 319(1): 247-251.

Turner, B. D., Binning, P. and Stipp, S. L. S. (2005). "Fluoride removal by calcite: evidence for fluorite precipitation and surface adsorption." Environ. Sci. Technol. 39(24): 9561-9568.

Wersin, P., Charlet, L., Karthein, R. and Stumm, W. (1989). "From adsorption to precipitation: Sorption of Mn^{2+} on $FeCO_3$ (s)." Geochim. Cosmochim. Ac. 53(11): 2787-2796.

Wu, N. L., Wang, S. Y. and Rusakova, I. A. (1999). "Inhibition of crystallite growth in the sol-gel synthesis of nanocrystalline metal oxides." Science 285(5432): 1375-1377.

Chapter 6 : Supplemental Information

Section 1: Tables

Table S1 Fluoride adsorption performance of aluminum oxide amended substrate materials

Samples	Q_{max}[a] or Q_e (mg/g)	$Q_{1.5}$[a] or Q_e (mg/g)
0.04[b]$AlCl_3$-Cellulose	$Q_{100}\approx 0$	$Q_{1.5}\approx 0$
0.04$AlCl_3$-Steel wool	$Q_{max}=2.22\pm0.39$	$Q_{1.5}=0.129\pm0.064$
0.04$AlCl_3$-Glass wool	$Q_{max}=0.50\pm0.28$	$Q_{1.5}=0.022\pm0.033$
0.04$AlCl_3$-750*Pinus patula* char[c]	$Q_{max}=1.608\pm0.072$	$Q_{1.5}=0.153\pm0.025$
0.04$AlCl_3$-Dowex 1×8	$Q_{100}\approx 0$	$Q_{1.5}\approx 0$
0.04$AlCl_3$-Dowex 50W	$Q_{100}=6.06$	$Q_{1.5}=0.177\pm0.019$
0.04$AlCl_3$-Amberlite FPC22H	$Q_{100}=5.84$	$Q_{2.3}=0.27$
0.04$AlCl_3$-IMAC HP333	$Q_{100}=3.88$	$Q_{1.5}=0.040\pm0.009$
0.04$AlCl_3$-Polystyrene-DVB	$Q_{100}\approx 0$	$Q_{1.5}\approx 0$
0.04$AlCl_3$-Molecular sieve 4A	$Q_{max}=2.82\pm0.17$	$Q_{1.5}=0.152\pm0.025$
0.04$AlCl_3$-Molecular sieve 5A	$Q_{max}=7.6\pm2.8$	$Q_{1.5}=0.24\pm0.18$
0.3$AlCl_3$-Molecular sieve 5A	$Q_{max}=9.16\pm0.54$	$Q_{1.5}=1.07\pm0.16$
0.04$AlCl_3$-Molecular sieve 13X	$Q_{max}=5.70\pm0.26$	$Q_{1.5}=0.333\pm0.038$
Raw molecular sieve 5A	$Q_{max}=1.29\pm0.28$	$Q_{1.5}=0.056\pm0.030$
0.04$AlCl_3$-MSU-H	$Q_{max}=2.54\pm0.26$	$Q_{1.5}=0.197\pm0.060$

[a] Uncertainties of Q_{max} are obtained directly from the Langmuir or Freundlich isotherm fitting; uncertainties of $Q_{1.5}$ are calculated using error propagation. Other reported Q_e are directly from experimental data when adsorption data cannot be fit by the Langmuir or Freundlich isotherms.

[b] 0.04 and 0.3 denote the concentrations of aluminum chloride (0.04 M and 0.3 M) used in the amendment process. Five day amendment was conducted for all substrate materials and the pH used in the amendment was not adjusted. After amendment, samples were rinsed with deionized water thoroughly and dried at 70°C in the oven.

[c] The *Pinus patula* was charred at 750°C for four hours, crushed and sieved with 40-80 mesh sieves.

Table S2 Properties of substrate materials (data from Sigma-Aldrich except *Pinus patula*)

Substrate	Pore size	Composition/Source	Notes
Cellulose[a]		$C_6H_{10}O_5$, D-glucose	
Steel wool		Iron oxide	
Glass wool	8 μm	SiO_2	
Pinus patula		Acquired from the Dancing Oak Nursery Company	
Dowex 1×8		Styrene-divinylbenzene (gel)/8% cross linkage	Gel-type strongly acidic CER[c]
Dowex 50W		Sulfonic styrene-divinylbenzene (gel)/8% cross linkage	Gel-type AER[c]
Amberlite FPC22H		Sulfonic polystyrene	Macroporous strongly acidic CER
IMAC HP333		Carboxylic polyacrylic	Macroporous weakly acidic CER
Polystyrene-DVB		Polystyrene-DVB	Inert resin
Molecular sieve 4A[b]	0.4 nm	1 Na_2O: 1 Al_2O_3: 2.0 ± 0.1 SiO_2 : x H_2O	10.5 pH_{slurry} (5% slurry)
Molecular sieve 5A	0.5 nm	0.80 CaO : 0.20 Na_2O : 1 Al_2O_3: 2.0 ± 0.1 SiO_2: x H_2O	10.5 pH_{slurry} (5% slurry)
Molecular sieve 13X	1 nm	1 Na_2O: 1 Al_2O_3 : 2.8 ± 0.2 SiO_2 : x H_2O	10.5 pH_{slurry} (5% slurry)
MSU-H	7.1 nm	SiO_2	Mesoporous material

[a] All substrate materials except *Pinus patula* wood were purchased from Sigma Aldrich.
[b] Molecular sieves are in the powder form with particle size of 2.5 μm.
[c] CER and AER indicate cation and anion exchange resins, respectively.

Section 2: Figures

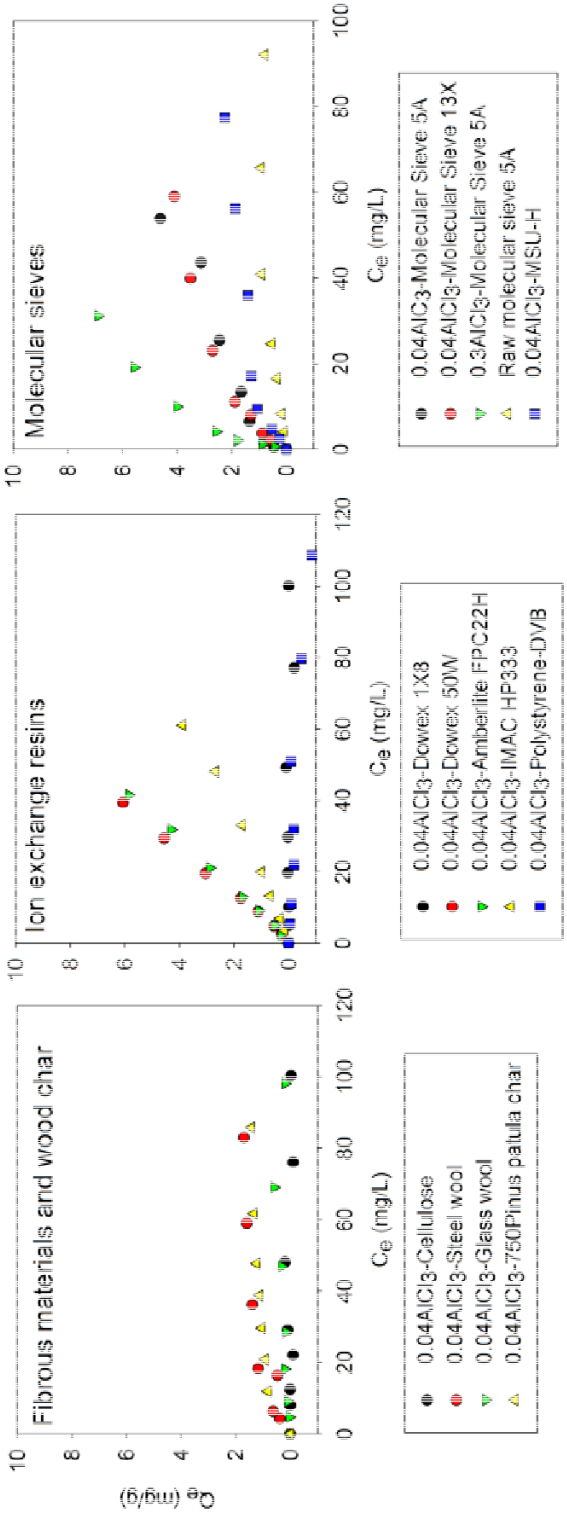

Figure S1 Preliminary fluoride adsorption screening tests on different substrate materials amended with 0.04 M or 0.3 M aluminum chloride (properties of substrate materials can be found in Table S2)

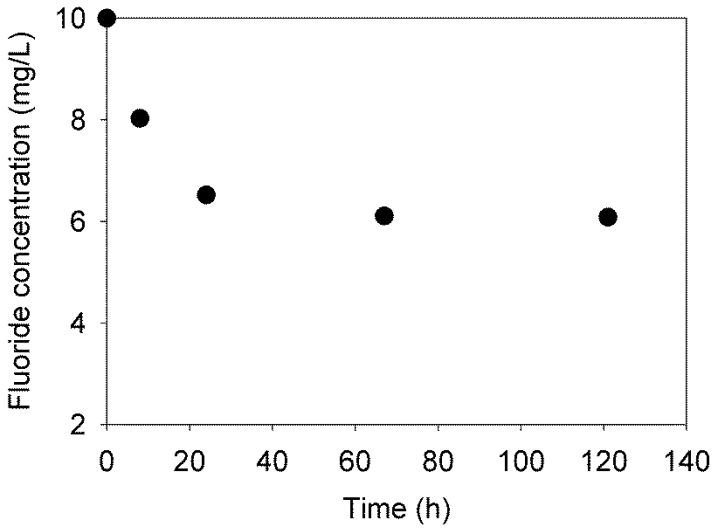

Figure S2 Solution fluoride concentration versus time using 0.04Al-MS-4A (molecular sieve 4A amended with 0.04 M aluminum (hydr)oxide) as the fluoride adsorbent. The initial fluoride concentration was 10 mg/L and the solid-to-liquid ratio was 4 g/L.

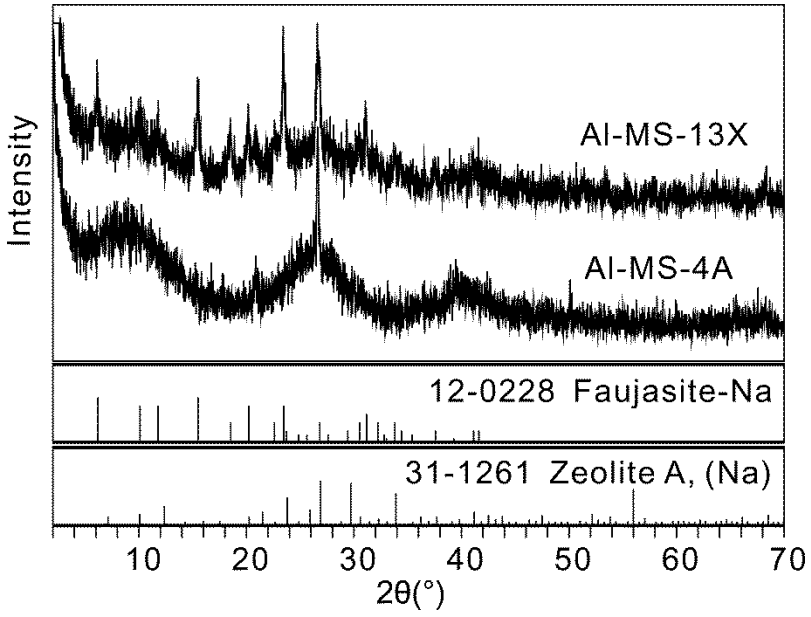

Figure S3 XRD patterns of Al-MS-4A, Al-MS-13X and reference minerals

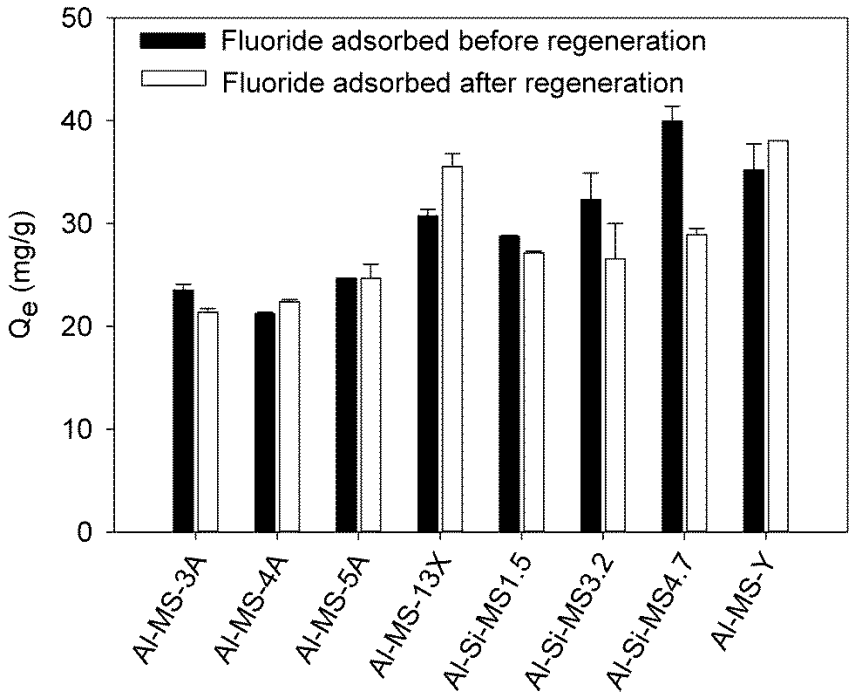

Figure S4 Fluoride adsorption to various aluminum (hydr)oxide amended molecular sieves before and after regeneration. The actual weight of samples after regeneration (i.e., accounting for the loss of mass due to dissolution and decanting) was used to calculate the equilibrium fluoride adsorption density (Q_e, mg F^- per g of adsorbent). The initial fluoride concentration was 100 mg/L and 10^{-4} M sodium hydroxide solution was used as regenerant.

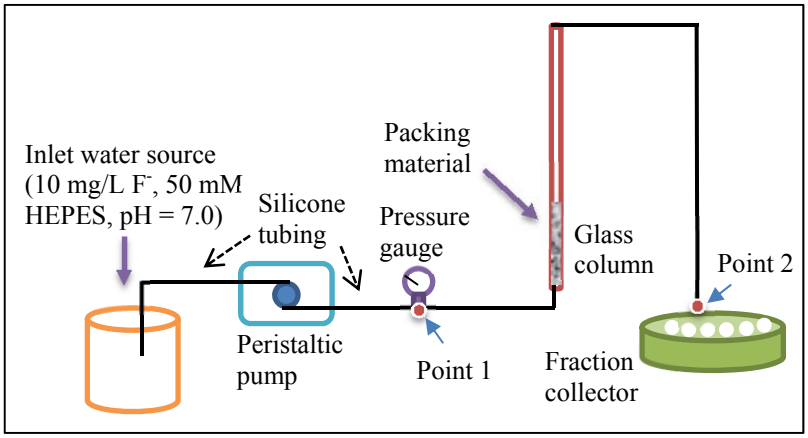

Figure S5 Column setup used in this study

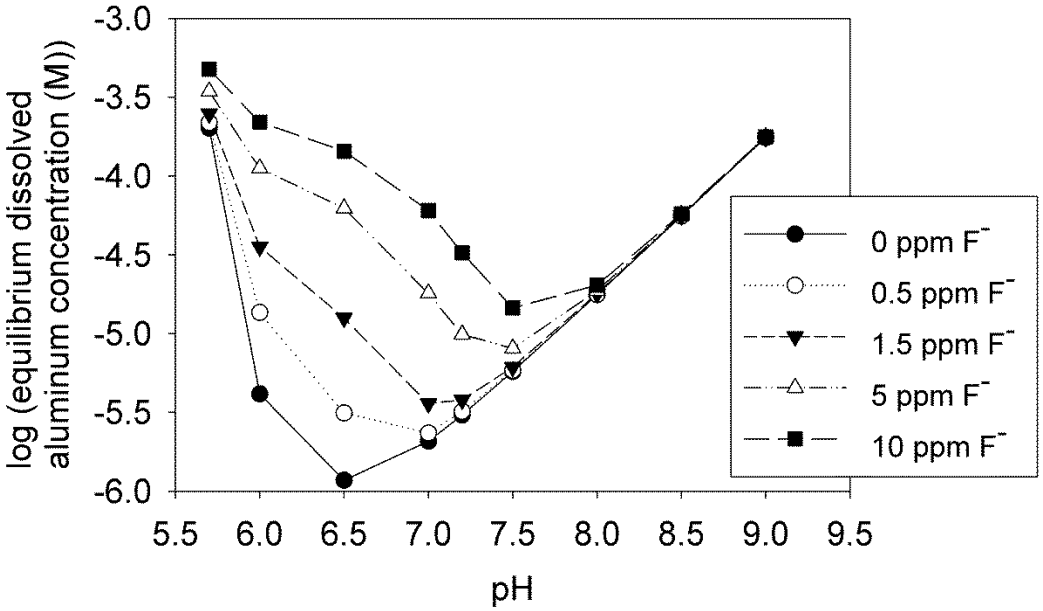

Figure S6 Equilibrium aluminum concentration dissolved from AlOOH (AlOOH (s) + 3 H^+ = Al^{3+} + 2 H_2O, pK_{sp} = 10.2) at different fluoride concentrations and pH values. Equilibrium reaction constants were from the Minteq database, Hem and Roberson (1967), Phillips et al. (1997), and Sanjuan and Michard (1987), see them in the SI Section 4.

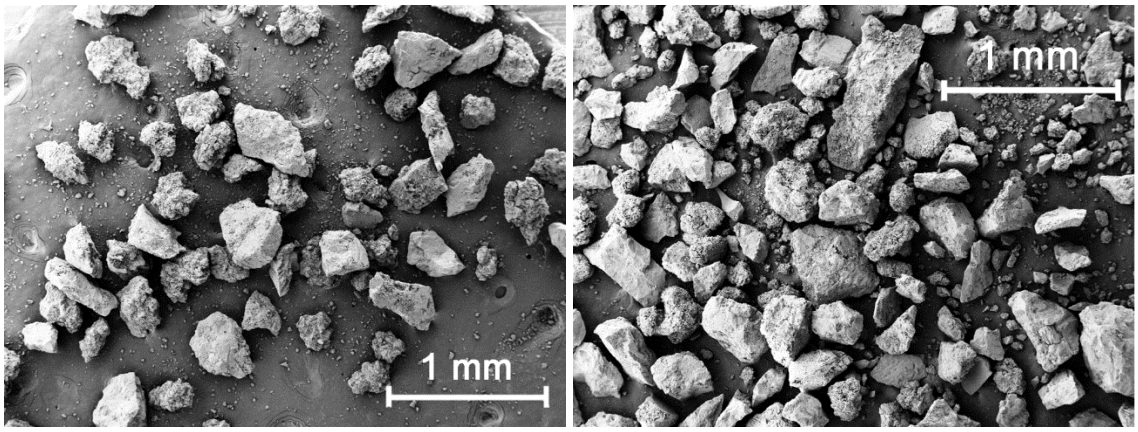

Figure S7 SEM images of 0.6Al-sodalite-5.3-1 before (left) and after (right) column fluoride adsorption

Section 3: Energy consumption

Nomenclature

Variables	Definition
A	Column cross-sectional area (m^2)
A_t	Tubing cross-sectional area (m^2)
D_f	Column filter inner diameter (m)
D_p	Adsorbent particle diameter (m)
D_t	Tubing inner diameter (m)
E_K	Kinetic energy density (Pa)
E_T	Total energy density (Pa)
E_{Po}	Potential energy density (Pa)
E_{Pr}	Pressure energy density (Pa)
HL_f	Head loss due to column filter friction (Pa)
HL_t	Head loss due to tubing friction (Pa)
k	Intrinsic permeability (m^2)
L	Height of column filter (m)
P_0	Atmospheric pressure (Pa)
P_P	Pump energy consumption per unit of time (W)
P_T	Total energy consumption per unit of time (W)
Q	Volumetric flow rate (m^3/s)
v	Velocity (m/s)
v_f	Superficial velocity in column filter (m/s)
v_t	Velocity in tubing (m/s)

z	Height above a reference level (m)
ΔE_T	Total energy density loss (Pa)
ε	Column filter porosity
μ	Dynamic viscosity of water (0.001 N·s/m^2 at 20°C (Haynes 2015))
ρ	Density of water (998.2 kg/m^3 at 20°C (Haynes 2015))

The pump efficiency was assumed to be 70% (typical range of pump efficiencies is between 60% and 85% (Horowitz 2006)). The energy consumed by the column operation includes kinetic, potential, and pressure energy, and energy loss due to fluid friction with the tubing and column. To calculate these items, energy density, equivalent to pressure (Pa), is frequently employed to calculate the final energy consumption. Simply put, energy density (Pa or kg/(m·s^2)) equals energy consumed per unit time (W or kg·m^2/s^3) divided by the volumetric flow rate Q (m^3/s) (Baaquie and Willeboordse 2009). The kinetic (E_K) and potential (E_{Po}) energy densities, according to Bernoulli's equation (Schetz and Fuhs 1999), can be expressed as $\frac{1}{2}\rho v^2$ and $\rho g z$, respectively. Total energy density (E_T) is the sum of E_K, E_{Po}, E_{Pr}, and energy density loss due to friction. E_{Pr} is the pressure energy density.

Calculations of energy consumption for large-scale filters

The community-scale filter was taken as an example of energy density calculation in the calculations below. For community-scale filters, equal empty bed contact time (EBCT, 6.5 min) and same adsorbent size were assumed to small bench-scale columns. The inner diameter of inlet tubing for community-scale filters was assumed to be 0.0127 m

(nominal pipe size 1/2"). The porosity was estimated to be 0.35 based on measurements with bench-scale columns. The friction loss due to tubing was omitted because preliminary calculations showed that the tubing energy density loss (less than 200 Pa) is much smaller than the energy density loss in packed column filter (e.g., 2×10^5 Pa).

- Calculation of kinetic energy density

  The diameter of community-scale filters was assumed to be 0.1 m and the length to be 0.7 m. Thus, the volumetric flow rate and tubing velocity are

  $$Q = \frac{Column\ bed\ volume}{EBCT} = \frac{\frac{\pi\times {D_f}^2}{4}\times L}{EBCT} = \frac{\frac{\pi\times(0.1\ m)^2}{4}\times 0.7\ m}{6.5\ min\times\frac{60\ s}{min}} = 1.41\times10^{-5}\frac{m^3}{s}$$ Eq. (1)

  $$v_t = \frac{Q}{A_t} = \frac{Q}{(\frac{\pi\times {D_t}^2}{4})} = \frac{1.41\times10^{-5}\frac{m^3}{s}}{(\frac{\pi\times(0.0127\ m)^2}{4})} = 0.11\frac{m}{s}$$ Eq. (2)

  Therefore, the kinetic energy density is

  $$E_K = \frac{1}{2}\rho v_t^2 = 0.5\times998.2\frac{kg}{m^3}\times(0.11\frac{m}{s})^2 = 6.18\ Pa$$ Eq. (3)

  Considering the small value of kinetic energy density, it is neglected in the calculation of total energy density.

- Calculation of potential energy density (at Point 2)

  Point 2 (Fig. S5) was assumed to be on the datum level (zero elevation). The potential energy density is thus

  $$E_{Po} = \rho g z = 998.2\frac{kg}{m^3}\times9.8\frac{m}{s^2}\times0\ m = 0\ Pa$$ Eq. (4)

- Calculation of energy density loss due to friction

To calculate the energy density loss due to friction, we selected two points, one of which is at the column inlet where the pressure gauge connects with the inlet tubing (Fig. S5, Point 1), and the other of which is at the point we collected sample using the fraction collector (Fig. S5, Point 2). Points 1 and 2 were at the same elevation. Based the Bernoulli equation, the total energy is conserved, i.e.,

$$\frac{1}{2}\rho v^2 + \rho g z + E_{Pr1} = \frac{1}{2}\rho v^2 + \rho g z + E_{Pr2} + HL_t + HL_f \quad \text{Eq. (5)}$$

Energy at Point Energy at Point Energy loss due to Friction

Because the pressure at Point 2 equals to the atmospheric pressure (P_0) and the head loss due to the friction of water flowing through tubing (HL_t) was omitted, eq (5) can be rewritten as

$$\frac{1}{2}\rho v^2 + \rho g z + E_{Pr1} = \frac{1}{2}\rho v^2 + \rho g z + P_0 + HL_f \quad \text{Eq. (6)}$$

Rearranging equation (6) to solve for HL_f

$$HL_f = E_{Pr1} - P_0 \quad \text{Eq. (7).}$$

(1) Calculation of head loss due to column filter friction using Ergun equation

To calculate the head loss, Ergun equation (Ergun 1952) was invoked with its expression as

$$HL_f = \frac{150\mu L}{D_P^2}\frac{(1-\varepsilon)^2}{\varepsilon^3} v_f \ (linear\ flow) + \frac{1.75L\rho}{D_P}\frac{(1-\varepsilon)}{\varepsilon^3} {v_f}^2 (nonlinear\ flow) \quad \text{Eq. (8)}$$

The average particle size of materials D_P was assumed to be 3×10^{-4} m (the average of 1.8×10^{-4} (80 mesh sieve size) and 4.2×10^{-4} m (40 mesh sieve size)).

The superficial flow velocity in the column is

$$v_f = \frac{Q}{A} = \frac{1.41\times10^{-5}\frac{m^3}{s}}{\frac{\pi\times {D_f}^2}{4}} = \frac{1.41\times10^{-5}\frac{m^3}{s}}{\frac{\pi\times(0.1\ m)^2}{4}} = 1.8\times10^{-3}\frac{m}{s}$$ Eq. (9)

According to Ergun equation (eq. 8), the head loss due to the packed material friction is

$$HL_f = \frac{150\times0.001\frac{N\cdot s}{m^2}\times0.7\ m}{(0.0003\ m)^2}\times\frac{(1-0.35)^2}{0.35^3}\times1.8\times10^{-3}\frac{m}{s}+\frac{1.75\times2\ m\times998.2\frac{kg}{m^3}}{0.0003\ m}$$
$$\times\frac{(1-0.35)}{0.35^3}\times\left(1.8\times10^{-3}\frac{m}{s}\right)^2$$
$$= \frac{150\times0.001\frac{kg\cdot m\cdot s}{s^2\cdot m^2}\times0.7\ m}{0.0003\ m^2}\times\frac{(1-0.35)^2}{0.35^3}\times1.8\times10^{-3}\frac{m}{s}+199.4\frac{kg}{m\cdot s^2}$$
$$= 20635\frac{kg}{m\cdot s^2}+199.4\frac{kg}{m\cdot s^2}$$
$$= 20834\frac{kg}{m\cdot s^2}$$
$$= 2.08\times10^4\ Pa$$ Eq. (10)

(2) Calculation of head loss due to column filter friction using Darcy's law

Darcy's law (Darcy 1856) was used to calculate intrinsic permeability and energy density loss with its expression as

$$Q = \frac{-k\cdot A\cdot\Delta E_T}{\mu\cdot L}$$ Eq. (11)

Rearranging eq. (11) to solve for the intrinsic permeability *k*,

$$k = \frac{-Q\cdot\mu\cdot L}{A\cdot\Delta E_T}$$ Eq. (12)

For the bench-scale column

$$Q = 0.6\frac{mL}{min}\times\frac{min}{60\ s}\times\frac{m^3}{10^6\ mL} = 1\times10^{-8}\frac{m^3}{s}$$

$$L = 0.05\ m$$

The area *A* in this case is

$$A = \frac{\pi \times {D_f}^2}{4} = \frac{\pi \times (0.01\ m)^2}{4} = 7.85 \times 10^{-5}\ m^2 \quad \text{Eq. (13)}$$

The energy density between Point 1 and Point 2 is

$$\Delta E_T = E_2(point\ 2) - E_1(point\ 1) = E_{Pr2} - E_{Pr1} \quad \text{Eq. (14)}$$

According to eq. (5)

$$E_{Pr2} - E_{Pr1} = -HL_f = \Delta E_T \quad \text{Eq. (15)}$$

The measured average total energy density loss for bench-scale columns (difference between the column outlet and inlet pressure, see Fig. S8) is about 0.018 psi by reading off pressure gauges before 700 bed volumes, i.e.,

$$\Delta E_T = E_{Pr2} - E_{Pr1} = 0.885\ psi - 0.903\ psi = -0.018\ psi \times \frac{6894.756\ pa}{psi} = -124.1\ Pa \quad \text{Eq. (16)}$$

Plugging values of Q, μ, L, A, and ΔE_T into eq. (12) to solve for k

$$k = \frac{-Q \cdot \mu \cdot L}{A \cdot \Delta E_T} = \frac{-1 \times 10^{-8} \frac{m^3}{s} \times 0.001\ Pa \cdot s \times 0.05\ m}{7.85 \times 10^{-5}\ m^2 \times (-124.1\ Pa)} = 5.17 \times 10^{-11}\ m^2 \quad \text{Eq. (17)}$$

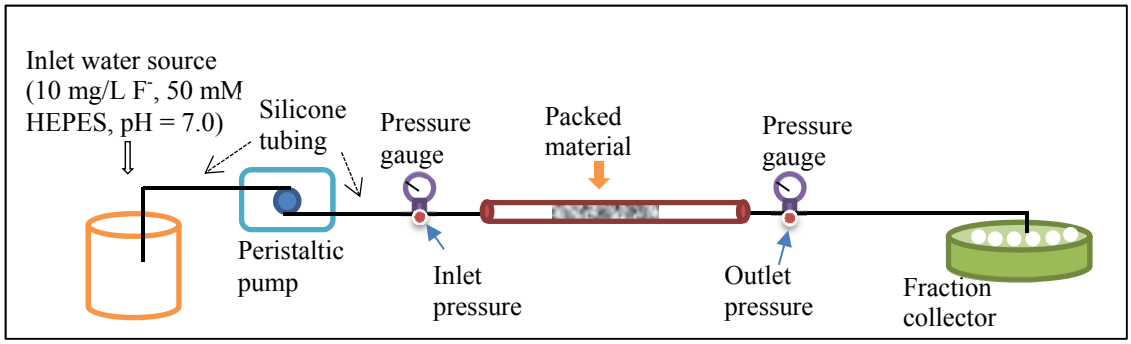

Figure S8 Column setup used to measure inlet and outlet pressure

The same intrinsic permeability k was applied in the calculation of total energy density loss of community-scale filter. Rearrange eq. (11) to get the expression of ΔE_T, i.e.,

$\Delta E_T = \frac{-Q \cdot \mu \cdot L}{A \cdot k}$ Eq. (18)

Since the same EBCT of community-scale filters were assumed as bench-scale columns, the volumetric flow rate is 1.41×10^{-5} m^3/s according to eq. (1).

For the community-scale filter,

$L = 2\ m$

$A = 7.85 \times 10^{-5}\ m^2$

Plugging values of Q, μ, L, A, k, and ΔE into equation (18) to solve for ΔE_T

$\Delta E_T = \frac{-Q \cdot \mu \cdot L}{A \cdot k} = \frac{-1.41 \times 10^{-5} \frac{m^3}{s} \times 0.001\ Pa \cdot s \times 0.7\ m}{7.85 \times 10^{-5}\ m^2 \times 5.17 \times 10^{-11}\ m^2} = -2.43 \times 10^4\ Pa$ Eq. (19)

According to eq. (15)

$HL_f = -\Delta E_T = 2.43 \times 10^4\ Pa$ Eq. (20)

- Calculation of total energy density required for community-scale filters operation

  Because of energy conservation, the total energy density required to operate community-scale filters is equal to that at the column outlet (Point 2, Fig. S5). According to eq. (5), the total energy density (E_T) at Point 2 (Fig. S5) is

  $E_T = \frac{1}{2}\rho v^2 + \rho g z + E_{Pr2} + HL_t + HL_f$ Eq. (21)

  With the HL_f calculated using Ergun equation,

  $E_T = 6.18\ Pa + 0\ Pa + 0\ Pa + 0\ Pa + 2.08 \times 10^4\ Pa = 2.08 \times 10^4\ Pa$ (Ergun equation) Eq. (22)

  Alternatively, the HL_f can be calculated using Darcy's law,

$E_T = 6.18\ Pa + 0\ Pa + 0\ Pa + 0\ Pa + 2.43 \times 10^4\ Pa = 2.43 \times 10^4\ Pa$ (Darcy's law) Eq. (23)

- Calculation of total energy required per unit of time for community-scale filters operation

  Total energy required per unit of time can be calculated with the total energy density E_T, i.e.,

  $P_T = E_T \times Q = 2.08 \times 10^4\ Pa\ \times 1.41 \times 10^{-5}\ \frac{m^3}{s} = 2.08 \times 10^4\ \frac{kg}{m \cdot s^2}\ \times 1.41 \times 10^{-5}\ \frac{m^3}{s} = 0.29\ \frac{kg \cdot m^2}{s^3} = 0.29\ W$ (Using the E_T calculated based on Ergun equation) Eq. (24)

  $P_T = E_T \times Q = 2.43 \times 10^4\ Pa\ \times 1.41 \times 10^{-5}\ \frac{m^3}{s} = 2.43 \times 10^4\ \frac{kg}{m \cdot s^2}\ \times 1.41 \times 10^{-5}\ \frac{m^3}{s} = 0.34\ \frac{kg \cdot m^2}{s^3} = 0.34\ W$ (Using the E_T calculated based on Darcy's law) Eq. (25)

- Energy supplied by the pump

  The energy supplied by the pump can be calculated by taking into account the pump efficiency (70%), i.e.,

  $P_p = \frac{Power_T}{efficiency} = \frac{0.29\ W}{0.7} = 0.42\ W$ (Using the P_T calculated based on Ergun equation) Eq. (26)

  $P_p = \frac{Power_T}{efficiency} = \frac{0.34\ W}{0.7} = 0.49\ W$ (Using the P_T calculated based on Darcy's law) Eq. (27)

- Energy consumed by the pump per day

  $Energy\ per\ day = P_p \times 1\ d = 0.42\ \frac{J}{s} \times 1\ d \times \frac{24\ h}{d} \times \frac{3600\ s}{h} = 3.63 \times 10^5\ J =$

  $36.3\ kJ = 36.3\ kJ \times \frac{kWh}{3600\ kJ} = 0.010\ kWh$ (Using the P_P calculated based on Ergun equation) Eq. (28)

  $Energy\ per\ day = P_p \times 1\ d = 0.49\ \frac{J}{s} \times 1\ d \times \frac{24\ h}{d} \times \frac{3600\ s}{h} = 4.23 \times 10^5\ J =$

  $42.3\ kJ = 42.3\ kJ \times \frac{kWh}{3600\ kJ} = 0.012\ kWh$ (Using the P_P calculated based on Darcy's law) Eq. (29)

Section 4: Adsorbent Production Cost

Production cost of pure AlOOH and amended sodalite

The production cost of pure AlOOH and amended sodalite, excluding labor and transportation fee which were surmised to be the same for all materials, was computed based on the price and consumption amount of raw chemicals. The prices of raw chemicals (aluminum chloride and sodium hydroxide) were taken from the International Conference on Information Systems website (2006), which can represent the market price of chemicals in the U.S., and the price of zeolite was from Virta (2002) (Table S1). The consumption of raw chemicals was estimated from experimental data.

The production cost of 0.6Al-sodaltie-5.3-0.3 is used as an example to show the calculation. Since the price of sodalite can vary significantly between countries, the price of general zeolite was used in lieu of sodalite (Table S3).

Table S3 Price of raw materials

Raw materials	Price ($ per kg)
$AlCl_3$	0.45
NaOH	0.59
zeolite	0.12

According to the amendment recipe, 30 g of zeolite is needed provided that 500 mL of 0.6 M aluminum chloride is used. Also, based on preliminary data, 141.12 mL of 5 M sodium hydroxide had to be applied to adjust the pH of half liter 0.6 M aluminum chloride to 5.3. In addition, assuming that all the aluminum in aluminum chloride precipitated during amendment and transformed to aluminum (hydr)oxide , 18 g of AlOOH (mw. 60) is formed in the amended material 0.6Al-sodaltie-5.3. The equation below could represent this process

$500\ \text{mL of 0.6 M}\ AlCl_3(40.05\ \text{g}) + 141.12\ \text{mL of 5 M NaOH}(28.224\ \text{g}) +$

$30\ \text{g zeolite} = 18\ \text{g AlOOH} + 30\ \text{g zeolite}$. After synthesis, 35% of the synthesized material was lost during crushing and sieving as indicated by the preliminary data.

In reference to the price of raw materials, the cost to prepare 48 g amended sodalite (sodalite (0.3 mm) amended with 0.6 M AlOOH) or 31.2 g sieved amended sodalite (excluding the 35% lost fraction) is $40.05\ \text{g} \times \frac{1\ \text{kg}}{1000\ \text{g}} \times 0.45 \frac{\text{dollar}}{1\ \text{kg}} +$

$28.224\ \text{g} \times \frac{1\ \text{kg}}{1000\ \text{g}} \times 0.59 \frac{\text{dollar}}{1\ \text{kg}} + 30\ \text{g} \times \frac{1\ \text{kg}}{1000\ \text{g}} \times 0.12 \frac{\text{dollar}}{1\ \text{kg}} = \$0.0383$. Considering the material used to pack one bed volume of bench-scale column, the mass of sieved material was 4.37 g and a total volume of 5.102 L of safe water could be produced (about 1300 bed volumes). The 1300 bed volumes of safe water was obtained by subtracting the first 70 bed volumes in which effluent aluminum concentration is above 0.2 mg/L from the service time (1370 bed volumes) of amended sodalite. Thus, the cost

to produce 4.37 g sieved material is $\frac{\$0.0383}{31.2\ \text{g}} \times 4.37\ \text{g} = \$0.0054$ or to produce 1 g sieved material is \$0.0012/g. The cost to treat one liter of water using 0.6Al-sodaltie-5.3 is $\frac{\$0.0054}{5.102\ \text{L}} = \$0.00105/\text{L}$, or to treat one cubic meters of water is \$1.05/m^3.

Production cost of activated alumina

Based on Onuoha (1983), the average fluoride capacity of activated alumina is 920-1480 g F^-/m^3 media, and the cost of activated alumina is \$435-530/m^3 media (1978 price) or \$0.57-0.69/kg media (density of activated alumina is 769 kg/m^3). To treat one liter of water containing 10 mg/L fluoride, at least $\frac{1\ \text{L} \times \frac{10\ \text{mg}}{\text{L}} \times \frac{\text{g}}{1000\ \text{mg}}}{1480 \frac{\text{g}}{\text{m}^3}} = 6.76 \times 10^{-6}\ \text{m}^3$ activated alumina is required.

Therefore, the cost of activated alumina to treat one liter of water is at least $6.76 \times 10^{-6}\ \text{m}^3 \times \frac{\$435}{\text{m}^3} = \$0.00294$ or the cost to treat a cubic meters of fluoride-containing water is \$2.94/m^3.

Section 5: Reactions used in equilibrium effluent aluminum modeling

The following reactions relevant to the dissolution of AlOOH and aqueous aluminum speciation in the presence of fluoride were used in equilibrium effluent aluminum modeling. All the reactions as well as their thermodynamic equilibrium constants are from the Visual Minteq ver. 3.1 (KTH, Stockholm) database except indicated otherwise.

$H_2O = OH^- + H^+$ $\qquad logK = -14.0$

$AlOOH(s) + 3H^+ = Al^{3+} + 2H_2O$ $\qquad logK_{sp} = -10.2$

$AlOOH(s) + 2H_2O = Al(OH)_4^- + H^+$ $logK_{sp} = 12.8$ (Hem and Roberson 1967)

$Al^{3+} + H_2O = Al(OH)^{2+} + H^+$ $logK = -5.0$

$Al^{3+} + 2H_2O = Al(OH)_2^+ + 2H^+$ $logK = -10.3$

$Al^{3+} + 3H_2O = Al(OH)_3(aq) + 3H^+$ $logK = -16.7$

$Al^{3+} + 4H_2O = Al(OH)_4^- + 4H^+$ $logK = -23.0$

$2Al^{3+} + 2H_2O = Al_2(OH)_2^{4+} + 2H^+$ $logK = -7.7$

$3Al^{3+} + 4H_2O = Al_3(OH)_4^{5+} + 4H^+$ $logK = -13.9$

$13Al^{3+} + 28H_2O = Al_{13}O_4(OH)_{24}^{7+} + 32H^+$ $logK = -98.7$ (Phillps et al. 1997)

$F^- + H^+ = HF$ $logK = 3.2$

$2F^- + H^+ = HF_2^-$ $logK = 3.8$

$Al^{3+} + F^- = AlF^{2+}$ $logK = 7.0$

$Al^{3+} + 2F^- = AlF_2^+$ $logK = 12.6$

$Al^{3+} + 3F^- = AlF_3(aq)$ $logK = 16.7$

$Al^{3+} + 4F^- = AlF_4^-$ $logK = 19.4$

$Al^{3+} + 5F^- = AlF_5^{2-}$ $logK = 19.3$ (Phillps et al. 1997)

$Al^{3+} + 6F^- = AlF_6^{3-}$ $logK = 19.5$ (Phillps et al. 1997)

$Al^{3+} + F^- + H_2O = AlF(OH)^+ + H^+$ $logK = 0.74$ (Phillips et al. 1997)

$Al^{3+} + F^- + 2H_2O = AlF(OH)_2 + 2H^+$ $logK = -5.7$ (Phillips et al. 1997)

$Al^{3+} + F^- + 3H_2O = AlF(OH)_3^- + 3H^+$ $logK = -12.8$ (Phillips et al. 1997)

$Al^{3+} + 2F^- + H_2O = AlF_2(OH) + H^+$ $logK = 5.2$ (Phillips et al. 1997)

$Al^{3+} + 2F^- + 2H_2O = AlF_2(OH)_2^- + 2H^+$ $logK = -1.7$ (Phillips et al. 1997)

$Al^{3+} + 3F^- + H_2O = AlF_3(OH)^- + H^+$ $logK = -31.8$ (Sanjuan and Michard 1987)

References

Baaquie, B. E. and Willeboordse, F. H. (2009). Exploring Integrated Science. CRC Press, pp. 133.

Darcy, H. (1856). Les fontaines publiques de la ville de Dijon: exposition et application. Victor Dalmont, Paris.

Ergun, S. (1952). "Fluid flow through packed columns." Chem. Eng. Prog. 48: 89-94.

Haynes, W. M. ed. (2015). CRC Handbook of Chemistry and Physics, 96th Edition. CRC press, pp. 6-7.

Hem, J. D. and Roberson, C. E. (1967). "Form and stability of aluminium hydroxide complexes in dilute solution." U.S. Geol. Surv. Water-Supply Pap. 1827-A.

Horowitz, F. B., Lipták, B.G. and Bain S. (2006). Pump controls. In: Lipták, B.G. (Eds.), *Instrument Engineers' Handbook: Process Control and Optimization*. CRC/Taylor & Francis, pp. 2088.

International Conference on Information Systems (2006). Indicative Chemical Prices. Retrieved on Jan. 7, 2016, from http://www.icis.com/chemicals/channel-info-chemicals-a-z/

Onuoha, U. O. (1983). Evaluation of an activated alumina sorption system for removal of fluoride from water. Master Thesis, Texas Tech. University.

Phillips, B. L., Casey, W. H. and Crawford, S. N. (1997). "Solvent exchange in $AlF_x(H_2O)_{6-x}^{3-x}$ (aq) complexes: Ligand-directed labilization of water as an analogue for ligand-induced dissolution of oxide minerals." Geochim. Cosmochim. Ac. 61(15): 3041-3049.

Sanjuan, B. and Michard, G. (1987). "Aluminum hydroxide solubility in aqueous solutions containing fluoride ions at 50°C." Geochim. Cosmochim. Ac. 51(7): 1823-1831.

Schetz J. A. and Fuhs A. E. (1999). Fundamentals of Fluid Mechanics, John Wiley and Sons, Inc., New York, pp. 9-14.

Virta, R. L. (2002). Zeolites. United States Geological Survey Mineral Resources Program, U.S. Geological Survey Publication.